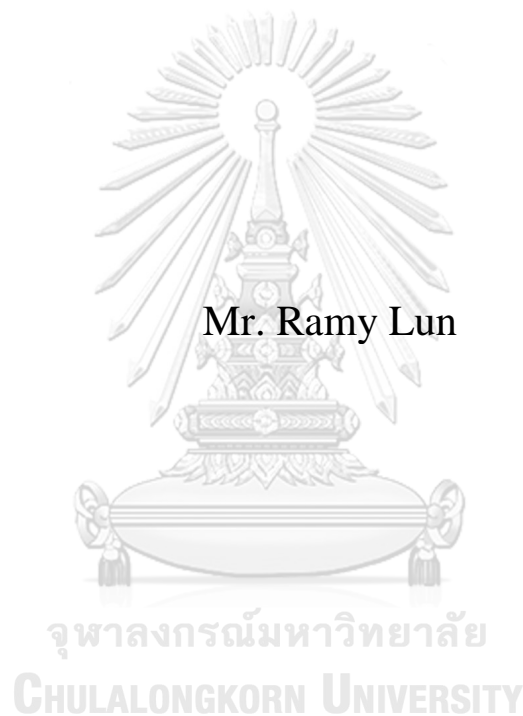# Heavy Metals Adsorption in Simulated Groundwater Using Iron Oxide Particles and Iron Oxide Coated Sand

Mr. Ramy Lun

A Thesis Submitted in Partial Fulfillment of the Requirements
for the Degree of Master of Engineering in Environmental Engineering
Department of Environmental Engineering
Faculty of Engineering
Chulalongkorn University
Academic Year 2018

การดูดซับโลหะหนักในน้ำบาดาลสังเคราะห์ด้วยอนุภาคเหล็กออกไซด์และทรายเคลือบเหล็กออกไซด์

นายรามี ลุน

วิทยานิพนธ์นี้เป็นส่วนหนึ่งของการศึกษาตามหลักสูตรปริญญาวิศวกรรมศาสตรมหาบัณฑิต
สาขาวิชาวิศวกรรมสิ่งแวดล้อม ภาควิชาวิศวกรรมสิ่งแวดล้อม
คณะวิศวกรรมศาสตร์ จุฬาลงกรณ์มหาวิทยาลัย
ปีการศึกษา 2561

Thesis Title   Heavy Metals Adsorption in Simulated Groundwater
                Using Iron Oxide Particles and Iron Oxide Coated Sand
By   Mr. Ramy Lun
Field of Study Environmental Engineering
Thesis Advisor Assistant Professor DAO SUWANSANG
                JANJAROEN, Ph.D.

Accepted by the Faculty of Engineering, Chulalongkorn University in Partial Fulfillment of the Requirement for the Master of Engineering

.... Dean of the Faculty of Engineering
(Professor SUPOT TEACHAVORASINSKUN, D.Eng.)

THESIS COMMITTEE

.... Chairman
(Associate Professor Pichaya Rachdawong, Ph.D.)
.... Thesis Advisor
(Assistant Professor DAO SUWANSANG
JANJAROEN, Ph.D.)
.... Examiner
(Jenyuk Lohwacharin, Ph.D.)
.... External Examiner
(Peerapong Pornwongthong, Ph.D.)

จุฬาลงกรณ์มหาวิทยาลัย
CHULALONGKORN UNIVERSITY

รามี ลุน : การดูดซับโลหะหนักในน้ำบาดาลสังเคราะห์ด้วยอนุภาคเหล็กออกไซด์และทรายเคลือบเหล็กออกไซด์.
(Heavy Metals Adsorption in Simulated Groundwater Using Iron Oxide Particles and Iron Oxide Coated Sand) อ.ที่ปรึกษาหลัก : ผศ.ดร.ดาว สุวรรณแสง จั่นเจริญ

งานวิจัยนี้มุ่งเน้นศึกษาเกี่ยวกับกลไกการดูดซับโลหะหนัก 3 ชนิดได้แก่แมงกานีส สารหนู และเหล็กในน้ำบาดาลสังเคราะห์ด้วยอนุภาคเหล็กออกไซด์ (IOP) และทรายเคลือบเหล็กออกไซด์ (IOCS) โดยอธิบายกลไกการดูดซับด้วยแบบจำลองทางจลนพลศาสตร์ pseudo first-order หรือ pseudo second-order และแลงเมียร์หรือฟรุนดิชไอโซเทอม โดยทดลองใช้ตัวกลางดูดซับปริมาณ 4 ถึง 24 mg/L และระยะเวลาระหว่าง 10 ถึง 60 นาที จากผลการทดลองพบว่าปริมาณตัวกลางดูดซับที่เหมาะสมสำหรับการดูดซับแมงกานีส สารหนู เหล็ก และโลหะหนักทั้ง 3 ชนิดรวมกันคือ 12, 12, 20 และ 16 mg/L ด้วย IOP และ 8, 12, 8 mg/L ด้วย IOCS นอกจากนี้ การดูดซับของโลหะหนักทั้ง 3 ชนิดเป็นแบบ pseudo-second order ซึ่งแสดงถึงการดูดซับแบบเคมี โดยการดูดซับของแมงกานีสเป็นแบบการดูดซับชั้นเดียว ในขณะที่การดูดซับของสารหนูและเหล็กเป็นการดูดซับแบบหลายชั้น นอกจากนี้ยังพบว่าซัลเฟตในน้ำขัดขวางการดูดซับโลหะหนักบนตัวกลางทั้งสองชนิดยกเว้นการดูดซับของเหล็ก แต่เมื่อโลหะหนักทั้งสามชนิดอยู่รวมกันในน้ำ พบว่าซัลเฟตไม่ขัดขวางการดูดซับสารหนูและเหล็กแต่อย่างใดเนื่องจากซัลเฟตจับตัวกับ IOP และ IOCS ด้วยแรงที่อ่อน นอกจากนี้ยังพบว่าผลการทดสอบการชะละลายโลหะหนักจากตัวกลางดูดซับที่ใช้แล้วผ่านมาตรฐานยกเว้นเหล็กที่ถูกชะละลายออกมาจาก IOP เกินมาตรฐาน จากผลการทดลองพบว่า IOP และ IOCS เป็นตัวกลางดูดซับที่มีความสามารถในการดูดซับโลหะหนักในน้ำเสียสังเคราะห์ให้ต่ำกว่าค่ามาตรฐานน้ำดื่ม Cambodian Drinking Water Quality (CDWQS) และ World Health Organization (WHO) Drinking Water Standard ได้

จุฬาลงกรณ์มหาวิทยาลัย
CHULALONGKORN UNIVERSITY

สาขาวิชา   วิศวกรรมสิ่งแวดล้อม   ลายมือชื่อนิสิต ....
ปีการศึกษา   2561   ลายมือชื่อ อ.ที่ปรึกษาหลัก ....

6070290821 : MAJOR ENVIRONMENTAL ENGINEERING
KEYWORD: Adsorption, Heavy Metals, Simulated Groundwater, Iron Oxide Particles, Iron Oxide Coated Sand

Ramy Lun : Heavy Metals Adsorption in Simulated Groundwater Using Iron Oxide Particles and Iron Oxide Coated Sand . Advisor: Asst. Prof. DAO SUWANSANG JANJAROEN, Ph.D.

This study aimed to understand adsorption mechanisms of single of heavy metals such as Mn, As and Fe and a combined heavy metal in simulated groundwater using iron oxide particles (IOP) and iron oxide coated sands (IOCS). The experiment was conducted in batch test. In order to understand mechanism of heavy metals adsorption, pseudo first-order and pseudo second-order of kinetic, and Langmuir and Freundlich isotherm models were applied by varying adsorbent dosages from 4 to 24 mg/L ,and 10 to 60 min of times. Optimal dosages for single heavy metals and a combined heavy metal removal were 12, 12, 20 and 16 mg/L of IOP, and 8, 12, 8 and 12 mg/L of IOCS, respectively. Moreover, heavy metals removal fitted well to the pseudo second-order kinetic model suggesting chemisorption process. For adsorption isotherm, Mn adsorbed using IOP and IOCS in single and combined heavy metal fitted better with Freundlich model which explained that Mn adsorbed on multilayer of IOP and IOCS surface. In contrast, Langmuir model was fitted with As and Fe in both single and combined heavy metals. Therefore, As and Fe adsorbed on monolayer surface for IOP and IOCS. Moreover, the presence of sulfate in water significantly reduced on single heavy metals adsorption except for Fe; however, sulfate had a negligible effect on combined heavy metals adsorption for As and Fe due to its weaker binding affinity for IOP and IOCS. Last but not least, after leaching test, IOP and IOCS were identified as non-hazardous waste except for Fe-adsorbed IOP. In conclusion, IOP and IOCS were effective adsorbents since they can remove heavy metals in simulated groundwater to an acceptable level according to CDWQS and WHO Standard.

จุฬาลงกรณ์มหาวิทยาลัย

CHULALONGKORN UNIVERSITY

Field of Study:	Environmental Engineering	Student's Signature	
Academic Year:	2018	Advisor's Signature	

ACKNOWLEDGEMENTS

TABLE OF CONTENTS

Page

LIST OF TABLES

จุฬาลงกรณ์มหาวิทยาลัย

CHULALONGKORN UNIVERSITY

LIST OF FIGURES

Page

ABBREVIATIONS

C_c	: Cavitation Coefficient
CDIC	: Cambodia Drinking Water Standard
C_u	: Uniformity Coefficient
DBP	: Disinfection by Products
DNA	: Deoxyribonucleic Acid
E_h	: Oxidation potential
Eq	: Equation
EPA	: Environmental Protection Agency
GAC	: Granular Activated Carbon
H.M	: Heavy Metal
Hr	: hour
ICP-OES	: Inductively Coupled Plasma-Optical Emission Spectrometry
IOCS	: Iron Oxide Coated Sand
IOP	: Iron Oxide Particles
MoIMAE	: Ministry of Industry, Mines And Energy
pH	: Power of hydrogen
pKa	: Negative base 10 logarithm of the acid dissociation constant
RO	: Reverse osmosis
SEM-EDS	: Scanning Electron Microscopy-Energy Dispersive Spectroscopy
TCLP	: Toxicity Characteristic Leaching Procedure
UNICEF	: United Nation International Children's Emergency Fund
WHO	: World Health Organization Standard
XRF	: X-Ray Fluorescence

CHAPTER 1
INTRODUCTION

1.1. Introduction

The population of Cambodian is approximately 13.3 million people among of those 80% living in rural area, and 20 % living in urban area in 2008 (National Institute of Statistic, 2008). In 2003, National target of access to safe drinking water sanitation is established as a part of the seventh goal of Cambodia Millennium Development Goals. Meanwhile, the target will be expected to achieve 50% and 75% of rural population with access drinking water sanitation in 2015 and 2020, respectively. It was reached 43.90% in 2011 as seen in Figure 1.1 (Ministry of Environment, 2012). Therefore, accessing safe drinking water in rural area is a challenge in Cambodia.
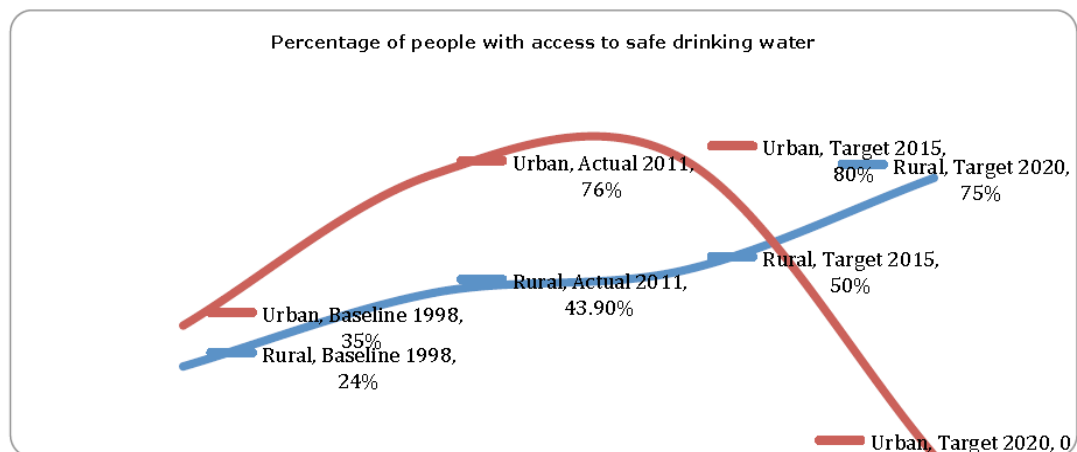
Figure 1.1. The percentage of Cambodian people with access to safe drinking water (Ministry of Environment, 2012)

In Cambodia, surface water from Mekong River and Tonle Sap Lake, groundwater, rainwater and others are main sources of drinking water. But, the quantity and quality usage of water resources are changed by season changes. For instance, Molis O'nilia (2016) it described that groundwater is the second largest source drinking water in dry season. During the last decade, family-based groundwater tube-wells are among popular sources of potable water in rural area (Figure 1.2). One million people have stopped using surface water since it has caused disease and illness in Kandal province and some rural areas. Poor water quality was a roof cause of high rate of infant

mortality (71 death/1000 live births) (Berg et al., 2007). However, groundwater in Cambodia is highly contaminated with arsenic and other heavy metals such as iron and manganese. (Buschmann et al., 2007). In addition, about 67%, 80% and 86% of the groundwater samples had higher concentrations of barium, manganese and lead greater than WHO Drinking Water Guidelines (Luu, Sthiannopkao, and Kim, 2009). The accumulation of these trace elements in the water can cause a potential risk to human health (Al Rmalli et al., 2005). The presence of the heavy metals in groundwater becomes a major concern, because it affects possible uses of water. For this reason, it is necessary to understand groundwater contamination, and to purify it for safe use.
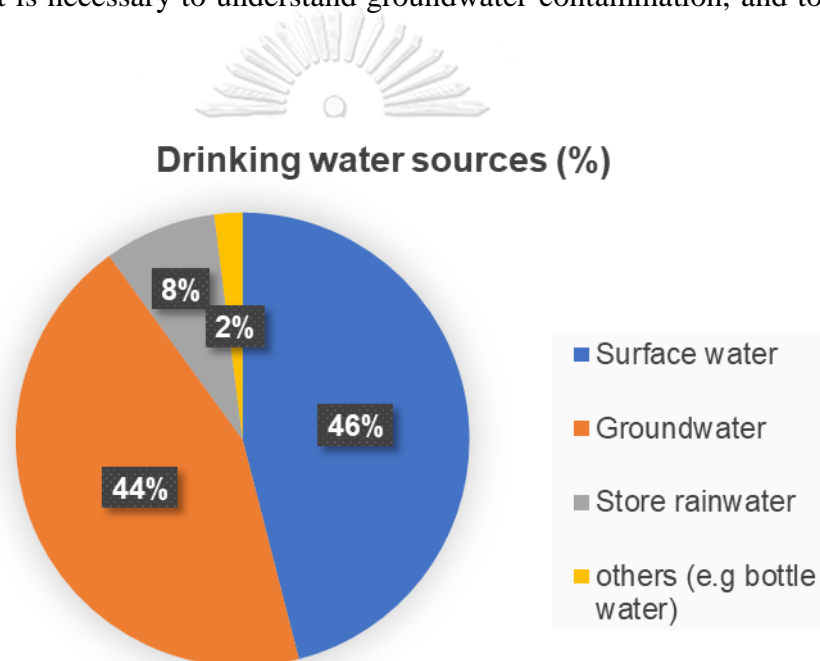
Figure 1.2. The modified primary water source for households during dry season in Cambodia by UNICEF (Molis O'nilia, 2016)

Naturally, groundwater quality in Cambodia has high heavy metal contents such as iron, arsenic, and manganese (CDIC, 2012). But these elevated concentration is typically associated with human actions that accumulate and distribute including improper human and animal waste management or heavy fertilizer usages (Sam Ol, 2011). Although heavy metals are generally occurred in the earth's crust, they are also generated from human activities in different sectors such as mining industry, smelting operations, industrial production, domestic usage, agricultural metals uses, and leachate from solid waste landfill (He, Yang, and Stoffella, 2005; Herawati et al., 2000; Shallari et al., 1998; Tiwari et al., 2015). Heavy metal contamination has a

number of negative impacts on the human health such as deoxyribonucleic acid (DNA) destruction, carcinogen and central nervous system damage (Stohs and Bagchi, 1995). Therefore, heavy metals pollution in groundwater needs to be removed for safe drinking water.

Not only Cambodia, but also the world, heavy metals pollution in water has become a major issue. Meanwhile, water treatment methods have been developed to remove heavy metals for purifying water including membrane, ion exchange, chemical precipitation, and adsorption (Carolin et al., 2017). In that technology, the membrane is a relatively fresh method which was initially developed for drinking water from saline and brackish water. Currently, this process has started to look for the application in the treatment of industrial wastewater by reducing the cost, and increasing pollutants removal efficiency (Qdais and Moussa, 2004). The membrane processes used to remove metals from wastewater are ultrafiltration, reverse osmosis, nanofiltration and electrodialysis. Moreover, the ion exchange is characterized as a physical process which ion in solution are transferred to a solid matric in turn releasing ions of different types with the same charge. The ion exchange resin can be categorized as the basis of functional groups such as cationic exchange resins, anions exchange resins and chelating exchange resin (Zewail and Yousef, 2015). In addition, chemical precipitation is a process that chemicals react with heavy metal ions to form insoluble precipitation. The precipitates formation can be separated from water by sedimentation or filtration. The conventional chemical precipitation processes include hydroxide precipitation and sulfide precipitation. (Fu and Wang, 2011). The adsorption is appearing as a potentially preferable alternative for heavy metals because it provides flexibility in design, high-quality treated effluent, and the possibility to regenerate adsorbent (Futalan et al., 2011).

Although, the technologies mentioned above are very suitable for heavy metals removal, there also have some of disadvantages such as sludge production, high cost, electricity requirement, and complexity of operation and maintenance (Lee et al., 2007; Sang et al., 2008; Subramani et al., 2012; Thakur and Mondal, 2017; Vaaramaa and Lehto, 2003; Zewail and Yousef, 2015). Therefore, adsorption is the best water treatment methods for rural communities than other methods (Agarwal and Singh,

2017). This method has provided an acceptable result in terms of heavy metals removal efficiency via physical and chemical interaction, however, it also requires other processes to separate the pollutants from water. The method has been found to be effective in removing several heavy metals such as arsenic in various pH. Adsorbent can be regenerated (Baig et al., 2013; Bradley et al., 2011; Snyder et al., 2016). The cost of treatment is mostly estimated depending on media uses in particularly the adsorbents price (Agarwal and Singh, 2017). Therefore, adsorbents selectivity has been considered on their adsorption ability, cost and environmental-friendly.

A good adsorbent, it should be non-toxic, show good resistance towards oxidizing and reducing agents, acids or bases, and very low solubility in water (Chaudhry, Zaidi, and Siddiqui, 2017). Among those adsorbents, iron oxide is naturally content, less soluble and has high adsorptive ability for the removal of heavy metals from contaminated water in term of removal efficiency (Benjamin et al., 1996; Cornell and Schwertmann, 2003; Washington and Off, 1962). The surface complexity of iron oxide can remove the soluble arsenic species in water because it reacted with the hydroxide on the surface (Katsoyiannis and Zouboulis, 2002; Thirunavukkarasu, Viraraghavan, and Subramanian, 2003). Moreover, iron oxide also adsorbed the heavy metals via electrostatic repulsion between negatively charged iron oxide surface and metals cation (Koretsky, 2000). The heavy metal was removed from water by physical and chemical adsorption mechanism (Janjaroen, Dilokdumkeng, and Jhandrta, 2018). Most iron oxide are only available as fine powder and the used of iron oxide powder is limited by difficulty in separation of the solid from solution (Phuengprasop, Sittiwong, and Unob, 2011). Recently, several studies have taken attention in synthesize the adsorbent by iron oxide particle coated on other materials to improve the performance of water treatment efficiency by adsorbents active site extension such iron impregnated with granular activated carbon, charred granulated attapulgite-supported hydrate iron oxide, nano impregnated iron with biochar, iron/cupper nanoparticle, nano iron ion enrich material, iron oxide coated sand (Hu et al., 2015; Mondal, Majumder, and Mohanty, 2008; Yin et al., 2017). Iron oxide coated sand is provided high heavy metals removal efficiency, and it is simple to synthesize, locally

and economically (Benjamin et al., 1996; V. Gupta, Saini, and Jain, 2005). Therefore, iron oxides particle and iron oxide coated sand were selected as adsorbents to remove heavy metals in simulated groundwater in Cambodia.

To address with groundwater quality issues, some researches have been conducted on centralized and decentralized groundwater treatment plan in rural area in Cambodia (Kang et al., 2014; Uy et al., 2009). Both researches was conducted with only arsenic removal, even though there have other heavy metals pollutants presence in groundwater (Buschmann et al., 2007; CDIC, 2012). However, Kang et al. (2014) conducted with the treatment using reverse osmosis illustrated the high removal efficiency. But treatment is required the electricity while household in rural area accessed with the electricity about 13.1 % (National Institute of Statistic, 2008). This reason is partially affected to access of drinking water in rural area by using this method. Moreover, Sand filtration was applied in rural communities by removing arsenic, but they used the high amount of adsorbent about 5 kg of iron nail rusted (Uy et al., 2009). When concentration of sulfate presence in water increase, the amount of iron precipitated also increase by changing the surface properties of the ferric oxyhydroxide precipitates (Kong et al., 2017). This anion can compete with heavy metals for available surface binding sites and interfere in the removal of heavy metals by alteration of the electrostatic charge on the surface of adsorbent (Yu et al., 2013). So, the effect of ligand such as sulfate in water might be competed with heavy metals reaction on adsorbent active site. Thus, the optimal adsorbent capacity and effect of sulfate concentration was considered to eliminate the waste generation and filter clogged. To complete the gap of these researches, the specifications of this work studied the small iron oxide particles and iron oxide coated with sand via their adsorption mechanisms to remove single and combined heavy metals in simulated groundwater. Furthermore, the effect of high initial sulfate concentration in groundwater was also conducted. The leaching test of adsorbents after adsorption process was studied before disposal to the environment.

1.2. Objectives

The general objective of this study aims to understand the heavy metals removal mechanism in simulated groundwater as groundwater quality in Kandal province, Cambodia by using the adsorption process. To achieve the general objective, there are three main objectives including:

1. To study adsorption process of heavy metals removal by using iron oxide particles and iron oxide coated sand in simulated groundwater.
2. To study the effect of sulfate on adsorption process on heavy metals removal.
3. To study the leachability of adsorbents.

1.3. Scopes of study

There were several scopes of this study which was described in this section following in order are:

1. The synthetic water was prepared similarly to the groundwater sources in Kandal province e.g., hardness and heavy metals.
2. Inorganic arsenate, ferrous, and manganese contaminants was considered as the heavy metal elements in groundwater due to some reasons. For arsenate is assume as total arsenic in water due to instrument can measure total arsenic, arsenate is less toxicity than Arsenite. In term of ferrous form in water, it was soluble in water. Therefore, Arsenic and Iron were studied in forms of arsenate and ferrous, respectively.
3. This study assumed that it has pretreatment before adsorption process to remove big particle sizes such as garbage and dissolved solid.
4. The experiment was conducted in a batch reactor.
5. The kinetic study was examined through varying the adsorbents doses and the initial concentration of sulfate (SO_4^{2-}) as the ligand competitor in water.
6. The experiment was conducted with individual heavy metal, followed by a combined heavy metals condition in a batch experiment.
7. Two different types of adsorbents such as iron particle and iron oxide coated sand were selected to be adsorbents in this study.

8. The adsorbents were synthesized only one time enough for all experiments and stored in desiccator.

9. The quantity and quality of iron contain on both adsorbents are assumed to be the same in every test. Iron characteristics will be measured to confirmation.

10. This research was conducted at the Department of Environmental Engineering, Faculty of Engineering at Chulalongkorn University, Thailand.

1.4. Hypothesis of research

The hypothesis of this research analyzed the effect of sulfate on heavy metals removal by using difference adsorbents. Therefore, there are a few hypothesizes such as:

- The iron oxide coated sand and iron oxide particle adsorbents will be able to remove heavy metals from groundwater.

- The initial concentration of sulfate in groundwater sources will affect heavy metals removal efficiency.

จุฬาลงกรณ์มหาวิทยาลัย
CHULALONGKORN UNIVERSITY

CHAPTER 2
THEORY AND LITERATURES REVIEW

2.1. Water quality in Kandal province, Cambodia

Several studies showed quality assessments of groundwater providing the summary background of quality sources in Kandal province, Cambodia as shown in Table 2.1. The Cambodian Drinking Water Standard and World Health Organization Standard for Drinking Water also includes in this table. In addition, there is the comparison between groundwater quality by the CDWS and WHO standards.

Table 2.1.Summary groundwater quality in Kandal province, Cambodia

Sources	Buschmann et al. (2008)	Luu et al. (2009)	CDIC (2012)	MoIMAE (2004)	WHO (2004)
As (μg/L)	155	-	1000	50	10
Mn (mg/L)	0.6	-	28	0.1	0.4
Fe (mg/L)	2.2	0.07	100	0.3	0.3
pH	6.92	7.2	7-8	6.5-8.5	-
Total hardness (mg CaCO$_3$/L)	-	319.4	1440	300	-
DOC (mg/L)	3.1	4.998	-	-	-
TDS (mg/L)	-	325	-	-	1800
SO$_4^{2-}$(mg/L)	-	175.9	-	-	-

To sum up, there are many heavy metals in the groundwater sources which have exceeded the WHO Drinking Water Standard and Cambodia Drinking Water Standard as is present in Table 2.2.

Table 2.2. WHO, Cambodia Drinking Water Standard and maximum real situation

Parameters	WHO (2004)	MoIMAE (2004)	CDIC (2012)
As (µg/L)	10	50	1000
Mn (mg/L)	0.4	0.1	28
Fe (mg/L)	0.3	0.3	100

2.1.1. Arsenic

The arsenic distribution is more homogenous in Cambodia, but restricted to the floodplains along the Mekong, Tonle Sap and Bassac rivers as shown in Figure 2.1. Arsenic is the most critical pollutant in groundwater in Cambodia. Its affects is very large regional and have the most severe health consequences for those consuming arsenic contaminated water for a long time generally 5 to 10 years. The concentration of arsenic in Kandal has been found as high as 1 to 1340 µg/L whereas WHO and Cambodia drinking water quality standards are 10 µg/L and 50 µg/L, respectively (MoIMAE, 2004; WHO, 2004).
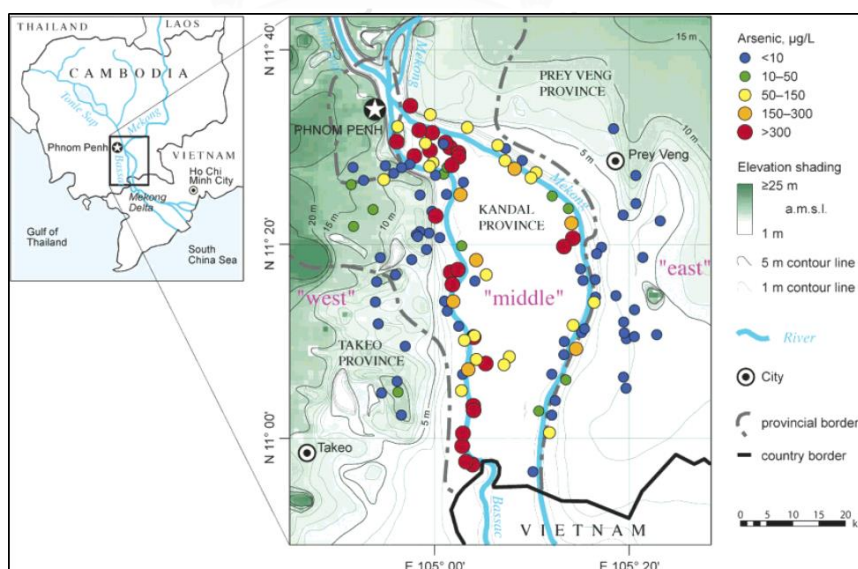
Figure 2.1. Arsenic concentration in Groundwater in Kandal map (Buschmann et al., 2007)

2.1.2. Manganese

Groundwater contaminated in Cambodia has been found that the manganese which is another health impact to the human. Manganese naturally occurs in the ground in soil and water. Many tube wells are polluted with manganese; however, the health effects are less visible than arsenic. Manganese is addressed as a neurotoxic element which impacts brain function. The Cambodian and WHO consumption drinking water standard for Manganese is 0.4 mg/L to prevent health impacts (MoIMAE, 2004; WHO, 2004). Consumption of manganese contaminated groundwater has been linked to lower test scores and hyperactivity in children (Sam Ol, 2011). At the small amount of manganese concentration, it is possible to produce the effects in desirable water taste and discoloration. Tube wells groundwater in Kandal, Prey Veng and Kompong Cham provinces was recognized that the manganese concentration has been hugely contaminated. Lastly, the range of manganese concentration in Kandal province is evaluated from less than 0.1 to 28 mg/L (CDIC, 2012).

2.1.3. Iron

In Cambodia, groundwater is usually contaminated by iron. Iron affects water characteristics leading to a cloudy, poor taste, burden laundry machine and discolor rice (Sam Ol, 2011). The WHO Drinking Water Quality Standard of iron is 0.3 mg/L which is appropriated to aesthetic effects, as Cambodia Water Drinking Standard (MoIMAE, 2004). Based on Table 2.1 shows that the iron concentration ranged from 0.07 to 100 mg/L that is exceeded the standard in Kandal province. Moreover, there also have research which is conducted to work on iron concentration in groundwater assessment map in Cambodia. In the map, iron concentration is exceeded 10 mg/L in Kandal province which is demonstrated in Figure 2.2.
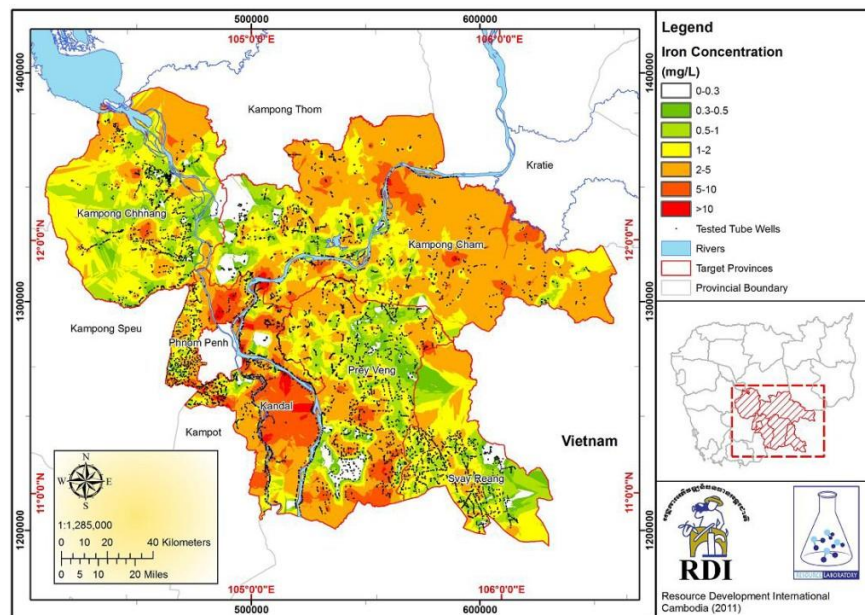
Figure 2.2. Iron concentration in groundwater in Kandal Map (CDIC, 2012)

2.2. Heavy metals solubility and precipitation

2.2.1. Arsenic

There have two types of arsenic forms in water sources. It includes organic and inorganic forms, however; the most present forms of arsenic in groundwater sources is in for inorganic form. Moreover, two species of arsenic in natural water sources include arsenite [As(III)] and arsenate [As(V)]. The pKa values are represented in Table 2.3 (Janga, Somannaa, and Kimb, 2016). In terms of inorganic form, the natural principles of arsenic in waters including $H_2AsO_4^-$, H_3AsO_3, $HAsO_4^-$ and $As_3O_4^{3-}$. The redox reaction in a system containing As^{3+} and As^{5+} and the possible reaction of arsenite with iron hydroxide is illustrated in the Equation 2.1 and 2.2.

$$H_3AsO_4 + 2H^+ + 2e- \rightarrow H_3AsO_3 + H_2O \qquad \text{Eq. 2.1}$$

$$Fe(OH)_{(s)} + H_3AsO_{3(aq)} \rightarrow FeHAsO_{3(s)}^{2-} + H_2O_{(aq)} \qquad \text{Eq. 2.2}$$

Table 2.3.The relative of pKa values and As^{3+} and As^{5+} species (Janga et al., 2016)

Arsenic Species	pKa$_1$	pKa$_2$	PKa$_3$
H_3AsO_4	2.19	6.94	11.5
H_3AsO_3	9.2	N/A	N/A

As shown in Figure 2.3 illustrated the relationship between pe and pH at which the types of arsenic species changed forms by given electron concentration under thermodynamic condition. The changed of As^{3+} to As^{5+} in oxidation state is feasibility with dissolved oxygen. At pH lower than 2, the predomination of arsenic acid is lower than the pH ranges from 2 to 11 that it is replaced by $H_2AsO_4^-$ and $HAsO_4^{2-}$. At higher Eh, the arsenic acid species such as H_3AsO_4, $H_3AsO_4^-$, $HAsO_4^{2-}$, and AsO_4^{3-} are stable and in the middle E_h the arsenous species either are stable. However, the arsenic oxide is formed insoluble. Under the pH conditions of most groundwater, arsenate is presented as the negatively charged oxyanions $H_2AsO_4^-$ or $HAsO_4^{2-}$, whereas arsenite is present as the uncharged species H_3AsO_3 (Ferguson and Gavis,
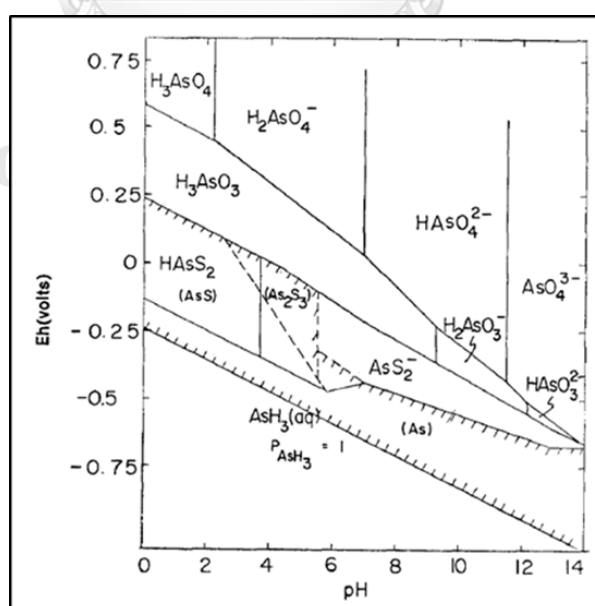
1972).

Figure 2.3. The speciation of arsenic under varying pH and redox conditions (Ferguson and Gavis, 1972)

2.2.2. Iron

Iron is generally a heavy metal containing in the earth' crust (soil and water). It occurs in two oxidation states, the divalent or ferrous form and the trivalent or ferric. The iron retained in solution is consequently affected by the pH of the solution such as the activity of the ions involved, both through the formation of hydroxide complexes and precipitation of solid hydroxides. Moreover, $Fe(OH)_3$ is mostly contained in natural water. Under equilibrium in the pH range of the 5 to 8, it will be solidification forms, thus low solubility (Washington and Off, 1962). Because of the low solubility of iron, it tends to precipitate under condition E_h lower than 0 and over pH in a range higher than 7. Iron tends to precipitate to $Fe(OH)_3$ when it is under oxidation value E_h higher than 0 and pH is exceed than 5 as shown in Figure 2.4. In free space, Ferrous is relatively soluble and a condition of groundwater that E_H range from 0.10 to 0.20 V and pH ranges from 5 to 9 (Crittenden et al., 2012).
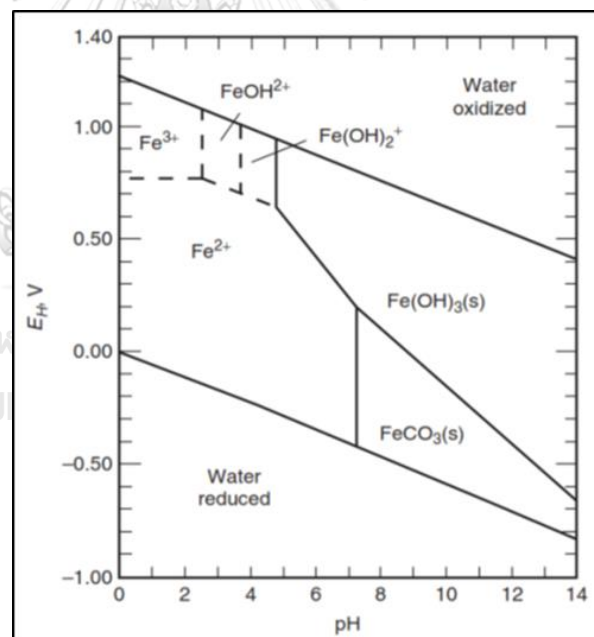
Figure 2.4. The speciation of iron under varying pH and redox conditions (Crittenden et al., 2012)

In addition, iron was formed many bulks and nano-sized iron oxides (Fe_2O_3 and Fe_3O_4) are synthesized from hydroxides. Iron (III) hydroxides, in the form of $Fe(OH)_3$ or the anhydrate from $FeO(OH)$. From Equation 2.3, it may be prepared from elemental iron:

$$4 \text{ Fe} + 3 \text{ O}_2 + 2 \text{ H}_2\text{O} \rightarrow 4 \text{ FeO(OH)} \qquad \text{Eq. 2.3}$$
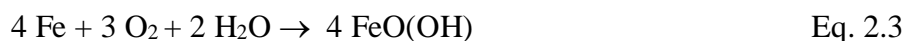
By via electrolysis, hydroxides may be readily prepared from the ion form following by the chemical stoichiometry as shown in Equation 2.4 and 2.5.

$$\text{Fe}^{3+} + 3 \text{ OH}^- \rightarrow \text{Fe(OH)}_3 \qquad \text{Eq. 2.4}$$

$$\text{Fe}^{3+} + 2 \text{ OH}^- \rightarrow \text{Fe(OH)}_2 \qquad \text{Eq. 2.5}$$
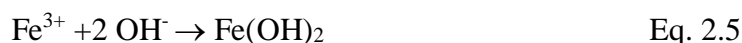
In the presence of hydroxide NaOH concentration as alkalinity condition. In water, hydroxides were easily made form hexacoordinated complexes and undergo deprotonation based on the pH of the environment. It has been taken the form of $[\text{Fe(OH)}_h(\text{H}_2\text{O})_6\text{-h}]^{(z-h)+}$ where z is the formal charge of iron and h is digit of hydroxylation actuating from 0 at pH 1. For ferrous, protonation occurs at pKa_1=9.5 and pKa_2=10.5. In order words, ferrous hydroxides in exist in forms in Equation 2.6.

$$[\text{Fe(H}_2\text{O})_6]^{2+} \leftrightarrow [\text{Fe(OH)(H}_2\text{O})_5]^+ \qquad \text{Eq. 2.6}$$
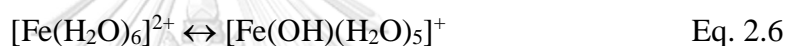
2.2.3. Manganese

Similarly, manganese is highly content in the natural environment such as water, soil, and groundwater. This chemical element is highly potential for metabolism process for plantation. In nature, there have four states of predominating such as +2, +3, +4 and +6 which form as oxides or hydroxides mostly presence in water and or nearby the earth surface. As the form a carbonate and a sulfide in divalent manganese species, it is oxidized at high pH with rapid rate. Because of the complexity of manganese in natural water, the Eh-pH diagram which was used to understand the stability and solubility of this element. As shown in Figure 2.5 represents a system would ordinarily be found in nature, the general relationships are interested. In the pH range commonly found in natural water, from about pH 5 to about pH 10, the solubility of manganese is considerably more than 0.01 mg/L over a wide range of Eh. At a pH of more than 12.3 the solubility can exceed 0.01 mg/L, at low Eh. Manganese is readily soluble at a pH of 7.0 and Eh equals to +0.50. In addition, the diagram indicated that manganese solubility is strongly affected by lower Eh or pH, in a system where oxides are the predominant solids (JohnD, 1963)
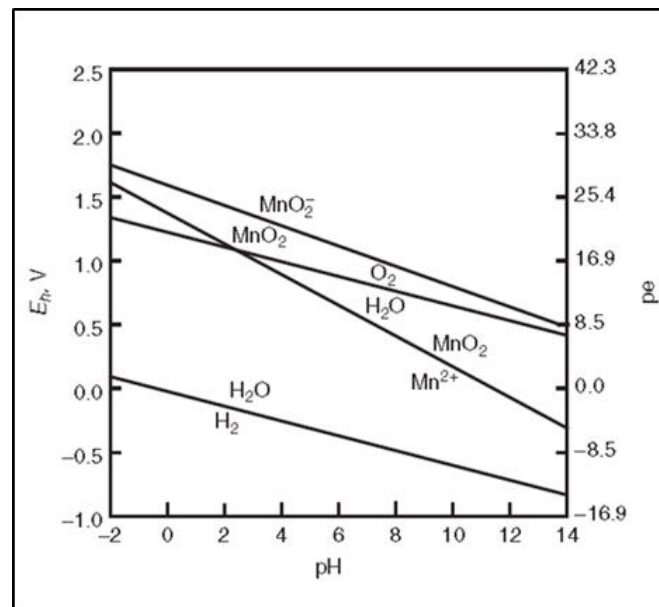
Figure 2.5. Predominance area diagram for permanganate system for total species concentration of 10^{-4} mol/L (Crittenden et al., 2012)

Moreover, manganese oxides have been comprehensively investigated as oxidizing agents for arsenite, and the overall oxidation reaction is illustrated in Equation 2.7 and 2.8. It was demonstrated that the oxidation of As(III) by a two steps pathways given in Equations 2.7 and 2.8. It was also involved the reduction of Mn(IV) to Mn(III) and then Mn(III) to Mn(II) (Zhang et al., 2007).

$$MnO_2 + H_2AsO_3 + 2\,H^+ \leftrightarrow Mn^{2+} + H_3AsO_4 + H_2 \qquad\qquad \text{Eq. 2.7}$$

$$2\,MnO_2 + H_3AsO_3 \leftrightarrow 2\,MnOOH^* \qquad\qquad \text{Eq. 2.8}$$

$$2\,MnOOH^* + H_3AsO_3 + 4\,H^+ \leftrightarrow 2\,Mn^{2+} + H_3AsO_4 \qquad\qquad \text{Eq. 2.9}$$
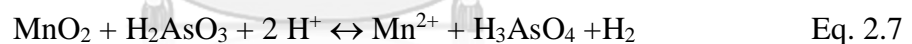
2.3. Current treatment technologies in Cambodia

Some studies on heavy metals removal from groundwater in Cambodia has described in this section. The studies have used the technology such as filtration process, membrane process and adsorption for purifying water to be safe drinking water. The summary of their process such as:

Uy et al. (2009) has studied on arsenic, iron, phosphate, and hardness removal in raw groundwater by using Kanchan Arsenic Filter. Arsenic contamination in drinking water is a critical issue in Cambodia. The groundwater had arsenic and phosphate

concentrations averaging 637 μg/L and 5.09 mg/L, respectively. It was representing challenging water quality source. It is the natural rusting process of these nails that provides the iron oxide adsorption sites to remove the arsenic from the water. The fine sand filter media below the 5 or 6 kg of nails performs as an intermittently operated slow sand filter. There has 20 L of raw groundwater has used for testing daily for 30 weeks in the morning and evening. As result, arsenic is removed averaged 95 to 97% for all configurations. Iron is removed 99% efficiency and hardness is acceptable range.

Kang et al. (2014) worked on developing arsenic removal technology from groundwater. This study surveyed and test the well water quality in 3 provinces in Cambodia including Kandal, Kompong Cham and Prey Veng. Amorphous iron (hydr)oxide was synthesized as adsorbent to study in this research. They have developed two types of As removal equipment. For type 1, they used a hand power without reverse osmosis (RO) membrane. Well water passes the pretreatment system that consists of a bag filter, 1 μm filter and a 0.2 μm filter. The water then moves to the adsorbent cartridge and As is removed by the adsorbent. Moreover, for type 2, they used the electric power with RO membrane. In the same manner as in Type1. Well water is passed through the pretreatment system then RO membrane. The adsorbent cartridge is packed in the layers consisting of 2 kg of the adsorbent, 4 kg of palm husk-activated charcoal, 0.5 kg of coarse sand, and 0.5 kg of fine sand. They based on the results of the field survey on well water. For field surveying, they found that As concentration in 68 % of the well water samples higher than WHO standard value for As concentration in drinking water and that in 35 % of the wells was higher than 500 μg/L. As a result, the As removal rate was 83.1 to 99.7 %, with an average of 93.7 %, indicating that the As removal equipment greatly lowered the risk of As exposure to the residents.

2.4. Heavy metals removal treatment methods

Pollutants generated in the effluent is characterized as organic and inorganic pollutants which have a different concentration of toxic level. Chemical, physical and biological treatment are commonly used in the treatment of organic pollutants.

However, these methods are not suitable for the inorganic pollutant like heavy metals. Because of their qualities like solubility, oxidation-reduction characteristics, and complex formation, the heavy metals composition plays a critical concern. Recently, many of water treatment technologies have been applied for heavy metals removal from groundwater sources to be drinking water. Hence, this section is described the definition and mechanism of those treatment processes in physical and chemical treatment. Each of techniques is studies by many researchers and the methods used for heavy metal removal includes ion exchange, membrane, oxidation, coagulation process, etc. All these methods removed the heavy metal is represented in the following below.

2.4.1. Ion Exchange process

Ion exchange is defined as the process through which ions in solution are transferred to a solid matrix which, in turn release ions of different types but of the same charge. Ion exchange is a physical separation process in which the ions exchanged are not chemically altered. Furthermore, the ion exchange resin can be categorized based on functional groups such as cationic exchange resins, anion exchange resins, and chelating exchange resin. This process has rapidly reacted with the pH of the solution (Barakat, 2011).

Based on the Zewail and Yousef (2015) found that the results of heavy metals removal efficiency of Ni^{2+} and Pb^{2+} are 98 % and 99%, respectively. Using an Ion exchange resins (AMBERJET 1200 Na) has been performed in batch conical air spouted vessel in the kinetic model, but it has been required checking the air spouted to the system. Meanwhile, the removal efficiency of the Ni^{2+} was dropped during the increasing of the initial concentration because of the fixed an exchange resin. Moreover, the study on heavy metals such as As, Fe, Mn removal in groundwater Vaaramaa and Lehto (2003), has been pointed that iron which was present as Fe(OH)3, it took up well by the cation exchangers, and arsenic, which presumably was sorbed on the iron species that was consequently sorbed on the exchangers. The quality of effluent is good compared to the WHO standard, and it stayed in the alkalinity condition.

Therefore, the main advantages of ion exchange include metal value recovery, selectivity, less sludge volume production and the meeting of strict discharge specifications, the high removal efficiency, and fast kinetic reaction. Recently, there have lots of different exchange materials to synthesis resins are available. On the other hand, the disadvantages of the ion exchange process that it cannot handle concentrated metal solution as the matrix as fouled by organics and solids.

2.4.2. Coagulation process

The coagulation process is a chemical process that use the chemicals such as Alum, Fe^{3+} as coagulants to destabilize the particles in the water. Recently, the process was categorized into two mains such as conventional coagulation process by chemical aid, the electro-coagulation process by using chemical charge. There are four mechanisms of this process include compression of the electrical double layer, adsorption and charge neutralization, adsorption and inter-particle bridging, and enmeshment in a precipitate, or sweep-floc. Typically, Jar test is required in this process (Crittenden et al., 2012).

Consequently, to remove heavy metals from groundwater the sweep co-precipitation by coagulants is the essential mechanism utilization that it changes the formation of metal to be metal-hydroxide and insoluble than precipitate (Lee et al., 2007). Based on the Lee et al. (2007) a process was used to treat the groundwater. Lime and calcium carbonate have been applied in term of their abandon quantity, economic, less toxicity to the environment. The heavy metals such as As, Ni, Cd, and Zn are the main pollutants in the groundwater sources. As a result, the research pointed out that granular calcium can remove Ni and Zn more effectively except arsenic can removal 50% efficiency. However, a combination of the lime and calcium, the performance of treatment in column test is pretty good, the sludge and hardness may be occurred by high Calcium in water.

Moreover, Electrocoagulation process is performed to remove heavy metals in groundwater by generated the metal hydroxides. It works as coagulants in an aqueous solution which provides the active sites for adsorption such as sweep coagulation,

bridge coagulation, co-precipitation. While the electro-coagulation process, the change of speciation and redox potential of arsenic and fluoride, the removal efficiency of Arsenic and Fluoride simultaneously depended on the pH ranges. In term of changing the pH, the ranges of pH which is suitable for removal was equal to or exceed 8.4 for all the initial pH values from 3 to 11. The percentages of removal decrease when the initial pH rises above 7 because of the presence of negative charge of arsenite and fluoride increasing. Sludge also was produced in this case with components of As(III) and Fluoride (Thakur and Mondal, 2017). Therefore, the advantages of this process cost effective, and removal efficiency. Nevertheless, the disadvantages are sludge production, depend on pH.

2.4.3. Membrane filtration

Membrane process is a new technology in term of physiochemical treatment that uses in any pollutants by separation mechanism (Crittenden et al., 2012). Membrane filtration technologies are the most commonly used to remove heavy metals with high efficiency, and space saving. Typically, there have 3 main processes in the membrane filtration to remove heavy metals such as ultrafiltration, reverse osmosis, nanofiltration and electrodialysis.

The reverse osmosis process has been defined as uses a semi-permeable membrane to remove high ranges of dissolved species. Based to Subramani et al. (2012) the RO process can recover about 60% of feed water recovery by using RO to treat mine-contaminated groundwater. However, without chemical softening and electrocoagulation in the primary treatment of heavy metals removal, the reverse osmosis process faces a problem by scaling on the membrane surface by $CaSO_4$. Regarding Sang et al. (2008) has been used the micellar-enhanced ultrafiltration using poly hollow fiber membrane can be achieve more than 99% of removal efficiency of metal in groundwater sources contaminated with heavy metals such as Pb^{2+} and Cd^{2+} in the feed of 100 mg/L but the process was used with high voltages to electro-spinning process.

In addition, in the last decade, Ellis, Bouchard, and Lantagne (2000) have worked on the microfiltration for iron and manganese removals in groundwater. The process performance is good; however, the oxidation process is required in pH is 8.5 for process completion. At pH 8 and 8 °C of temperature was achieved 20 % manganese removal. Because of the microfiltration is allowed the pore size 1 µm of pollutants size, this research found that the artificial and natural groundwater quality in form of iron oxide and manganese oxide, their pores size distribution ranged from 1.5 to 50 µm. Thus, the iron and manganese physically were separated from groundwater. The phenomena introduce the adsorption process between iron oxide and manganese. Unfortunately, the membrane was fouled by oxide particles that were retained on the surface membrane and pressure was needed either.

In sum up, the advantages of the membrane are high removal efficiency, high binding selectivity, highly concentrated metal concentrates for reuses, and spacing operation, etc. Besides, the benefits of using membrane filtration, the disadvantage also occurs such as using high energy consumption, scaling on the membrane surface, high cost, clogging, and membrane fouling.

2.4.4. Electrochemical treatment

The electrochemical method is defined as the combination of other the electrical combination and other techniques that made highly development to remove heavy metals from wastewater. Electrodes in the reactor shift the electrons which result in a reduction of pollutants(Carolin et al., 2017). The method is based on the electrode material and cell parameters such as mass transport, current density, chemistry compound in water (Silva et al., 2018). An electrocoagulation reactor consists of two electrodes including anode and cathode in which the external energy is generated the coagulants such as aluminum and iron at the anode and hydrogen at the cathode in the contaminated water. The advantage of using electrocoagulation process is compact sludge production, easy to operate, small retention time. The disadvantage of this method is limited to certain applications because of the short lifespan of electrode material, low mass transfer rates, increase in temperature during the process (Carolin et al., 2017).

2.4.5. Summary

In summary, heavy metals pollutants have been treated by different methods. Most researchers have been improved the technology to remove heavy metals from groundwater to be drinking water due to disadvantages to meet the standard. However, each method has its own advantages and disadvantage as shown in Table 2.4. Different technologies, conditions, need different methods for treating heavy metals in groundwater sources.

Table 2.4.Summary the advantages and disadvantages of treatment methods

Treatment methods	Heavy metals	Advantages	Disadvantages
Ion Exchange	As, Fe, Mn, Pb, Ni	Metal recovery, high removal efficiency, fast kinetic reaction, less sludge production	Cannot handle concentrated metal solution as the matrix as fouled by organics and solids
Coagulation	As, Ni, Cd, F, Zn	Cost effective, high removal efficiency	Jar test, Sludge and hardness production, and pH dependence
Membrane Filtration	Fe, Mn, Pb, Cd	High removal efficiency, reusable heavy metals	High cost, membrane fouling, scaling, high energy consumption
Electrochemical treatment	Cu, Cr, and Ni	Efficient metal ions removal, low chemical usage	High initial investment and electricity requirement

2.5. Adsorption process

2.5.1. Theory of adsorption process

Adsorption process is defined a mass transfer operation in which substances present in a liquid phase are adsorbed or accumulated on a solid phase and removed from the liquid. It has been used in drinking water treatment for the removal of taste and odor-causing compounds, synthetic organic chemicals, color-forming organics, and disinfection by product (DBP) precursors. Moreover, adsorption application was used to remove inorganic compounds including that represent a health hazard such as perchlorate, arsenic and some heavy metals (Crittenden et al., 2012). The mechanisms of this method were categorized into three steps including transportation sorbate to the outer surface of sorbent, diffusion of sorbate into the pore of sorbent and adsorption of sorbate on sorbent as shown in Figure 2.6.
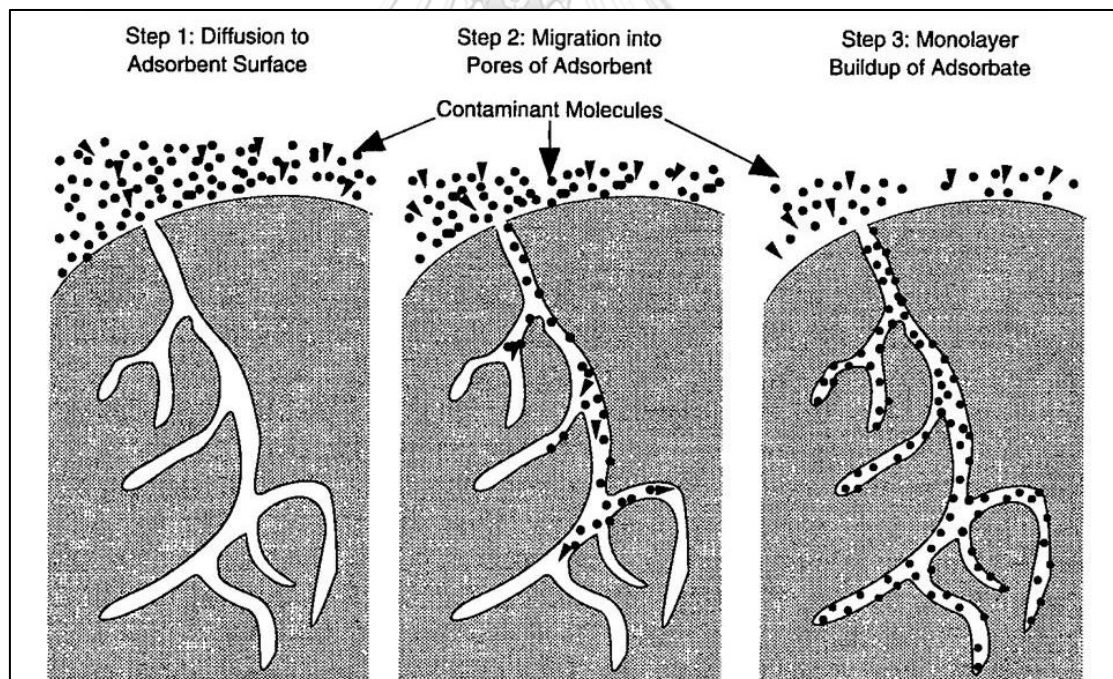
Figure 2.6.Adsorption process mechanism Source:
https://slideplayer.com/slide/10567105/

Adsorbate is the constituent retained onto a surface which is referred to as the adsorbent in phenomenality. In terms of the removal mechanism processes, the dissolved species are transported into the porous solid adsorbent granule by diffusion

and are then adsorbed on to the extensive inner surface of the adsorbent. This process is affected by temperature, the nature of the adsorbate and adsorbent, the presence of other pollutants, satmospheric and experimental conditions such as pH, the concentration of pollutants, contact time, and particle size of the adsorbent (Ali and Gupta, 2006). For most applications in water treatment, the amount of adsorbate adsorbed is usually a function of the aqueous-phase concentration and this relationship is commonly called an isotherm (Crittenden et al., 2012). Langmuir and Freundlich models are the well-known models and can explain the adsorption efficiency of the pollutants in isotherm which is described detail in the next part. Moreover, the batch and column test in the laboratory has been used to carry out the development and optimization of the adsorption parameters.

In adsorption process, the interaction between the adsorbate and adsorbent in aqueous solution is occurred by physical and chemical forces within and surrounding the adsorbate compounds. In physical adsorption process is divided into 3 interaction competations such as adsorbate water interactions, adsorbate surface interactions, and water surface interactions. These physical adsorption interactions have been determined by the strength of adsorbate surface interactions, surface chemistry and solubility of adsorbate the surface chemistry such as hydrophobic and hydrophilic, respectively. For chemisorption is happened while the adsorbate reacts with the surface to form a covalent bond or an ionic bond. Some of the chemical forces occur between the adsorbent surface and adsorbates are shown Figure 2.7. The chemical reaction on surface is strongly effected to the high reaction rate. So, the volumetric of small pores and abundant surface area is really essential and potential in adsorption process. Moreover, the attraction between adsorbent and adsorbate methods are caused by a covalent or electrostatic chemical bond between atoms, with shorter bond length and higher bond energy.
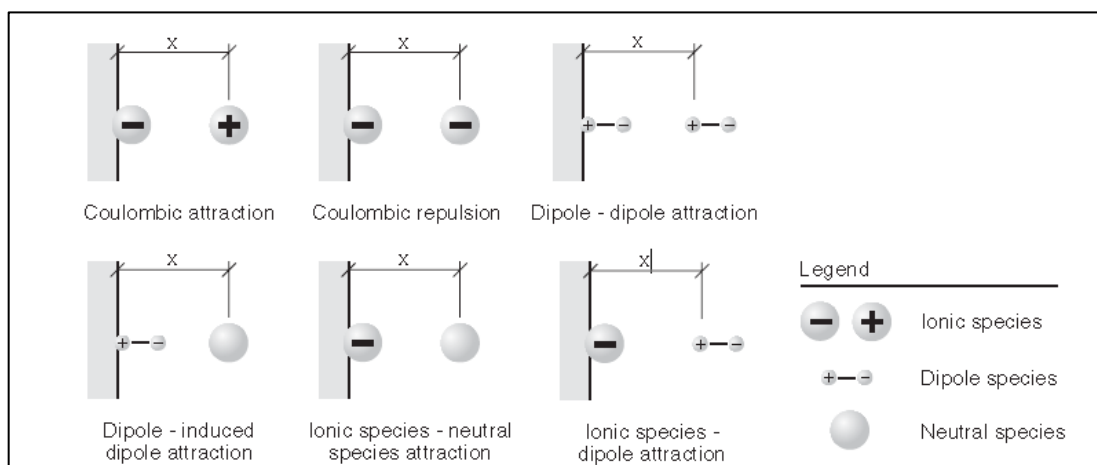
Figure 2.7. Surface functional groups and forces of attraction (Crittenden et al., 2012)

In addition, being more detail on adsorption with respect to ionic species, one class of the chemical bonding to specific surface sites is the acid-base reaction at a functional group. An example is the reaction of hydrated metal ions from solution with hydroxide sites on metal oxides as presented in the reaction of Equation 2.10. For adsorption of ionic species to surfaces, the most important mechanism is electrostatic attraction, which is highly dependent on pH and ionic strength (Crittenden et al., 2012).

$$MeOH_{(aq)} + SOH_{(surface)} \rightarrow SOMe_{(surface)} + H_2O \hspace{2cm} \text{Eq. 2.10}$$
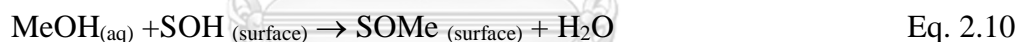
where MeOH is the metal ion adsorbate, and SOH is the hydroxide site on metal oxide adsorbent.

2.5.2. Adsorption kinetic

The kinetic adsorption model is used to demonstrate the rate of adsorbate which is uptake on the metal controls at equilibrium time. The mechanism of sorption process includes chemical reaction, diffusion control and mass transfer were examined by the several kinetic models were used to test experimental data. The Kinetics data are interpreted and discussed by calculating values of enthalpy (ΔH), free energy (ΔG), the energy of activation (E_a) and entropy (ΔS) by using well known kinetics equations. Pseudo-first order, pseudo-second order were applied to study the kinetics of the adsorption process. At the end of the equilibration period, the aqueous-phase

concentration of the adsorbate is measured and the adsorption capacity is calculated by using the mass balance expression in Equation 2.11.

$$q_t = \frac{V}{M}(C_0 - C_t)$$ Eq. 2.11

Where qt is adsorbent-phase concentration of adsorbate along the times (mg adsorbate/g adsorbent), Co is the initial aqueous-phase concentration of adsorbate (mg/L), Ct is aqueous-phase concentration of adsorbate along the times (mg/L), V is the volume of aqueous phase added to bottle (L), and M is mass of adsorbent (g).

a. The pseudo first-order kinetic

The pseudo first-order was used in the equation (Lagergren's equation) to explain adsorption in solid and liquid systems based on the sorption capacity of solids to understand the adsorption rate (Yuh-Shan, 2004). The linear equation predicts this model is explained as shown in Equation 2.12.

$$\log(q_e - qt) = \log q_e - \frac{k_1}{2.303}t$$ Eq. 2.12

Where qe and qt are the adsorption capacity at equilibrium and time, respectively (mg/g), k_1 is the pseudo-first order rate constant(1/min).

b. The pseudo second-order kinetic

The pseudo-second-order rate equation used to examine kinetic equation based on adsorption capacity from the concentration of a solution by analyzing the chemisorption in the solution (Ho, 2006). The Equation 2.13 is expressed the linear pseudo-second-order rate.

$$\frac{t}{q_t} = \frac{1}{k_2 q_e^2} + \frac{1}{q_e}t$$ Eq. 2.13

Where k_2 is the rate constant for pseudo second-order adsorption (mg/gmin) and $k_2 q_e^2$ or h (mg/mgmin) is the initial adsorption rate.

2.5.3. Adsorption isotherm

At equilibrium, adsorption isotherm examined the proposition of sorbate molecules that are partitioned between liquid and solid phases. Two well-known models determine the isotherm process in adsorption technique including Langmuir and Freundlich (Dada et al., 2012) which described as following:

a.   Langmuir adsorption isotherm

Model describes the quantitatively the formation of a monolayer adsorbate on the outer surface of the adsorbent, and after that no further adsorption takes place. Thereby, the Langmuir represents the equilibrium distribution of metal ions between the surface and solution as a reversible chemical equilibrium between species. The Langmuir isotherm is valid for monolayer adsorption onto a surface containing a finite number of identical sites. The model assumes uniform energies of adsorption onto the surface and no transmigration of adsorbate in the plane of the surface. Based upon these assumptions, Langmuir represented the following Equation 2.14.

$$q_e = \frac{Q_0 K_L C_e}{1 + K_L C_e}$$ Eq. 2.14

Langmuir adsorption parameters were determined by transforming the Langmuir equation into form as Equation 2.15.

$$\frac{1}{q_e} = \frac{1}{Q_0} + \frac{1}{Q_0 K_L C_e}$$ Eq. 2.15

Where C_e the equilibrium concentration of adsorbate (mg/L), q_e is the amount of metal adsorbed per gram of the adsorbent at the adsorbent at equilibrium (mg/g), Q_o is maximum monolayer coverage capacity (mg/g), and K_L is Langmuir isotherm constant (L/mg).

Therefore, the value of q_{max} and K_L were computed from the slope and intercept of the Langmuir plot of C_e/q_e versus C_e. The essential features of the Langmuir isotherm may be expressed in terms of equilibrium parameters R_L, which is a unitless constant referred to as separation factor or equilibrium parameter, calculated by Equation 2.16.

$$R_L = \frac{1}{1+(1+K_L C_0)}$$ Eq. 2.16

Where Co is the initial concentration (mg/L), K_L is the constant related to the energy of adsorption (Langmuir Constant). R_L is valued indicates the adsorption nature to be either unfavourable is $R_L<1$, Linear if $R_L=1$, favourable if $0<R_L<1$ and irreversible if $R_L=0$. The graph of the adsorption capacity with a concentration in equivalents is represented in Figure 2.8.
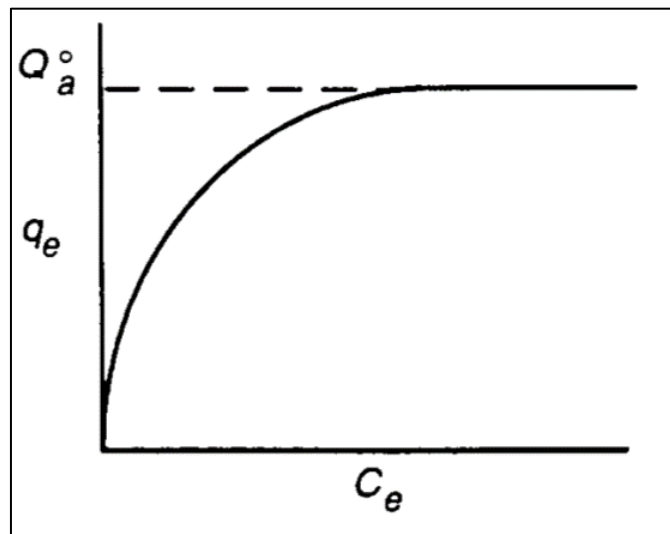
Figure 2.8. Langmuir adsorption curve (Alexandar S and Pharm M, 2015)

b.   Freundlich Adsorption Isotherm

It is originally an empirical model which is the first known relationship describing the non-idea and reversible adsorption, not restrict to the formation of monolayer and apply with multilayer adsorption with non-uniform distribution of adsorption heat and affinities over the heterogeneous adsorbents (Freundlich, 1906). Historically, its equation can be derived using the Langmuir equation to describe the adsorption onto sites of a given free energy and considering the following assumptions including the site energies for adsorption follow a Boltzmann distribution and the mean site energy is ΔHMo , and the change in site entropy increase linearly with increasing site enthalpy $-\Delta H_{ado}$ and the proportionality constant (Crittenden et al., 2012). The equation was illustrated as following Equation 2.17.

$$q_e = K_f C_e^{\frac{1}{n}} \qquad \text{Eq. 2.17}$$

Where K_f is Freundlich isotherm constant (mg/g), n is adsorption intensity, Ce is the equilibrium concentration of adsorbate (mg/L), and q_e is the amount of metal adsorbed per gram of the adsorbent at equilibrium (mg/g). In addition, the linear equation can be derived as Equation 2.18.

$$\log q_e = \log K_f + \frac{1}{n} \log C_e \qquad \text{Eq.}$$

2.18

The constant K_f is an approximate indicator of adsorption capacity, while 1/n is a function of the strength of adsorption in the adsorption process. If n=1 then the partition between the two phases are independent of the concentration. If the value of 1/n is below one, it indicates a normal adsorption. However, if the 1/n is higher than one, it indicates the cooperative adsorption (Dada et al., 2012). As the temperature increases, the constants K_f and n reflectively change the empirical observation that the quantity adsorbed increases more slowly and higher pressures are required to saturate the surface. Where K_f and n are parameters characteristic of the sorbent-sorbate system, that must be determined by data fitting and whereas linear regression is typically used to determine the parameters of kinetic and isotherm models. The curve can be plotted with adsorption capacity and concentration is represented in Figure 2.9.
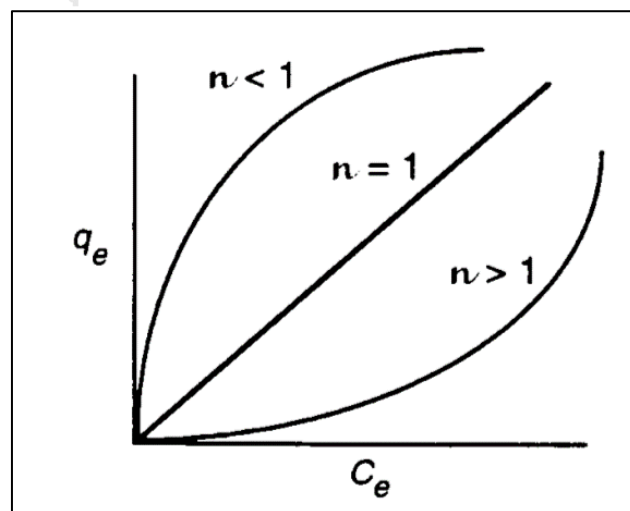
Figure 2.9. Freundlich isotherm curve (Alexandar S and Pharm M, 2015)

2.5.4. Adsorption experiment procedures

a.   Batch adsorption experiment

The batch adsorption process was developed by starting with the isotherm plotting graph as shown in Figure 2.10. that illustrated a typically equilibrium graph plotted between adsorbate concentrations of adsorbed per gram of adsorbent and in the aqueous phase, respectively at equilibrium (C_e). Basically, maximum adsorption of pollutants on a particularly adsorbent can be achieved by optimizing various parameters of adsorption. Adsorption batch experiments can be carried out the kinetics which is also a very important step to understand the adsorption mechanism
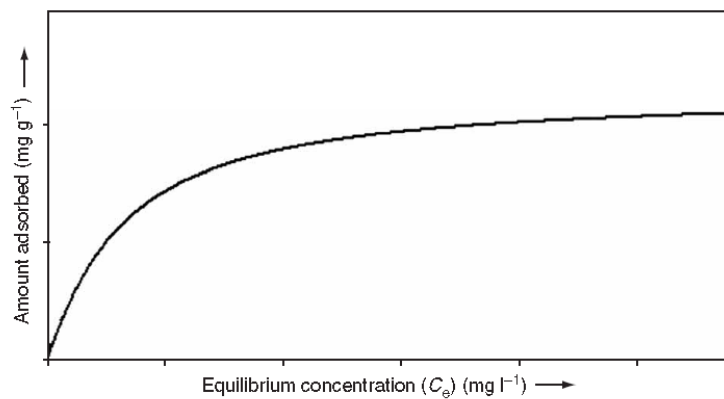
and to design columns on laboratory, pilot and industrial scales (Ali and Gupta, 2006).

Figure 2.10. A typical batch adsorption isotherm indicating equilibrium stage at Adsorption (Ali and Gupta, 2006).

b.   Column adsorption experiment

Ali and Gupta (2006) has pointed out that the optimized conditions of adsorption are determined by batch experiments, these can be transferred to column operations. The designing of a column starts with laboratory testing to determine the breakthrough capacity. A mass transfer zone is formed in the column bed by passing contaminated water through. The depth of this zone is controlled by the characteristics of the adsorbent, pollutants and hydraulic factors. The depth of the mass transfer zone is a measure of the physical and chemical resistance to mass transfer. This zone moves down and reaches the bottom of the column, where pollutant concentrations and

breakthrough point of the column occurs. This situation is illustrated in Figure 4. The breakthrough curve is idealized by the assumption that the removal of the pollutants is completed over the initial stages of operation. The breakpoint is chosen considerately at some value, C_b for the effluent concentration. At considerately selected effluent concentration, C_x closely approaching C_o which is the sorbent by considering to be importantly exhausted. Total mass quantity of effluent V_b is passing per unit cross-section at the break point, and the nature of breakthrough curve (between the values of V_b and V_s) are used for design purposes. The primary adsorption zone in the fixed bed adsorbent is that part of the bed where there is a concentration reduction from C_x to C_b. It is assumed to be of constant length (L_m) as seen in Figure 2.11. Total time x related for primary adsorption zone formation maybe calculated by Equation 2.19.

$$t_x = \frac{V_x}{F_m}$$

<div align="right">Eq. 2.19</div>

Where F_m is the mass rate of flow to the adsorbents expressed as mass per unit time per unit cross-sectional area of the bed. The fractional capacity (f) of the adsorbent at breakpoint may be calculated by Equation 2.20.

$$f = \int_0^1 \left[1 - \frac{C}{C_0} \right] d \left[\frac{V_e - V_b}{V_x - V_b} \right]$$

<div align="right">Eq. 2.20</div>

Moreover, the percent column saturation at the breakpoint is given by the Equation 2.21.

$$\% saturation = \frac{[D + L_m(f-1)]}{D}$$

<div align="right">Eq. 2.21</div>

Where D is adsorbent bed depth (mm)
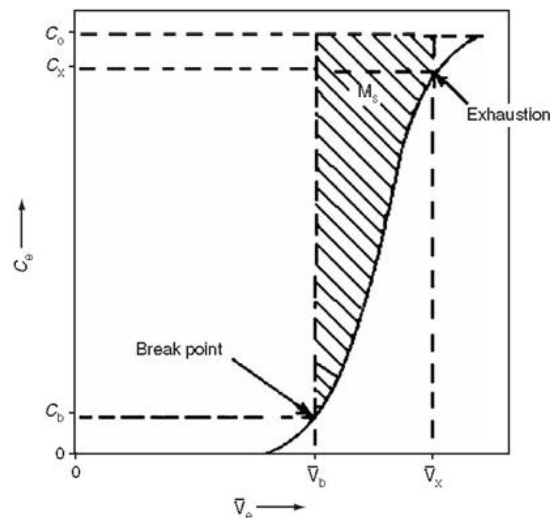
Figure 2.11. A typical column breakthrough curve (Ali and Gupta, 2006)

2.6. Adsorbent properties

2.6.1. Iron oxide particle

The chemical compositions of iron oxide include iron and oxygen which is presented in the environment and locality. Typically, iron forms as Fe^{2+} and Fe^{3+} in the iron oxide material which are magnetic. There have 16 iron oxides composition such as ferric oxide (Fe_2O_3), magnetite (Fe_3O_4), maghemite (γ-Fe_2O_3), hematite (α-Fe_2O_3), ferrihydrite ($Fe_2O_3.0.5H_2O$), hydratediron(III) oxide (Fe(O)OH), goethite (α-FeO(OH)), akaganeite (β-FeOOH), lepidocrocite (γ-FeOOH), feroxyhyte (δ-FeOOH) and limonite (FeO(OH).nH_2O) are well known iron oxide derivatives. The point of zero charge pH_{PZC} of iron oxides was in 6 to10 (Cornell and Schwertmann, 2003). If in aqueous solution have pH value lower than pH_{PZC} of iron oxide, the surface hydroxyl sites could be protonated and positively charged. Unlike, the active sites are deprotonated when the solution pH is higher than pH_{PZC}, resulting in negatively charged sites and the adsorption of metal cations on iron oxide could possibly take place via electrostatic interaction with the negatively charged sites on iron oxide surface (Koretsky, 2000).

The study focused on the iron oxide with sand filtration by Thirunavukkarasu et al. (2003) shown that the surface area of iron oxide coated with sand filtration was in the specified range of goethite and hematite that suggested that the iron oxide was

probably a combination of goethite and hematite. Moreover, the possible reaction happened which is made the goethite and hematite as Equation 2.22, 2.23, 2.24, and 2.25.

$$2\ Fe(NO_3)_3.9H_2O + 2\ H_2O \rightarrow 2\ Fe + 6\ HNO_3 + 17\ H_2O + 1.5\ O_2 \qquad Eq.\ 2.22$$

$$2\ Fe + 6\ HNO_3 + 17\ H_2O + 1.5\ O_2 + 4\ NaOH \rightarrow 2\ Fe(OH)_2 + 2\ HNO_3 + 4\ NaNO_3 + 19\ H_2O + 0.5\ O_2 \qquad Eq.\ 2.23$$

$$2\ Fe(OH)_2 + 2\ HNO_3 + 4\ NaNO_3 + 19\ H_2O + 0.5\ O_2 \rightarrow (dehydration) \qquad Eq.\ 2.24$$

$$\alpha Fe_2O_3 + 2HNO_3 + 21H_2O + 4NaNO_3, \alpha\text{-}FeOOH + 2HNO_3 + 20H_2O + 4NaNO_3 \quad Eq.\ 2.25$$
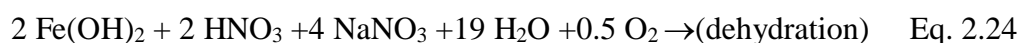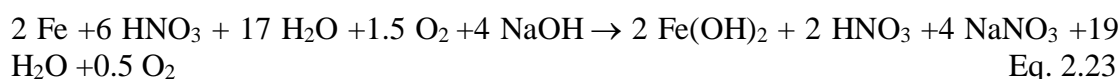
The adsorption is specific, which may involve the replacement of surface hydroxyl groups by the adsorbing ligand. The reactions between arsenic species and goethite may be represented by Equation 2.26 and 2.27.

$$\alpha\text{-}FeOOH + H_2AsO_4^- + 3\ H^+ \rightarrow FeH_2AsO_4 + 2\ H_2O \qquad Eq.2.26$$

$$\alpha\text{-}FeOOH + H_3AsO_3 + 2\ H^+ \rightarrow FeH_2AsO_3 + 2\ H_2O \qquad Eq.2.27$$

2.6.2. Nano iron particle

Small sized metal oxide particles (iron oxides nanoparticles) have a large surface area, higher active sites, and magnetic characteristic, make them potentially technology for remediation pollution from water typically from 1 to 100 nm of diameter size. In solution, the iron oxide nanoparticles are largely diffusion with particle sizes of less than 40 nm. Iron oxide nanoparticle such as Fe_3O_4 or $\gamma\text{-}Fe_2O_3$ and ferrites are commonly used in an aqueous medium which chemical reaction of formation as Equation 2.28.

$$M^{2+} + 2\ Fe^{3+} + 8\ OH^- \rightarrow MFe_2O_4 + 4\ H_2O \qquad Eq.\ 2.28$$
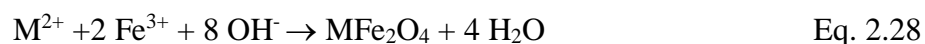
Where M can be Fe^{2+}, Mn^{2+}, Co^{2+}, Cu^{2+}, Mg^{2+}, Zn^{2+}, and Ni^{2+}. The Magnetite nanoparticles (Fe_3O_4) are not stable under atmospheric condition. The mean diameter of Fe3O4 nanoparticle ranged from 9 to 37 nm which the percentages of ferrous ions is depended on the total iron ion raised from 33 to 100 %. (Faraji, Yamini, and Rezaee, 2010). Specially, the iron oxides nanoparticles were functionalized with dimercaptosuccinic acid to remove heavy metals successfully. The nanoparticles have the usefully high surface area of 114 m^2/g, particles sizes of 5.8 ± 0.9 nm, and

magnetic collectability under a suitable condition (Yantasee et al., 2007). Unfortunately, due to the particles size is a too small dispersion in solution highly, the coated process was used to develop adsorbents such as Fe_3O_4 coated with humid acid to remove heavy metals in water (Liu, Zhao, and Jiang, 2008).

2.6.3. Previous researches on the adsorption process

As mentioned in the previous section, day by day the modification of low-cost adsorbents has been investigated to remove heavy metals such as arsenic, iron and manganese is common sense in groundwater and wastewater. However, the adsorption process typically effected by the initial concentration of pollutants, pH, sorption capacity, adsorbent dose, contact time, specific area, the pore size of adsorbent. Therefore, this section was carried out the research studies which have been focused on the adsorption process generated with low-cost adsorbent and iron oxide coated sand particles to remove arsenic, manganese, and iron that focused on the mechanism and their affectivity.

Mondal et al. (2008) have investigated the arsenic removal presence with Mn and Fe in groundwater simulation by comparing between granular active carbon (GAC) and Fe3+ impregnated with GAC. They studied on the effect of adsorbent dose, particles size and initial concentration of arsenic. The experiment selected the pH about 7 in a neutral condition, and adsorbent dose 0 to 40 g/L, particle size 2 to 4 mm, and initial concentration of arsenic ranges from 0 to 3200 µg/L. After the adsorption process was done, they generated with the 0.45 µm membrane filter. Again, the adsorbent dose was affected by the removal efficiency of arsenic by their surface-active site. They have found that the GAC-Fe have specific area site higher than GAC. It caused to removal efficiency higher in the optimal value 8 g/L and 24 g/L of both adsorbents that used SEM for morphology and X-ray a Thermo FTIR. For Fe and Mn removal, 98 % and 99 % of removal were achieved, by using GAC and GAC-Fe with an adsorbent dose of 24 g/L and 8 g/L, respectively. Fe^{3+} form as negatively charged was obtained on GAC-Fe and Mn and Fe also removed by precipitation. Moreover, particles size does not create the surface pore size, so it is not affected by Arsenic removal. However, Mn and Fe were adsorbed by physical adsorption mechanism

better than chemical adsorption. The initial concentration of the arsenic is the most effected by constant adsorbent dose 8 g/L to 24 g/L. the optimal value of the initial concentration of arsenic is lower than 500 µg/L in term of surface coverage and As (III) species is oxidized to be As (V) fast in the simulation. Conversely, Fe removal is not affected by the initial concentration of As. They have found that only Mn removal was performed high, when initial arsenic increase. The amount of 8 g/L of GAC-Fe possibly removes 95% of the initial concentration of arsenic about 200 µg/L   In sum up, GAC-Fe impregnation is very effective adsorbent for heavy metal removal. Therefore, this research gap is not mentioned in a contact time of adsorbent with pollutants and adsorption capacity.

Yin et al. (2017) have found low cost adsorbent which is the porous charred granulated attapulgite-supported hydrate iron oxide for removal arsenic. This research has studied on the effect initial of iron concentration on arsenic sorption of charred GAP, adsorbent dose, pH, co-exiting anion such as SO_4^{2-}, HCO_3^- and PO_4^{3-}, and the reusability of adsorbent in batch and column fixed test experiment. Physical and chemical components of the Fe modified charred GAP include 1 to 2 mm of particle size, 52.2 m^2/g of surface area, 0.177 cm^3/g pore volume, 14.6 nm of average pore diameters in 8.33 of pH_{pzc}. Arsenic species are changed form in different pH, so they have pointed the pH value which is suitable for arsenic removal is 5 to 9 indicated the removal efficiency increase dramatically while the initial arsenic concentration is 20 mg/L. For the batch experiment, pH is 7 for isotherm and kinetic model. For Adsorption kinetic, the temperature is 25 °C, arsenic solution 5, 20, 100 mg/L, adsorption dose 10 g of Fe modified charred GAP. Moreover, Adsorption isotherm was used the 0.50 g of Fe modified charred GAP to remove initial arsenic concentration range 0.05 to 200 mg/L. After that the water flows into the 0.45µm membrane filtration. As a result, the Fe modified charred GAP dose was selected at the optimum values 20 g/L to 40 g/L at 1 mg/L and 10 mg/L of arsenic concentration, respectively. The study has found that the adsorbent ability for arsenic removal about 78% within using 1 mol/L of adsorbent. The presence of anion does not potentially affect the arsenic removal except PO_4^{3-}. This adsorbent can reuse by using NaOH regeneration.

Hu et al. (2015) have worked to remove the arsenic that co-exiting with anion by using adsorption process with iron nanoparticles impregnate with biochar. The batch and column test was examined in this study. Again, this study selected the pH was varied from 5.8 ± 0.2 by adjusting NaOH. For the batch experiment, the adsorbent was added 0.1 g at 20 ± 2 $^{\circ}$C, arsenic concentrations between 0.1 and 55 mg/L, and co-existing anions are 5 mg/L of SO_4^{2-}, NO_3^-, and Cl^- and 5 and 50 mg/L of PO_4^{3-}, on arsenic 5 mg/L. For the column test, 5 mm of the column was measurable about 1 g of the test biochar adsorbents, and 0.5 to 0.6 mm of the average size of sand. The pH keeps the same as batch test. The isotherm model such as Langmuir, Freundlich and Temkin isotherm were applied in this research. As a result, the Langmuir isotherm indicated that the maximum capacity of the adsorbent is 2.36 mg/g and K_L is 2.36 L/mg. Likely, Freundlich and Temkin isotherm which are used to understand chemisorption described that arsenic was adsorbed by Fe impregnated biochar by chemisorption. This study has focused on the arsenic capacity sorption which 2.16 mg/g was carried out and the initial concentration of arsenate is 0 to 55 mg/L. The Fe-impregnated biochar is 3.88%. For this adsorbent the specific was not the main parameters. About 85 % of arsenic initial concentration was removed by this process.

Babaee, Mulligan, and Rahaman (2018) have been studied on arsenite and arsenate by using new adsorbent Fe/Cu nanoparticle in term of removal efficiency that effect of different parameters including adsorbent dose and initial concentration. The experiments were conducted in the batch test. By using 50 mL of centrifuge tubes, pH 7, 100 and 10 mg/L of the initial concentration of arsenite and arsenate, respectively which is prepared in 1 L of DI water for the batch test. To understand the effect of contact time, 48 hours of contact time have applied with an initial concentration of As (III) 100, 500, 1000 µg/L and 50 mg/L of nanoparticles. Arsenic influence and effluent were measured by using ICP-MS methods. Fe/Cu nanoparticles were characterized by their physico-chemicals properties by X-ray diffraction (XRD), transmission electron microscopy (TEM), and Brunauer Emmett-Teller (BET) surface area. The result of this study has shown that Fe_2O_3, CuO were obtained, particle diameter ranges from 4 to 22 nm with an average size of 13.17 nm, and BET surface area of 79.5 m^2/g higher than granular iron approximately 40 times. As a result, by

using 100 mg/L of nanoparticles, the effect of the initial arsenic concentration of 1000, 500, and 100 μg/L on removal efficiency is 69%, 78%, 80 % of removal As(III), and 89%, 96%, and 97% of removal As(V), respectively. Thus, the adsorbent dose is related to the arsenic removal. Moreover, pH also effects on the arsenic removal in ranges from 4 to 11. The presence of coexisting ions such as PO_4^{3-}, SO_4^{2-}, and CO_3^{2-} have no effect on adsorption capacity for decreasing arsenic concentration. Therefore, the synthesis of nanoparticles by using the reduction method that is the easy technique, was successfully for arsenic removal.

Asmel et al. (2017) have researched on the arsenic removal in adsorption process by using nano iron ion enrich material (NIIEM) super adsorbent. In their study, both arsenic species As(III) and As(V) was added in 100 mg/L of each at pH of 2.5. They have investigated the effect of adsorbents dose from 0.5 to 40 mg of mass NIIEM at equilibrium time 24 hours in batch test in 1 mg/L of arsenic. After that, they have varied the contact times form (0, 1, 2, 4, 8, 16 and 24 hr) with rotary shaker 200 rpm and suspensions to 6000 rpm for 10 minutes before filtration. The effect of pH and initial concentration of Arsenic have investigated in a range of 2 to 13, and 10 to 100 mg/L, respectively. As a result, the adsorbent dose of 40 mg/L is possibly removed about 97 to 98 % of As (III) and As(V), respectively. In effect of beyond neutral pH onto adsorption NIIEM is indicated that significantly increased on arsenic removal and while pH range 3.5 to 10 results the same remaining of a decrease in arsenic removal by positively charged surface species of adsorbent. The cost analysis also determined and analyzed for pollutant remediation approximately 0.284 US$/kg and 1.630 US$/kg of adsorbents.

Benjamin et al. (1996) have been worked on an iron oxide coated on the sand to treat heavy metals on water treatment. There have been two types of iron oxides coated with sand as the low-cost adsorbents that are divided by difference coated methods running in the conventional filtration process. The heavy metals have been studied such as Cu, Cd, Pb, Ni, and Zn and its complexation. In process treatment operation, pH was changed from 8, 9 and 10 in different conditions such as uncomplication and complexed of metals cations. As results, the soluble heavy metals Cu, Pb, and Cd were typically reduced about 80%, 90%, and 98%, respectively while the removal

efficiency of these three metals complexity is 99%. The reason for high efficiency removal is responded by the mechanism of adsorption and filtration between heavy metals and adsorbents in majority happen in accidental treatment. The study is concluded that the process was a success to remove these heavy metals in simultaneous and individual contaminated in water or wastewater.

Day by day, the iron oxide coated sand has been developed and modified to be low cost adsorbent for heavy metals and toxicity pollutants removal from water. V. Gupta et al. (2005) have been investigated the research on adsorption of arsenic by using iron oxide coated sand and uncoated sand as an adsorbent. The study has found that the effect of initial pH in water about 5 to 7.6, which is carried out the arsenic removal greater than 95%. The optimal pH is 7.5 can uptake the arsenic concentration of 400 μg/L by using iron oxide coated sand and uncoated sand. Unlike, uncoated sand is pursued about 10% of arsenic removal. Otherwise, the effect of contact time was studied on 20 to 180 minutes. Caused by contact times, the study has pointed that the maximum removal of 93% was achieved at the end of 180 minutes. The adsorption plays important roles by pore diffusion which is effect to rate reduction. Moreover, it caused by the mass transfer between the initial and final stages of the adsorption process. Focusing on dose concentration effective, the range from 5 to 20 g/L has been investigated in this research. As result, the 20 g/L achieved arsenic 94 %, and 12.5 % removal efficiency, operated with iron oxide coated and uncoated sand, respectively. For column study, the effect of filtration rate is 4mL/min highly adsorb 94 % of arsenic by iron oxide coated sand. This studied has not been a focus on the adsorbent regeneration.

Deka and Bhattacharyya (2018) have been conducted the research on the adsorption process to remove iron in the water. This study has been purchased with the influence of contact time, pH, initial metal ion concentration, and adsorbent dosage on the rate of iron removal. The synthetic adsorbate solution in water was prepared from anhydrous FeCl$_3$. It weights about 162.21g to dissolve FeCl$_3$ in distilled water for each required ferrous concentration. For contact time about 60 to 120 minutes for sand and dust/sand, respectively, are examined with the initial concentration of 50 mg/L and normal pH. For the pH effect, during the pH increase to 4, the result was

successfully demonstrated that 94 and 98 % iron removal sand and dust/sand adsorbents, respectively. In term of dose concentration, the 1 to 5 g/L has been investigated because of a large surface area iron adsorbed.

2.6.4. Effect sulfate on adsorption process

Effects of sulfate on As(V) and As(III) sorption may have derived from different experimental conditions. Decreased sorption of both As(V) and As(III) on hydrous ferric oxide were reported in the presence of sulfate from pH 4 to 7. In alkalinity condition, the effect of sulfate has been reduce (Su and Puls, 2001). Moreover, during concentration of sulfate presence in water increase, arsenic removal decreased due to the amount of iron precipitated also increase by changing the surface properties of the ferric oxyhydroxide precipitates. It was competition for adsorption sites with sulfate onto iron precipitates adsorption (Kong et al., 2017). Moreover, the effect of sulfate decreases markedly with increasing pH and is slightly more pronounced at the lower total As(III) concentration (Wilkie and Hering, 1996). According to Jeong, Fan, et al. (2007) explained that the As(V) adsorption isotherm curves were hardly affected by lower concentrations of sulfate, however; the isotherms illustrated moderate decreasing trends with the higher of sulfate concentrations. The effect of sulfate on the adsorption of cadmium was determined for different sulfate concentrations and various ionic strength. The effect of sulfate is to increase cadmium adsorption. This increase is positively correlated to the sulfate concentration. The effect of sulfate on heavy adsorption can partly be attributed to changes in electrostatic conditions as results of sulfate adsorption, and for the other reason, this effect can be explained by the formation of ternary surface complexes (Hoins, Charlet, and Sticher, 1993). Therefore, sulfate presence in water has potentially affected to adsorption process on heavy metals removal.

2.6.5. Summary

This part demonstrates in the summary of the previous researches on heavy metals removal by adsorption process in different adsorbents iron existing. Table 2.5

represents the adsorbent types, pollutants, pH operation, adsorption dosages, co exiting ion and removal efficiency.

Table 2.5. Summary the previous research by using adsorption process

Adsorbents	Pollutants	pH	Adsorbent dosage(mg/L)	Co-ions existing	Removal efficiency
GAC/Fe^{3+} Impregnated with GAC	As, Fe, Mn	7	800 and 2400	-	95%, 98 % and 99 %
Fe Charred GAP	As	5 to 9	20000 and 40000	SO_4^{2-}, HCO_3^- and PO_4^{3-}	78%
Nano Impregnated iron with biochar	As	5.8 ± 0.2	10	SO_4^{2-}, NO_3^-, Cl^- and PO_4^{3-}	85%
Fe/Cu nanoparticle	As (III), As (V)	7	50	PO_4^{3-}, SO_4^{2-}, and CO_3^{2-}	69%, 78%, 80 % As (III), 89%, 96%, and 97% (As(V)
Nano iron ion enrich material (NIIEM)	As	2 to 13	40	-	97 to 98 %
Iron oxide coated on sand	Cu, Zn, Cu, Cd, Pb, Ni, Cu, Zn	8, 9 and 10	12.4, 0.6 to 4.0, 5 each, 0.1 to 0.9 0.2	-	80%, 90%, and 98%, 99% of H.M complexation
Iron oxide coated sand and uncoated sand	As	5 to 7.6	5 to 20	-	94 %, and 12.5 %
Sand and Dust/sand	Fe	4	1 to 5	-	94 and 98 %

CHAPTER 3
MATERIALS AND METHODS

3.1. Study overview

This section describes an overview of methodology in this study. The first objective of this research work was to investigate the removal behavior of heavy metals in synthetic groundwater using the iron oxide coated sand (IOCS) and iron oxide particle as adsorbents. The adsorbents doses and its equilibrium were obtained from a batch test in the presence of single and combined heavy metals such as arsenic, iron, and manganese. After that, to reach the second objective, the effect of initial concentration of sulfate in groundwater was studied by using optimal adsorption capacity that was obtained from first experiment. Lastly, the leachability test was studied on both adsorbents for answering the third objective. The study overview is portrayed in Figure 3.1.

Heavy Metals Adsorption in Simulated Groundwater Using Iron Oxide Particles and Iron Oxide Coated Sand

Groundwater pollutants
- Hardness (320 mg $CaCO_3.L^{-1}$) , pH=8 ± 0.5
- Mn (15 $mg.L^{-1}$), As (500 $\mu g.L^{-1}$), Fe(10 $mg.L^{-1}$), Combined heavy metals

Adsorbents synthesis
- Iron oxide particles
- Iron oxide coated sand
✓ Sieve analysis, SEM-EDS, XRF

1st objective

Adsorption experiments
✓ Varied both adsorbents dosages
✓ Varied time

- Optimal adsorbents doses
- Equilibrium
- Best fit Kinetic models
- Best fit isotherm models

2nd objective

SO_4^{2-} effect on adsorption experiment
✓ Varied sulfate (SO_4^{2-})
✓ Optimization of adsorbent dose

- Effect of SO_4^{2-} on heavy metals adsorption removal

3rd objective

Leaching experiment
✓ Leaching adsorbents dosage optimal

- Leachability of adsorbents

Legend
-Process
-Outputs

Figure 3.1. Framework of study overview of the research study

จุฬาลงกรณ์มหาวิทยาลัย

CHULALONGKORN UNIVERSITY

3.2. Experimental set-up

In this research, the experiment carried out in the batch test. The study conducted in 1 L beaker at ambient temperature. The condition of Jar testing was performed at 130 rpm (revolution per minute) agitation until achieved equilibrium (Figure 3.2).
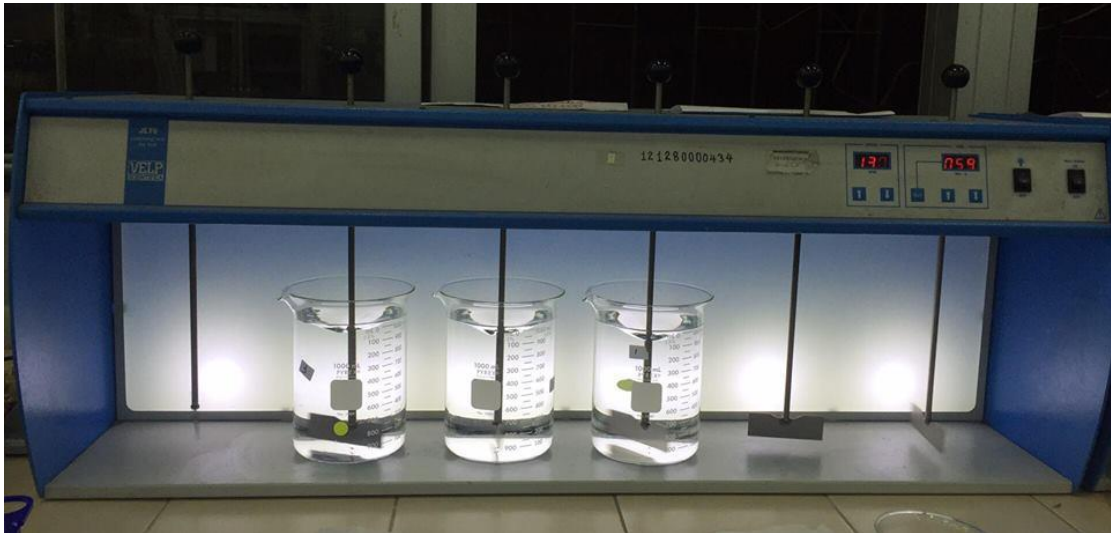
Figure 3.2. Jar test apparatus for batch adsorption experiment

3.3. Materials and equipment

3.3.1. Apparatus

The apparatus employed for adsorption experiment, and equipment's for analyzing parameters in synthetic groundwater including:

- Beaker 1 L: was used to contain the sample for an experiment in every batch test.
- Jar test apparatus: Model of Twister JR D-Series Multi-positions with 6 paddles (6D) will be used for operating in Jar test as a mixing o 130 rpm. The model dimensions are 235 x 1125 x 400 mm of width, length, and height. The roller size (L x H) is 75 length x 25 mm axial.
- pH meter: The pH meter model METTLER-TOLEDO was used to measure the pH and temperature of the solution.
- A scanning electron microscope and energy dispersive X-ray Spectrometer (SEM-EDS) model (JEOL, JSM-7610F and Oxford, X-MaxN 20): EDS

function in SEM was used to look at metal composition on the iron-coated sand, iron oxide particle surface, and on the pure sand surface. The SEM will be Scanning electron micrograph of iron oxide particles and iron oxide coated sand at magnifications of 500X and 5000X.

- X-ray fluorescence (XRF), model (Rigaku Supermini200): was used to analyze the chemical composition of adsorbents, detection limit 10 g of samples.

- Inductively coupled plasma optical emission spectroscopy (ICP-OES) is applied to measure the initial and final concentration heavy metals of water with the detection limit are 5 μg/ L of As, 0.05 μg/ L of Mn and 0.01 mg/ L of Fe.

- Stopwatch: was used to determine the adsorption time for running all experiments.

- Sieve: is used for the sieve analysis to get the sand for the experiment by using opening size such as 4.750, 2.800, 2.000, 0.710, 0.425, 0.300, 0.150, and 0.075 mm and pan.

- Balance was used to weight of amount adsorbents, chemical substances and waste after adsorption with detection limit at 0.1 mg and maximum at 220 g.

- The oven was used to dry the sand and iron oxide particles and iron oxide coated sand in the process of sieve analysis and coating.

- Pipet 10 mL was used for sampling stock for groundwater preparation.

- Syringes filters with 0.45 μm of membranes was used to take all samples for analysis.

- Multi RS-60 programable rotator was used for leaching test to rotate solution.

- Centrifuge tubes 25 mL was taken for keeping samples.

3.3.2. Chemical reagents

All solution in this study was prepared with the chemical reagents which bought from commercial grade. It used for a stock solution that portrays as follow:

- Sodium arsenate dibasic heptahydrate ($Na_2HAsO_4.7H_2O$) was used to generate arsenate in groundwater.

- Ferrous chloride tetrahydrate ($FeCl_2.4H_2O$) was used to generate ferrous in groundwater as pollutants sources.

- Manganese (II) chloride tetrahydrate ($MnCl_2.4H_2O$) was generated the manganese.

- Hardness calcium carbonate ($CaCl_2$) was generated the hardness contaminated in water.

- Sodium hydroxide (NaOH) was used to examine the pH in water.

- Hydrochloric acid (HCl) was used to generate the pH in water.

- Ferric nitrate $Fe(NO_3)_3.9H_2O$ was used to generate the iron oxide coated particle adsorbent.

- Milling cast iron were used to the adsorbent sources to prepare the iron oxide.

- Nitric acid (HNO_3) was used to preserve samples before ICP-OES analysis.

- Sodium sulfate salt (Na_2SO_4) was prepared for conducting the optimal initial concentration of sulfate.

- Sodium bicarbonate ($NaHCO_3$) was used as a buffer in groundwater to maintain pH in water.

- Acetic acid (CH_3COOH) was examined in the leaching test for making the acid condition of heavy metals extraction.

- Sand was examined the iron oxide coated sand as an adsorbent. Sand bought from The Concrete Products and Aggregate Co., Ltd. (CPAC) company, Thailand.

These chemical reagents and materials are described in Table 3.1 of each part utilization.

Table 3.1. Chemical reagents and material utilization in the study

Synthetic Groundwater Composition	
RO: Reverse osmosis water	Arsenic: Sodium Arsenate ($Na_2HAsO_4.7H_2O$)
Iron: ($FeCl_2.4H_2O$)	Manganese: $MnCl_2.4H2O$
Hardness: Calcium cloride ($CaCl_2$)	Sulfate: Sodium Sulfate salt (Na_2SO_4)
pH: hydrochloric acid and (HCl) and Sodium Hydroxide (NaOH)	Buffer: Sodium bicarbonate ($NaHCO_3$)
Adsorbents Synthesis	
Ferric nitrate: $(Fe(NO_3)_3).9H_2O$	Cast Iron steel
Analytical method	
Nitric acid: (HNO_3)	Acetic acid: CH_3COOH

3.4. Experimental procedures

Overall, the study was conducted by four main parts to achieve the objectives. Synthesis groundwater contains the As, Fe, Mn, pH, hardness, buffer and sulfate. Firstly, studying adsorbent dose in term of kinetic and isotherm sorption on heavy metals removal the single and a combined heavy metal in the batch test. Then, studying the concentration sulfate presence in groundwater effect to heavy metals treatability as individual and simultaneous heavy metals with optimal adsorption dose. Lastly, the leaching test is applied to leach heavy metals on adsorbents after the treatment process. These experiments were summarized in Figure 3.3.
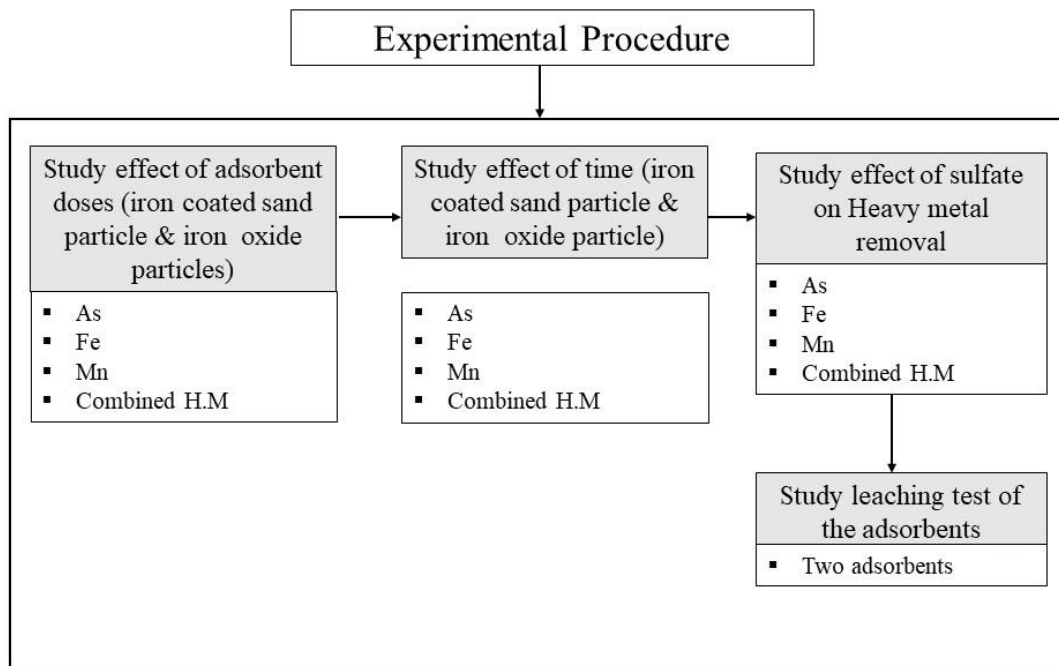
Figure 3.3. The overall framework of experimental procedures

3.4.1. Groundwater synthesis

The feed solution is the results of mixing a concentrated solution of arsenic, iron and manganese with reverse osmosis (RO) water for the batch test.

- Arsenic

Basically, the concentration arsenic was the case study presented as the total inorganic arsenic concentration. It was approximately 500 μg/L. So, the synthesis of arsenic species for the study was decided to choose arsenate as a presence of arsenic pollutants in groundwater. Its solution of chemical was prepared by 500 μg/L by dissolving $Na_2HAsO_4.7H_2O$ of 2.08 mg in deionized water solution with 2% nitric acid to 1 L of RO water.

- Iron

Ferrous chloride heptahydrate ($FeCl_2.4H_2O$) was used as the source of iron in synthetic. The concentration of ferrous containing in the groundwater was set at 10

mg/L of Fe (II). It was generated from $FeCl_2.4H_2O$ about 35.53 mg by dissolving in deionized water in 1 liter.

- Manganese

At the concentration of 15 mg Mn/L in synthetic groundwater was prepared by dissolving manganese (II) chloride tetrahydrate ($MnCl_2.4H_2O$) in RO water. To obtain the desired concentration, 0.053 g of ($MnCl_2.4H_2O$) was dissolved in 1 L of RO water and dilute to desired concentration of Mn.

- Hardness

Calcium chloride ($CaCl_2$) was examined to make the hardness presence in groundwater. Basically, the amount of the hardness contaminated in groundwater 320 mg of $CaCO_3$/L was synthesis 355 mg of $CaCl_2$ to the RO water.

- pH

Based on groundwater quality assessment, pH ranges from 7 to 8. Therefore, in this study focused on pH about 8 ± 0.5 as the maximum pH in groundwater. Sodium hydroxide and hydrochloric acid was employed to adjust the solution pH. The 1 M of NaOH and 1 M of HCl are adjusted into the RO water to synthesize groundwater as a function of pH about 8 ± 0.5.

- Buffer

Sodium bicarbonate ($NaHCO_3$) of 0.5 M was used as a buffer to maintain pH of water in range of 8.0 ± 0.5.

- Sulfate ion

Sodium Sulfate Salt (Na_2SO_4) was prepared for conducting the optimal initial concentration of SO_4^{2-}. The concentration of sulfate ion content from 50, 100, 150 mg/L were synthesized by 73.96 mg/L, 147.91, and 221.88 mg, respectively of Na_2SO_4 dissolved in 1 liter of RO water.

3.4.2. Adsorbents preparation

This part focuses on the methods to synthetic both adsorbents including iron oxide particles and iron oxide coated sand. Raw sand was chosen by using sieve analysis following the ASTM standard method analysis shaker in 15 minutes. Before analysis, sand was dried at 105 °C in 24 hr. After that, dry sand particles about 459.94 g were analyzed at department of Mining and Petroleum Engineering, Chulalongkorn University. Likely IOP, sand was sieve in the same sieve number includes 4, 10, 25, 40, 50, 100, 200 and pan, opening size are 4.750, 2.800, 2.000, 0.710, 0.425, 0.300, 0.150, and 0.075 mm, respectively.

a. Iron oxide particles

Iron oxide particles were obtained from milling cast iron to be small particles at a Mechanical Shop at the Department of Mechanical Engineering, Chulalongkorn University (Janjaroen et al., 2018). Then, sieve analysis was used to get size distribution of iron oxide particle. After that, the chemical components, and morphology at difference magnification X500 and X5000 of iron oxide particle was characterized by XRF model (Rigaku Supermini200), and SEM-EDS model (JEOL, JSM-7610F and Oxford, X-MaxN 20) instrument after this adsorbent was generated.

b. Iron oxide coated sand

Iron oxide coated sand was prepared using the procedure following describes. Firstly, raw sand was washed by acid washed pH of 1 by 0.1 M of HCl in 24 hr, rinsed with RO water and dried in oven at 105 °C to removed heavy metals contaminated on sand. After cleaning, 200 g dried sand was coated by mixing in 2 min with 80 mL of a 2 M (Fe $(NO_3)_3$)9H_2O in order to coated chemical solution on the surface of sand, then dropped 1 mL of 10 M of NaOH into solution and pH of solution is about 2 (Thirunavukkarasu et al., 2003). Then, the mixture was then dried at 110 °C in an oven for 14 hr to volatile HNO_3 from adsorbent from Fe($NO_3)_3$ solution (Benjamin et al., 1996). The coated sand was washed with distilled water until the runoff was clear, dried at 105 °C and store in capped bottles (V. Gupta et al., 2005). To make sure about the iron oxide possible coated on sand as uniform, SEM-EDS model (JEOL,

JSM-7610F and Oxford, X-MaxN 20) was examined the surface morphology of iron oxide coated on the sand. About 10 g of adsorbent chemical composition of iron oxide was characterized by XRF model (Rigaku Supermini200). Again, mass of iron oxide on IOCS was obtained by XRF.

3.4.3. Batch adsorption experiment

Adsorption capacities is one of the adsorption parameters that plays an important role for heavy metals removal. In order to understand the adsorption capacities of IOP and IOCS addition heavy metals adsorption, the concentration of heavy metals at 10, 20, 30, 40, 50, 60 min were after IOP and IOCS analyzed. Then, the kinetic and isotherm adsorption were determined. The testing conditions were set at pH of 8 ± 0.5 and 130 rpm jar test agitation for 1 hr to achieve equilibrium in 1 L beaker. The purpose of this experiment was to determine the optimal adsorbent doses and times for effective treatment of heavy metals. In this study, the effect of sulfate in water was also investigated with the presence of calcium hardness in synthetic groundwater. After sulfate anion at different amount was supplemented to illustrate this effect. The overall batch experiment procedure is described in Figure 3.4**Error! Reference source not found.**.

จุฬาลงกรณ์มหาวิทยาลัย

CHULALONGKORN UNIVERSITY
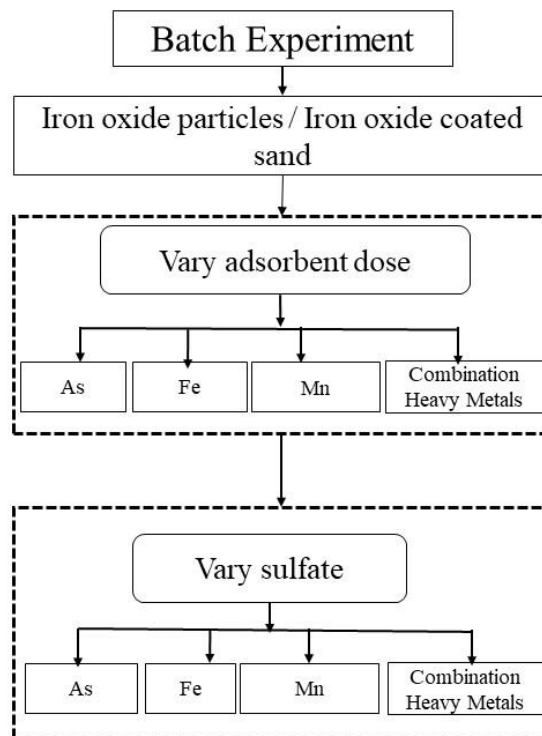
Figure 3.4. The framework of the batch experimental study

    a.   Study the adsorbent doses and contact times in heavy metals removal

The main purpose of this experiment was investigated the optimal condition of adsorbents doses iron oxide particle and iron coated sand particle for each initial concentration of these heavy metal's removal. In this experiment, the primarily study by using synthetic groundwater was contained with the hardness and buffer. The steps experiment was followed by:

➢ Put 1 L of synthesis groundwater into the 1 L of beakers, there have 4 types of synthesis in this experiment which hardness 320 mg of calcium carbonate/L, and buffer maintaining pH 8 ± 0.5 with

- The initial concentration of arsenic 500 μg/L
- The initial concentration of ferrous 10 mg/L
- The initial concentration of manganese 15 mg/L
- The simultaneous initial concentration of the heavy metals (500 μg/L, 10mg/L, 15 mg/L) of arsenic, ferrous, and manganese, respectively.

- ➢ Weight the adsorbents doses vary from 4, 8, 12, 16, 20 and 24 mg of both adsorbents.
- ➢ Then, it was shaken on a rotary shaker at 130 rpm of 1 hr by jar test.
- ➢ The experiment was employed 1 hr of equilibration, initial pH is 8 ± 0.5.
- ➢ The final concentration was sampled after every 10 minutes of the rotary.
- ➢ 10 mL samples were filtered by a 0.45 μm syringe membrane filter prior the fixation by 2% nitric acid. The concentrations of heavy metals in each sample were analyzed by an ICP-OES.
- ➢ Finally, the adsorbent doses optimal appropriate and equilibrium with those initial concentration of heavy metals removal efficiency were obtained to answer first objective of this study based on removal efficiency.

The framework of the experiment study, and the fixed, controlled, and responded parameters were illustrated in Figure 3.5.
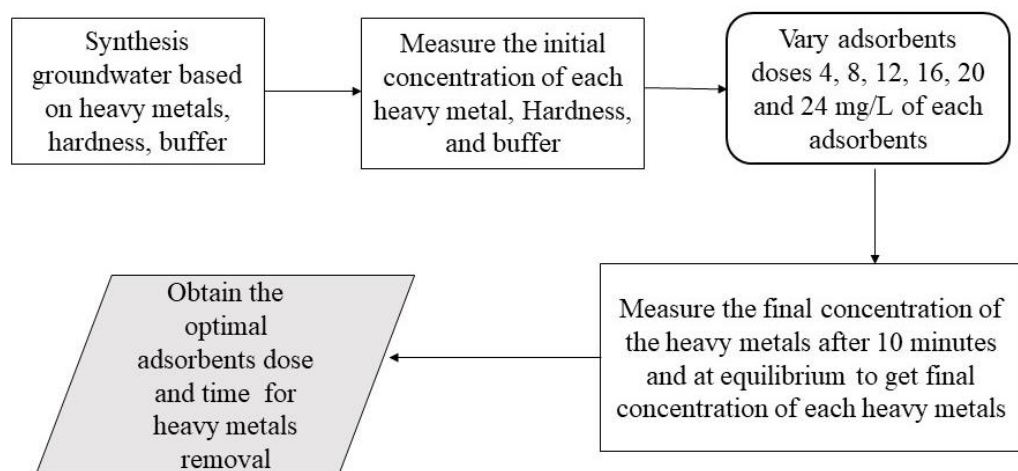
Figure 3.5. Flowchart of study on adsorbents dosages and contact times

The optimal adsorbents dose and times were determined using the parameters described in Table 3.2.

Table 3.2. Study parameters on adsorbents dosages and contact times

Parameters	Name or Value
• Fixed parameter	
Experimental condition (Batch / Cont.)	Batch experiment
Reactor	1 L
Liquid phase	Synthetic groundwater (hardness, buffer)
As	500 μg/L
Fe	10 mg/L
Mn	15 mg/L
pH	8 ± 0.5
Temperature	$30 \pm 2°C$
Equilibrium time	1 hr
Jar test	130 rpm
• Studied parameter	
Adsorbent doses	4, 8, 12, 16, 20 and 24 mg
• Responded parameter	
Directly measured parameter	The final concentration of heavy metals after 10 min
Analytical parameter	% Removal

b.   Study the effect of concentration sulfate in groundwater

The essential point of this experiment part was investigated the effect of initial concentration sulfate to the individual and simultaneous of heavy metals removals efficiency in batch test. In literature, the maximum of initial concentration of sulfate is 176 mg/L is consisted in groundwater sources. Hence, this study will be conducted by varied sulfate containing in specifically range from 50, 100, 150 mg/L. The steps of experiment was followed by:

- ➢ Put 1 L of synthesis groundwater into the 1 L of beakers. There have 4 types of synthesis in this experiment which hardness 320 mg $CaCO_3$/ L, and buffer maintaining the pH 8 ± 0.5.
  - The initial concentration of As (500 μg/L)
  - The initial concentration of Fe (10 mg/L)
  - The initial concentration of Mn (15 mg/L)
  - The simultaneous initial concentration of the heavy metals (500 μg/L,10 mg/L,15 mg/L) of arsenic, ferrous, and manganese, respectively.
- ➢ Put the concentration of sulfate content from 50, 100, 150 mg/L in the synthesis groundwater.
- ➢ Put the optimal adsorbents dose concentration in the previous experiment to 1 L of the backer.
- ➢ Then, it was shaken on a rotary shaker at 130 rpm of 1 hr by jar test.
- ➢ The final concentration was sampled after every 10 min of the rotary.
- ➢ Then sample was filtered by membraned filter 0.45 μm and maintain with 2% HNO_3.
- ➢ Plot the effect of sulfate with heavy metals removal efficiency. It was become the outcomes to obtain the second main objective of this study.

The flowchart of this experiment is shown in Figure 3.6.
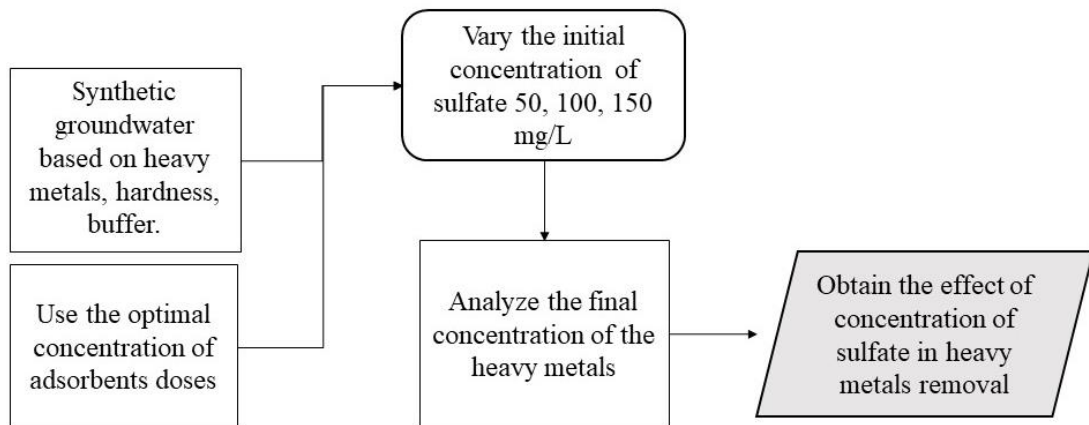
Figure 3.6.Flowchart study effect of sulfate on heavy metals removal

To conduct of the above experiments, the parameters were considered as fixed and responded is shown in Table 3.3.
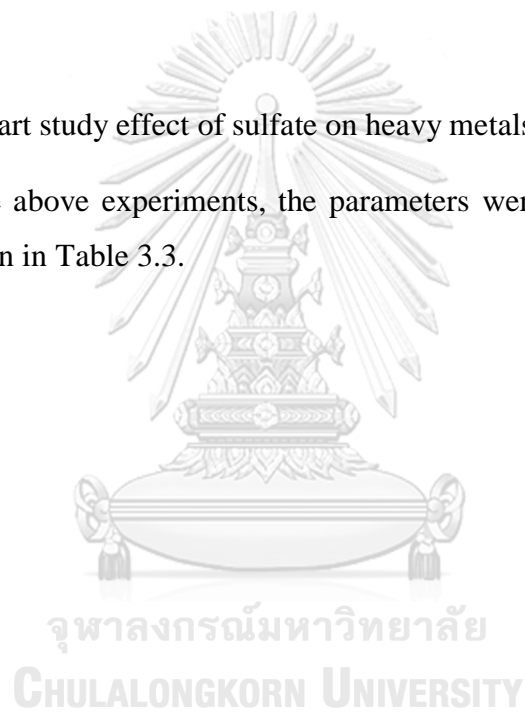
Table 3.3. Parameters for study effect of sulfate in the study

Parameters	Name or Value
• Fixed parameter	
Experimental condition	Batch experiment
Reactor	1 L
Liquid phase	Synthetic groundwater
As	500 μg/L
Fe	10 mg/L
Mn	15 mg/L
Adsorbent dose selected	The optimal dose
pH	8 ± 0.5
Equilibrium time	1 hr
Jar test	130 rpm
• Studied parameter	
Initial sulfate	50, 100, 150 mg/L
• Responded parameters	
Directly measured parameter	The final con. of heavy metals after 10 min
Analytical parameter	% removal

3.4.4. Leaching test

This main purpose of this experiment was examined the possibility of heavy metals leaching from adsorbents. Moreover, this test was followed by batch leaching method namely as Toxicity Characteristic Leaching Procedure (TCLP) (EPAmethod1311, 1992). TCLP required an extraction fluid made of buffered acidic medium to run the test and a direct acid digestion method to carry out for heavy metals determination. The concentration of heavy metals will be answered to third objective of this study. The leaching test using the TCLP method wass described as:

➤ First, adjust pH of buffer acetic acid to obtain pH 2.88 ± 0.05 of solution by adding 5.7 mL of acetic acid (CH_3COOH) to 1 L of RO water.

➤ Then, extract heavy metals from the adsorbents with acetic acid at the solid/liquid ratio of 1: 21 (g: mL).

➤ The suspension contains the heavy metals loaded solid was shaken by rotating at 30 rpm for 18 hr by Multi RS-60 programable rotator.

➤ After agitation, an aliquot was filtered by micro auto-pipet.

➤ Heavy metals concentration was analyzed by ICP-OES.

3.5. Analytical methods

3.5.1. Removal efficiency

The removal efficiency was illustrated by the proportion between the initial and final concentration of heavy metals concentration in the synthetic groundwater in Equation 3.1. The arsenic, iron, and manganese removal efficiency (*%R*) can be determined by the Equation 3.1, where C_i and C_f are the initial and along the time or final concentration of heavy metals concentration (mg/L), respectively.

$$\% R = \frac{C_i - C_f}{C_i} \times 100 \qquad \text{Eq. 3.1}$$

3.5.2. Heavy metals concentration

Analytical methods for determination heavy metals concentration of influence and effluence samples were analyzed by an inductively coupled plasma optical emission

spectroscopy (ICP-OES) techniques. In this study, ICP-OES was used to measure the concentration of heavy metals, followed the standard method. Detection limit are 5 µg/ L of As, 0.05 µg/ L of Mn and 0.01 mg/ L of Fe.

3.5.3. Adsorption models

To study the kinetic this research was used the well-known kinetic models such as pseudo first-order and pseudo second-order model. In addition, in order to investigate mechanisms of heavy metals adsorption on IOP and IOCS, Langmuir and Freundlich models were carried out the adsorption isotherm in this study. These popular models were described in the literatures review part and summarized again in Table 3.4

Table 3.4. Summary of adsorption kinetic and isotherm model equations

Models	Equations
Adsorption capacity	$q_t = \dfrac{V}{M}(C_0 - C_t)$
Pseudo first-order kinetic model	$\log(q_e - q_t) = \log q_e - \dfrac{k_1}{2.303}t$
Pseudo second-order kinetic model	$\dfrac{t}{q_t} = \dfrac{1}{k_2 q_e^2} + \dfrac{1}{q_e}t$
Langmuir isotherm model	$q_e = \dfrac{Q_0 K_L C_e}{1 + K_L C_e}$, or $\dfrac{1}{q_e} = \dfrac{1}{Q_0} + \dfrac{1}{Q_0 K_L C_e}$
Freundlich isotherm model	$q_e = K_f C_e^{\frac{1}{n}}$, or $\log q_e = \log K_f + \dfrac{1}{n}\log C_e$

Where k_1 is the pseudo-first order rate constant (1/min), k_2 is the pseudo-second order rate constant ($mgFe_2O_3$/mg.min), q_t is the number of heavy metals adsorbed at time t (min), K_F and K_L are Freundlich and Langmuir constants, respectively, q_e is the uptake at equilibrium (mg/$mgFe_2O_3$), Ce is the equilibrium concentration (mg/L), q_0

is the initial adsorption capacity (mg/mgFe$_2$O$_3$), and 1/n is the heterogeneity coefficient.

3.5.4. Summary experiments

All amount of experiments conducted in this study was summarized in Table 3.5 which was represents with types of metals reduction, adsorbents types and amount of experiment. The total experiments in this research were about 86 experiments without including the adsorbents preparation test.

Table 3.5. Summary the number of experiments in the study

Test type	Description	Heavy metals	Types of test	Amount of experiment
Adsorbents	Iron oxide particle, Iron oxide coated sand	-	-Sieve analysis, SEM-EDS, XRF	6
Batch test	Study adsorbent dose and contact time	As,Fe,Mn	IOCS,IOP	12
		As	IOCS,IOP	12
		Fe	IOCS,IOP	12
		Mn	IOCS,IOP	12
	Study effect of anion sulfate in groundwater	As,Fe,Mn	IOCS,IOP	6
		As	IOCS,IOP	6
		Fe	IOCS,IOP	6
		Mn	IOCS,IOP	6
Leaching test	Leaching test	As,Fe,Mn	IOCS,IOP	8

CHAPTER 4
RESULTS AND DISCUSSION

This section describes about the results and discussion that responding to the three main objectives of this study. The section was divided into four main results parts including (1) adsorbents synthesis, (2) effect of adsorbents dosage and contact times, (3) effect of sulfate on heavy metals adsorption, and (4) leaching adsorbents results. For more detail each part has sub-result and discussion such as

- Synthetic adsorbents
  - For adsorbent generation: Sieve analysis, Surface morphology by SEM-EDS analysis, Chemical composition by X-Ray Fluorescence (XRF) analysis.
- Effect of adsorbents dosages and times
  - Adsorbent dosages and contact times of heavy metals removal efficiency
  - Kinetic models: Pseudo first-order and pseudo second-order
  - Isotherm models: Langmuir and Freundlich models
- Effect of sulfate on heavy metals adsorption,
  - Effect of sulfate on single and combined heavy metals by varied 0, 50, 100 and 150 mg/L of SO_4^{2-}.
- Leaching test for IOP and IOCS.

4.1. Study physical and chemical composition of adsorbents

4.1.1. Size distribution of adsorbents

a. Iron oxide particles

Oven-dried iron oxide particles and sand particles weighed about 504.6 g and 459.94 g, respectively. The data has been shown in Table 4.1. To understand about the grade of iron oxide particles distribution, uniformity coefficient (C_u) and cavitation coefficient (C_c) were applied by using the following Equation 4.1 and 4.2 as described in (ASTM, 2017). Size distribution of iron oxide particles is 0.20 mm in effective size diameter, 0.850 mm in mean diameter, 0.550 mm of 30% in passing diameter, and 1 mm of 60 % of passing dimeter (Figure 4.1). As a result, the coefficient of uniformity and cavitation of iron particles is 5 and 1.512, respectively. Based on ASTM (2017), the classification of sand aggregates was divided into two groups including well graded sand and poorly graded sand. The division of grades depends on C_u and C_c as (well graded sand is $C_u \geq 6$ and $1 \leq C_c \geq 3$) and (poorly graded sand $C_u < 6$ and $1 < C_c < 3$). Therefore, the iron oxide particles after milling is expressed in poorly graded.

Table 4.1 Size distribution of Iron Oxide Particles

Total dry weight of iron oxide particle 506 g					
Sieve N°	Opening size(mm)	Weight Sample Retained (g)	Percent Retained	Cumulative % Retained	Percent Passing
4	4.750	0.000	0.000	0	100
7	2.800	0.765	0.152	0.15	99.85
10	2.000	2.888	0.572	0.72	99.28
25	0.710	292.300	57.924	58.65	41.35
40	0.425	113.200	22.432	81.08	18.92
50	0.300	27.695	5.488	86.57	13.43
100	0.150	30.688	6.081	92.65	7.35
200	0.075	24.510	4.857	97.51	2.49
Pan		12.592	2.495	100.00	0.00

$$C_u = \frac{D_{60}}{D_{10}}$$ Eq. 4.1

$$C_c = \frac{D_{30}^2}{D_{10} \times D_{60}}$$ Eq. 4.2

Where, C_u is uniformity coefficient, C_c is cavitation coefficient, D_{10} is IOP or IOCS dimeter passing 10% of passing (mm), D_{30} is IOP or IOCS dimeter passing 30% of passing (mm), D_{50} is IOP or IOCS dimeter passing 50% of passing (mm), D_{60} is IOP or IOCS dimeter passing 60% of passing (mm).
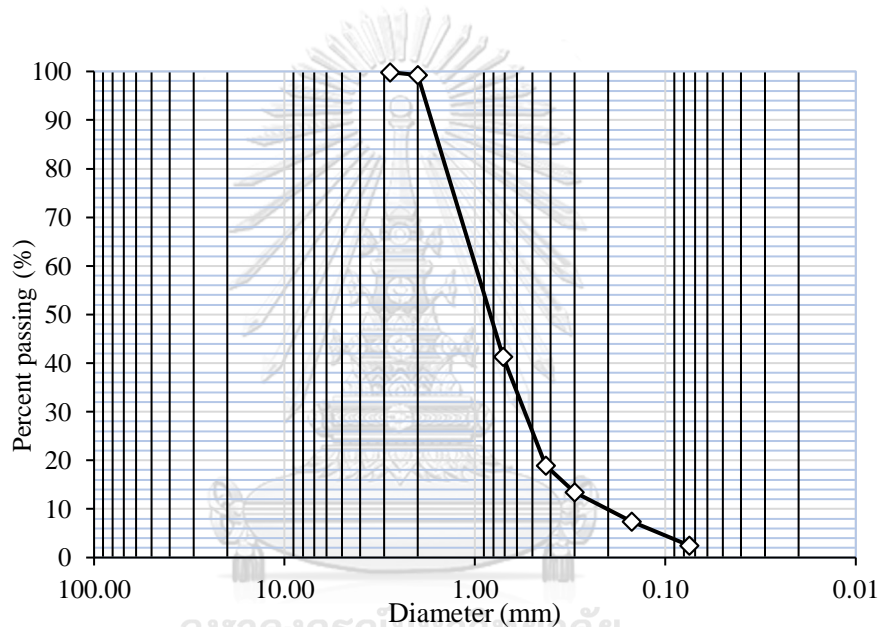
Figure 4.1 Iron oxide particles size distribution by sieve analysis

b. Iron oxide coated sand

Dried-sand particles weighed about 459.94 g. Then it was used for coated process directly. The weight of dried sand retained on sieve as well as 0, 4.040, 385.70, 69.270, 0.213, 0.153, 0.140, 0.104 and 0.231 g, respectively. The data calculated and showed in Table 4.2. Size distribution curve demonstrated the steepest, so the mean, effective, 60 and 30 percent passing diameters as 2.30 mm, 1.5 mm, 2.45 mm and 1.5mm, respectively (Figure 4.2). Uniformity and cavitation coefficient values obtained 1.63 and 1.22, respectively. Hence, these coefficient values indicated the uniformity grade because Cu is lower than 5. The uniformity values explained that the particles mass consists of identical sizes of the particles (Viswanadham, 2015).

Table 4.2. Size distribution of iron oxide coated sand

Total dry weight of IOCS 459.94 g					
Sieve N°	Opening size size (mm)	Weight sample retained (g)	Percent retained	Cumulative % retained	Percent passing
4	4.750	0	0	0	100
7	2.800	4.040	0.878	0.88	99.12
10	2.000	385.700	83.875	84.75	15.25
25	0.710	69.270	15.063	99.82	0.18
40	0.425	0.213	0.046	99.86	0.14
50	0.300	0.153	0.033	99.90	0.10
100	0.150	0.140	0.030	99.93	0.07
200	0.075	0.104	0.022	99.95	0.05
Pan		0.231	0.050	100.00	0.00
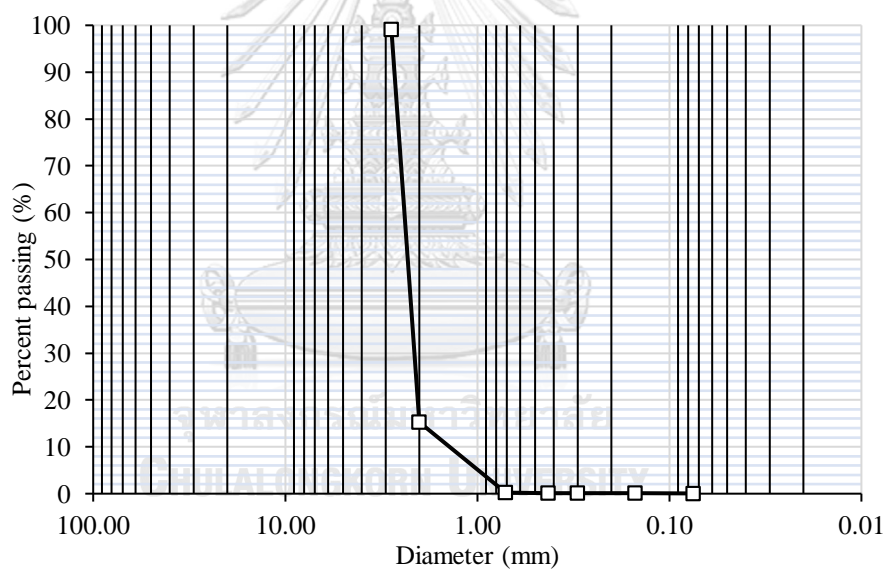
Figure 4.2 Iron oxide coated sand size distribution by sieve analysis

Therefore, the diameter of both IOP and IOCS was selected the ranges from 0.7 to 2 mm for adsorption process based on the mean diameters for make sure the same ranges of diameter size's between IOP and IOCS.

4.1.2. Scanning Electron Microscopy-EDS analysis

The surface morphology and chemical composition on surface of both adsorbents have been found by scanning through SEM-EDS at 500 and 5000 magnification. First, the color of IOP and IOCS was black and dark red, respectively. For SEM analysis, the result has shown the shape of IOP are rough and amorphous on surface layer. This structure information was enhanced the effective site adsorption mechanism with heavy metals contaminated in water (Crittenden et al., 2012). Figure 4.3 shows that surface layer of sand is a plate layer and has a small surface area. For IOCS, surface layer become like circle. It explained that surface layer increased with iron coating. For IOP, high Fe was presented the surface about 55.28% of weight and O about 2.1% Fe is the composition at 60.67%. The photograph of IOCS from EDS scanned showed that Fe and O are the main chemical elements with 33.17% and 39.64% by weight, respectively (Figure 4.4). However, Fe was the lowest compound on raw sand. Hence, it concluded that Fe_2O_3 was coated on surface of sand successfully.
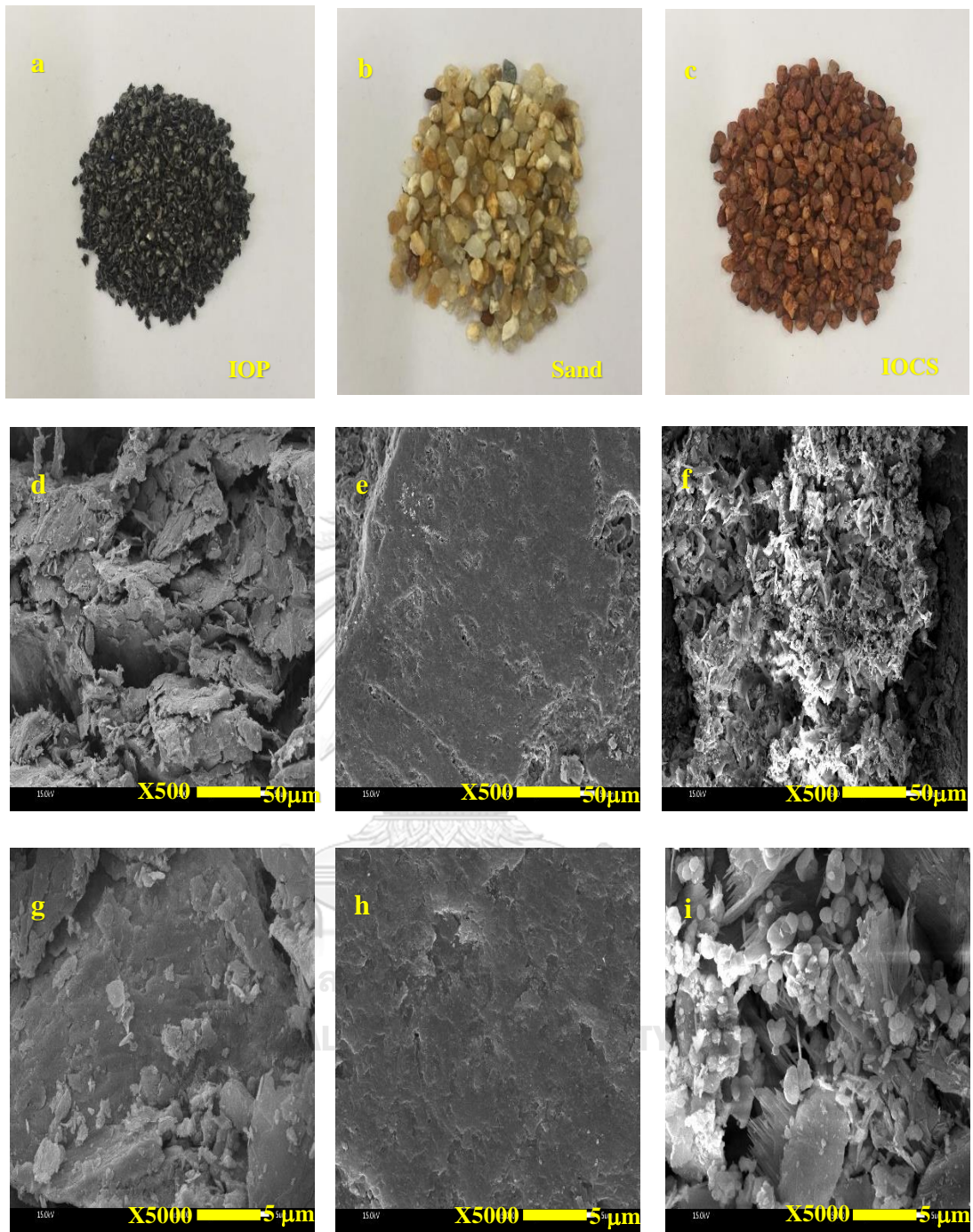
Figure 4.3 Scanning electron micrographs of a) Iron oxide particles, b) Sand, c) Iron oxide coated sand at500 and 5000X
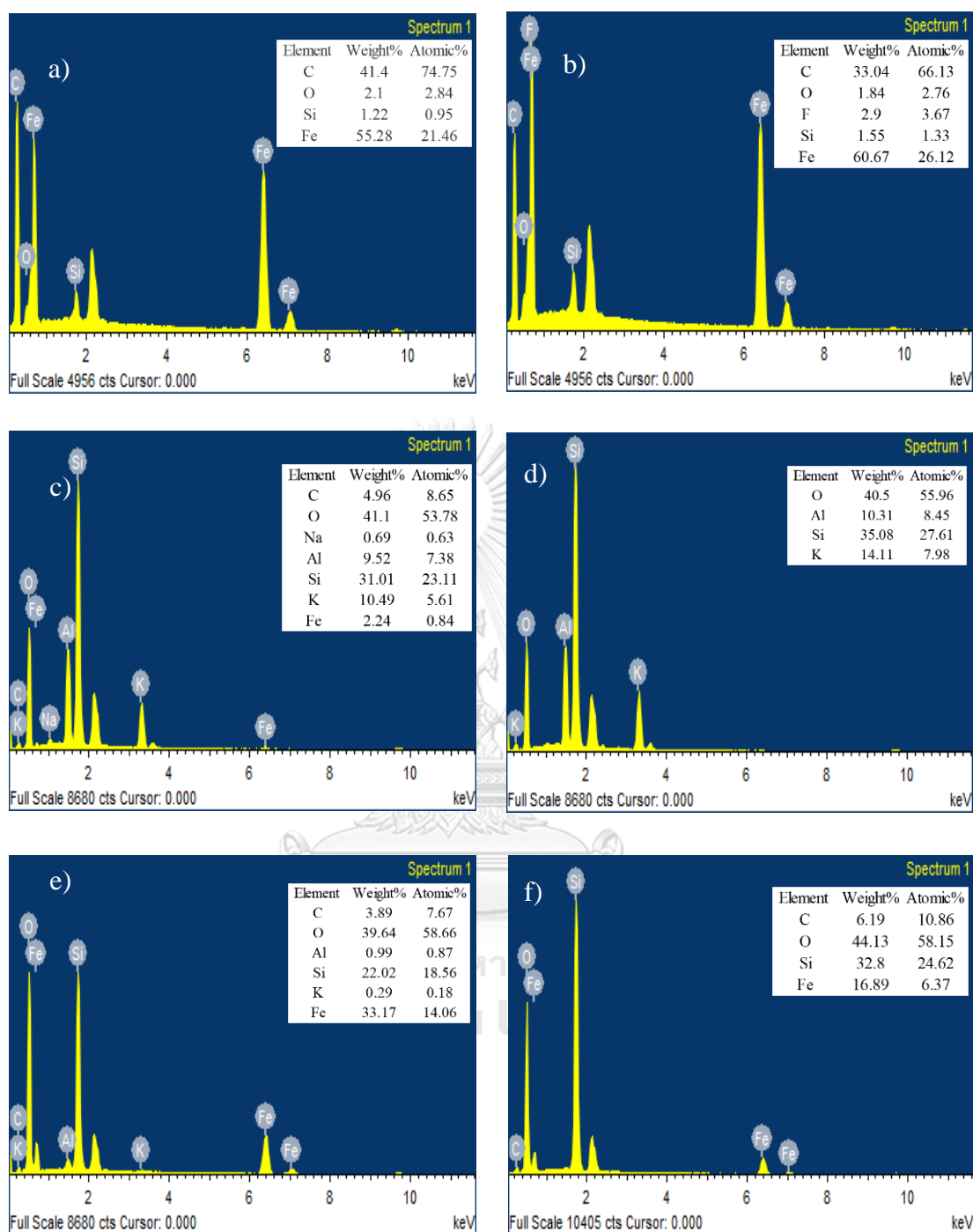
Figure 4.4 Elements composition on surface layer of a, b) Iron oxide particles scanned by EDS at 500 and 5000X, c, d) Sand scanned by EDS at 500 and 5000X and e, f) Iron oxide coated sand scanned by EDS at 500 and 5000 X

4.1.3. X-Ray Fluorescence analysis

Table 4.3 shows chemical composition on IOP and IOCS. For IOP results, Ferric oxide Fe_2O_3 was the main compound around 95.7% by mass, while SiO_2 and MnO constituent only 2.62% and 0.40% by mass, respectively. After coated, chemical compound presented on Iron oxide coated sand such as Fe_2O_3 was occurred about 1.87 % by mass that Fe_2O_3 composition on the sand is 0.778 %. It means Fe_2O_3 consisted approximately 0.187 g of IOCS. Hence, it was evident with EDS results that IOCS was coated successfully on sand surface.

Table 4.3 Chemical composition on IOP and IOCS by using X-Ray Fluorescence

Iron Oxide Particles (IOP)		Iron Oxide Coated Sand (IOCS)		Sand	
Chemical Components	Percent by mass (%)	Chemical Components	Percent by mass (%)	Chemical Components	Percent by mass (%)
Fe_2O_3	95.700	Na_2O	0.338	SiO_2	89.9
SiO_2	2.6200	MgO	0.035	Al_2O_3	5.28
MnO	0.401	Al_2O_3	4.304	K_2O	3.03
CuO	0.224	SiO_2	90.019	Fe_2O_3	0.778
SO_3	0.216	Cl	0.018	Na_2O	0.437
Cr_2O_3	0.214	K_2O	2.646	CaO	0.229
K_2O	0.179	Fe_2O_3	1.874	MgO	0.131
P_2O_5	0.147	Co_2O_3	0.156	TiO_2	0.084
Al_2O_3	0.108	Rb_2O	0.016	P_2O_5	0.035
NiO	0.073	SrO	0.008	BaO	0.032
Na_2O	0.035	ZrO_2	0.007	Rb_2O	0.017
MnO_3	0.030	WO_3	0.573	SO_3	0.014
Cl	0.015	RS1100	0.100	MnO	0.011

4.2. Effect of adsorbents dosages and times heavy metals adsorption

Responding to the first objective is to understand adsorption of heavy metals in synthetic groundwater, this part described about effect of adsorbents dosages on heavy metals removal by varied the adsorbent ranging from 4, 8, 12, 16, 20, and 24 mg/L of iron oxide particles (IOP) and iron oxide coated sand (IOCS) in 1hr. Based on (Babaee et al., 2018) found that 1 hr could reach equilibrium of adsorbate on adsorbent in small amount of adsorbents, so this study considered 1 hr as equilibrium. The initial concentration of 15 mg/L of Mn, 500 μg/L of As and 10 mg/L of Fe were prepared for adsorption process. This part divided into two main parts starting with single Mn, As, Fe and a combined heavy metal of IOP and IOCS. Removal efficiency of heavy metals was calculated from Equation 4.3.

$$\%R = \frac{C_i - C_f}{C_i} \times 100 \qquad \text{Eq. 4.3}$$

Where R is removal efficiency (%), C_i and C_f are the initial and final concentration of heavy metals concentration (mg/L), respectively.

4.2.1. Effect of IOP dosages on heavy metals removal

a. Single heavy metals adsorption

Figure. 4.5 represents relationship between different IOP dosage with removal efficiency of heavy metals in. The maximum removal efficiencies of Mn, As and Fe started to 44.4, 31, 97.4 % by using IOP dosages 12, 12, and 20 mg/L, respectively (Figure 4.5). However, Mn removal efficiency started to decline from 44.4 % to 10.3% at 16 mg of IOP and continued to raise up to 26.8% and 36.7% at 20 and 24 mg/L of IOP, respectively. These results showed that IOP was adsorbed the lowest as 0.7% at 4 mg/L of IOP and highest as 44.4% at 12 mg/L of IOP. Like Mn results, As removal efficiency initially increased from 2.5% to 31% when adding more IOP from 4 to 12 mg/L. However, it decreased significantly from 31% to 8.7% at 16 mg of IOP. Concentration of Fe present in 10 mg/L in water was decreased higher than Mn and As shown in Figure 4.5. The results expressed the higher removal efficiency of Fe were around 80 % to 97% within varying IOP dosage mentioned above. The result

was fluctuated when increasing IOP doses. At 4 mg/L of IOP, Fe was removed about 97.1% and became stable around 8 to 16 mg/L above 90% removal efficiency. Moreover, the maximum Fe removal efficiency was 97.4% at 20 mg/L of IOP. 20 mg/L was chosen as an optimal dosage for Fe removal. Similar to previous research which Fe removal is higher than Mn removal by using mordenite as adsorbent to remove Mn and Fe with initial concentration 1.66 and 0.492 mg/L, respectively (Zevi et al., 2018). It is apparent that the percent removal of heavy metals increases rapidly with increase in the dose of the adsorbents due to the greater availability of the exchangeable sites or surface area. Moreover, the percentage of metal ion adsorption on adsorbent is determined by the adsorption capacity of the adsorbent for various metal ions (Meena et al., 2005).
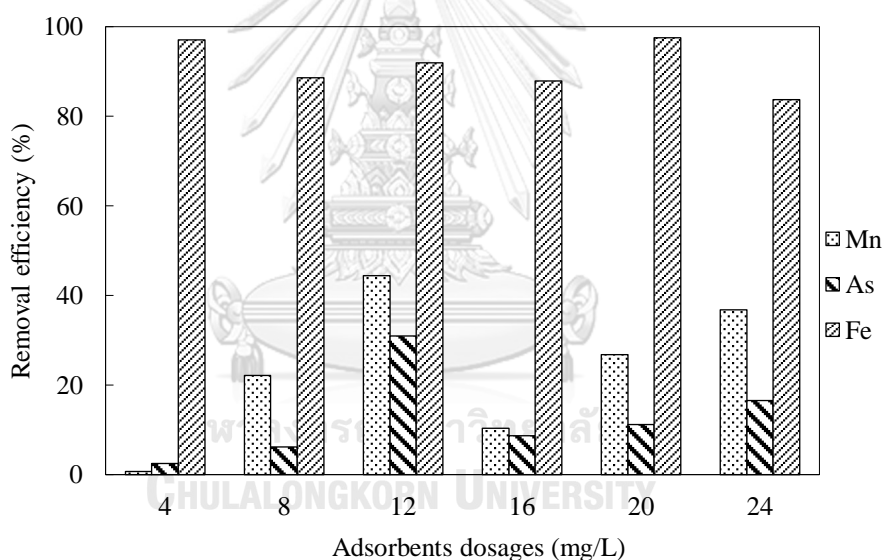
Figure 4.5 Removal efficiency of single heavy metals (Mn, As, and Fe) at 1 hr, pH about 8 ± 0.5 and temperature 30 ± 2 °C

a. Combined heavy metals adsorption

The combined heavy metals removal efficiency related with difference IOP dosages as previous ranges is shown in Figure 4.6. The highest removal efficiency of combined heavy metals (Mn, As and Fe) was approximately 29, 97 and 92 %, respectively by using 16 mg/L of IOP. The removal of Mn decreased from 26% to 5 % at 4 and 12 mg/L of IOP, respectively. But it started to increase to 29 % at 16 mg/L of IOP then continuously declined to about 5% removal at 24 mg/L of IOP. This

results increasement is caused by co-precipitation arsenic occurred with iron in water (V. Gupta et al., 2005). In pH around 8 ± 0.5, Fe was oxidized to be agglomeration of iron from chemical reaction followed Equation from 4.4 to 4.10. Moreover, As removed about 100% by the Fe/As ratio approximately 12 (Meng et al., 2001). Therefore, 16 mg/L of IOP was selected to be optimal dosages in combined heavy metals removal by Mn removal as a baseline.
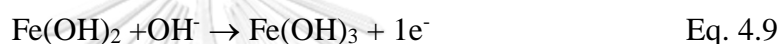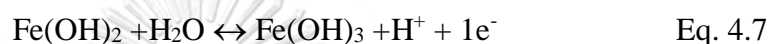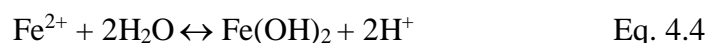
$$Fe^{2+} + 2H_2O \leftrightarrow Fe(OH)_2 + 2H^+ \qquad \text{Eq. 4.4}$$

$$2H^+ + 2OH^- \rightarrow 2H_2O \qquad \text{Eq. 4.5}$$

$$Fe^{2+} + 2OH^- \rightarrow Fe(OH)_2 \qquad \text{Eq. 4.6}$$

$$Fe(OH)_2 + H_2O \leftrightarrow Fe(OH)_3 + H^+ + 1e^- \qquad \text{Eq. 4.7}$$

$$H^+ + OH^- \rightarrow H_2O \qquad \text{Eq. 4.8}$$

$$Fe(OH)_2 + OH^- \rightarrow Fe(OH)_3 + 1e^- \qquad \text{Eq. 4.9}$$

$$3H_3AsO_4 + 3Fe(OH)_3 \rightarrow Fe_3(AsO4)_3 + 9H_2O \qquad \text{Eq. 4.10}$$

Comparing removal efficiency of single heavy metals and combined heavy metals, the results showed the removal of single As is lower than combined As due to co-precipitation of As and Fe occurred. Only single Fe removal were like combined Fe.
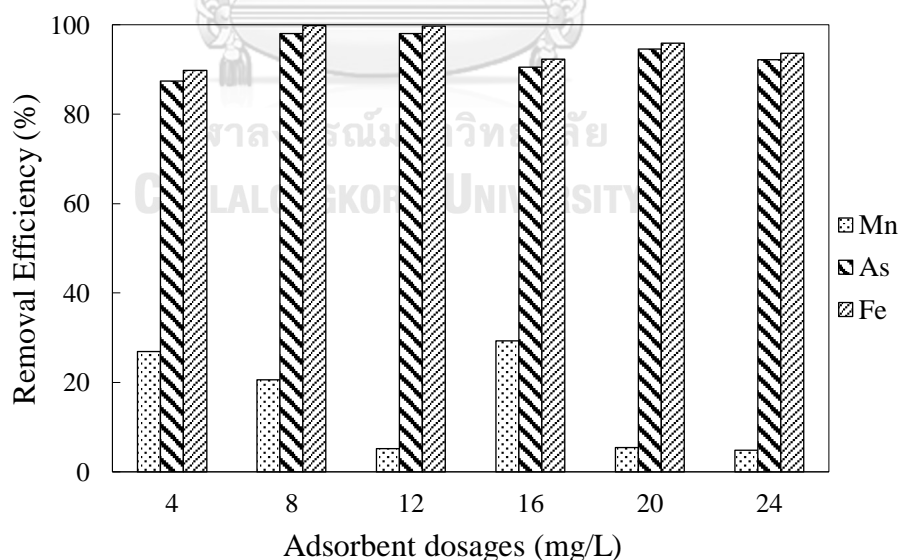
Figure 4.6 Removal efficiency of combined heavy metals (Mn, As, and Fe) at 1 hr, pH about 8 ± 0.5 and temperature 30 ± 2 °C

4.2.2. Effect of IOCS dosages on heavy metals removal

a. Single heavy metals

In this part, normalized mass of IOCS is used to obtain the mass of Fe_2O_3 as mass of IOCS. Hence, amount of adsorbent dosages was ranged from 4, 8, 12, 16, 20 and 24 mg/L of Fe_2O_3. After 1 hr as equilibrium, removal efficiency of individual Mn, As and Fe was represented with IOCS dosages from 0.4 to 2.4 mg/L of Fe_2O_3 (Figure 4.7). Regarding the Figure 4.7, the maximum of single heavy metal Mn, As and Fe removal efficiency are 13, 6, 99 % by using 0.8, 1.2, 0.8 mg/L of IOCS, respectively. As a result, removal efficiency of Mn provided about 7.04% and 13.18% as maximum of removal efficiency by using 0.4 and 0.8 mg/L of IOCS, even though, increasing dosages from 1.2 to 2.4 mg/L, there has no increasing removal efficiency almost lower than 5%. For As removal, the maximum removal efficiency was approximately 6 % at 1.2 mg/L of IOCS. Better than Mn and As, single heavy metal removal of Fe increased from 93.76 % to about 99 % removal at 0.4 to 0.8 mg/L of IOCS. Then, the Fe removal efficiency was stable 99% of Fe removal at 0.8 to 2.4 mg/L of IOCS. Therefore, optimal IOCS dosages for single of Mn, As and Fe include 0.8, 1.2 and 0.8 mg/L of IOCS, respectively.
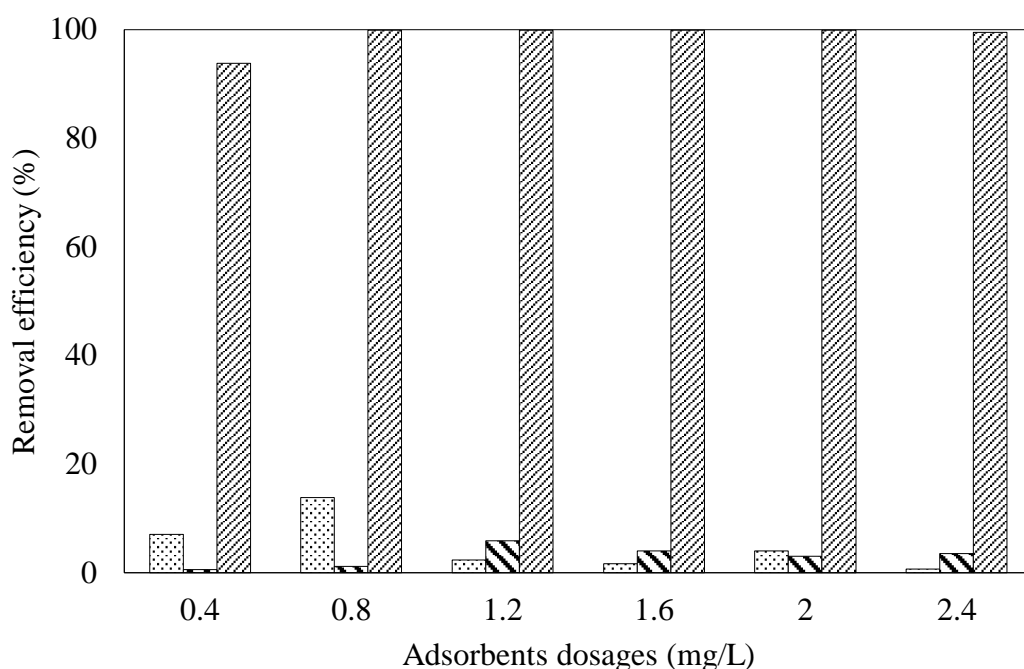
Figure 4.7 Removal efficiency of single heavy metals (Mn, As, and Fe) at 1 hr, pH about 8 ± 0.5 and temperature 30 ± 2 °C

b. Combined heavy metals

Figure 4.8 represents the effect of IOCS dosages on combined heavy metals adsorption efficiency. Removal efficiency of all heavy metals increased comparing to their single solutes heavy metal adsorption. As a result, the highest removal efficiency of Mn, As and Fe was found to be 27, 99 and 100 % by 1.2 mg/L of IOCS, respectively. Firstly, Mn removal efficiency remained statically constant (around 27% removal) between 0.4 and 2.4 mg/L of IOCS. As removal efficiency increased higher than single As to about 99 % of removal efficiency. Initial concentration of As about 500 µg/L was reduced since using 0.4 mg/L of IOCS, then its removal efficiency were constant from 0.8 to 2.4 mg/L at approximately 99 % of removal. Moreover, Fe were removed about 99.9% by using only 0.8 mg/L of IOCS. The results were similarly to combined of heavy metals by using IOP except for Mn. As a baseline of Mn removal, this part found the optimal IOCS dosages is 1.2 mg/L for combined heavy metals.

Comparing removal efficiency of single heavy metals and combined heavy metals, the results showed the removal of single Mn, As was less than combined Mn, As. Only single Fe removal was as high as combined heavy metals Fe.
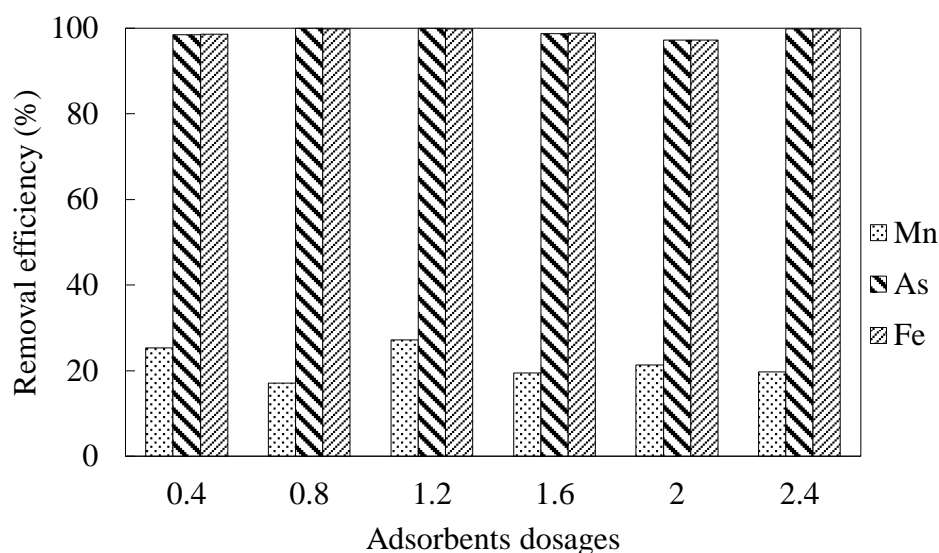
Figure 4.8 Removal efficiency of combined heavy metals (Mn, As, and Fe) at1 hr, pH about 8 ± 0.5 and temperature 30 ± 2 °C

4.3. Determination of adsorption equilibrium

Equilibrium is one of the adsorption parameters that plays an important role for heavy metals isotherm adsorption. In order to determine the equilibrium point on heavy metals adsorption, the results were obtained by sampling along the times from 10 to 60 min. The results of equilibrium were varied all value range of IOP and IOCS dosages such as 4, 8, 12, 16, 20 and 24 mg/L. However, this part explained only the best optimal dosages.

4.3.1. Equilibrium on heavy metals removal by IOP

This part was explained the effect of time from 10 to 60 min using IOP. The optimal dosage of IOP were 12, 12, 20 and 16 mg/L for single metals Mn, As,

a. Single heavy metals

The removal of single heavy metals Mn, As and Fe related with time using different IOP dosages were illustrated in Figure 4.9. The removal Mn rapidly increased from 0 to 46.01% during 0 to 20 min and then remained constant at 12 mg IOP. Therefore,

Mn concentration reached its equilibrium after 20 min. Moreover, according to As removal graph (Figure 4.9b), As removal was approximately 31% during 60 min. However, a small increase of As removal was from approximately 28 to 31 % between times of 30 and 60 min. This implied that the removal efficiency of As on IOP reached equilibrium at 30 min. This result was similar to the reported by Babaee et al. (2018) that As adsorption by Fe/Cu nanoparticles was occurred between 15 and 30 min. Lastly, the removal efficiency of Fe by IOP was about 99 % during 10 min; however, it decreased to 97% at 60 min. The order of effect of contact time about 10 min to single heavy metals adsorption provided by removal efficiency, the results consequently shown that 99 % of Fe removal > 46% of Mn removal > 21 % of As removal. The reduction of heavy metals concentration was gradually faster due to adsorbent has available active site during the short contact time (Abuh et al., 2013; Kitkaew et al., 2018).
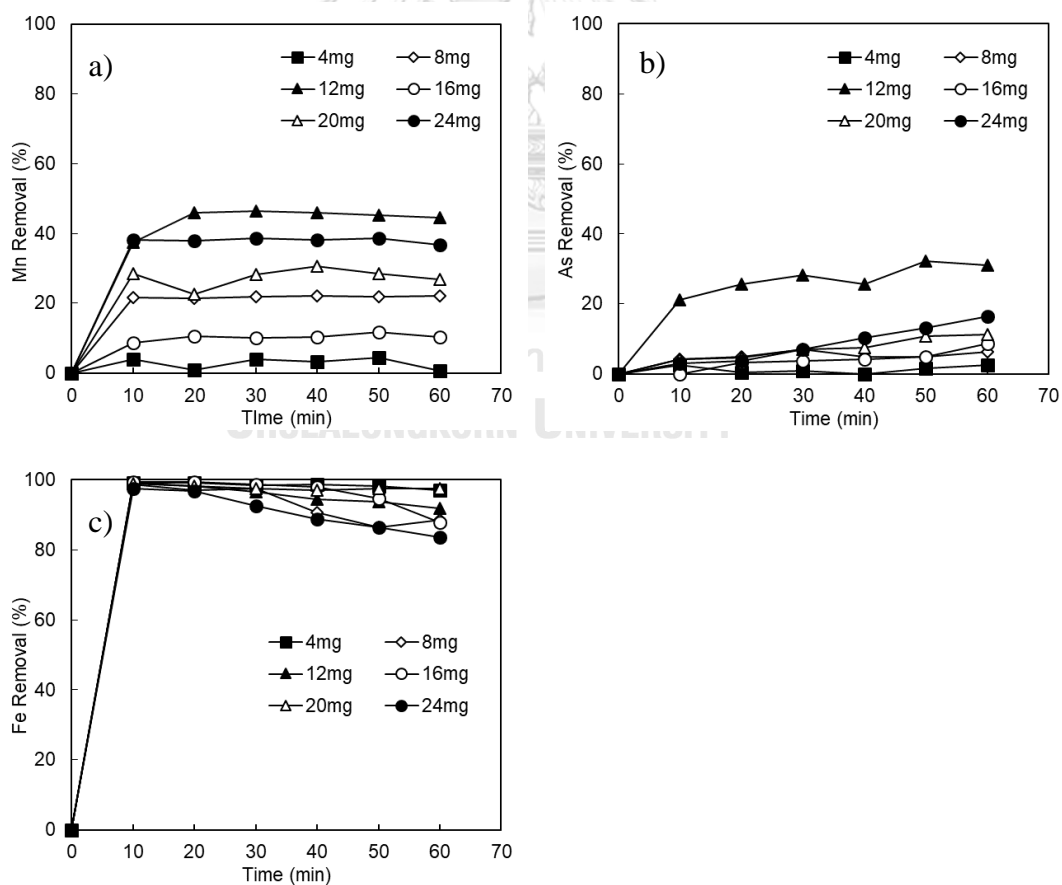
Figure 4.9 Removal efficiency at equilibrium on single heavy metals removal by IOP
a) Mn, b) As and c) Fe at pH = 8 ± 0.5 at 1 hr

b. Combined heavy metals

The removal efficiency of combined heavy metals related with time using different IOP dosages were exhibited in Figure 4.10. The removal of Mn is increased from 0 to 34 % during 10 min. Mn removal reached equilibrium in 10 min. However, As adsorbed faster than As single adsorption within 10 min. Based on figure 4.10 b. As removal increased rapidly from 0 to 98 % in 10 min of contact time. Similar to single Fe adsorption, Fe removal efficiency highly increased from 0 to 99% at 10 min contact time. The order of highest to lowest removal efficiency was 99 %of Fe > 98% of As > 34% of Mn removal. To sum up, Fe adsorbed faster than As and Mn in combined heavy metals. In the same aqueous solution, this may relate to adsorbates characteristics in terms of electronegativity and ionic radius (bin Jusoh et al., 2005). The electronegativity of As, Fe is higher than the Mn which are 2.1 1.8 and 1.5 respectively. In fact, electronegativity is a evaluate the strength for chemical elements to attract electron. In this case, it would measure the strength of Fe, As and Mn attached to negative charge on surface of IOP.
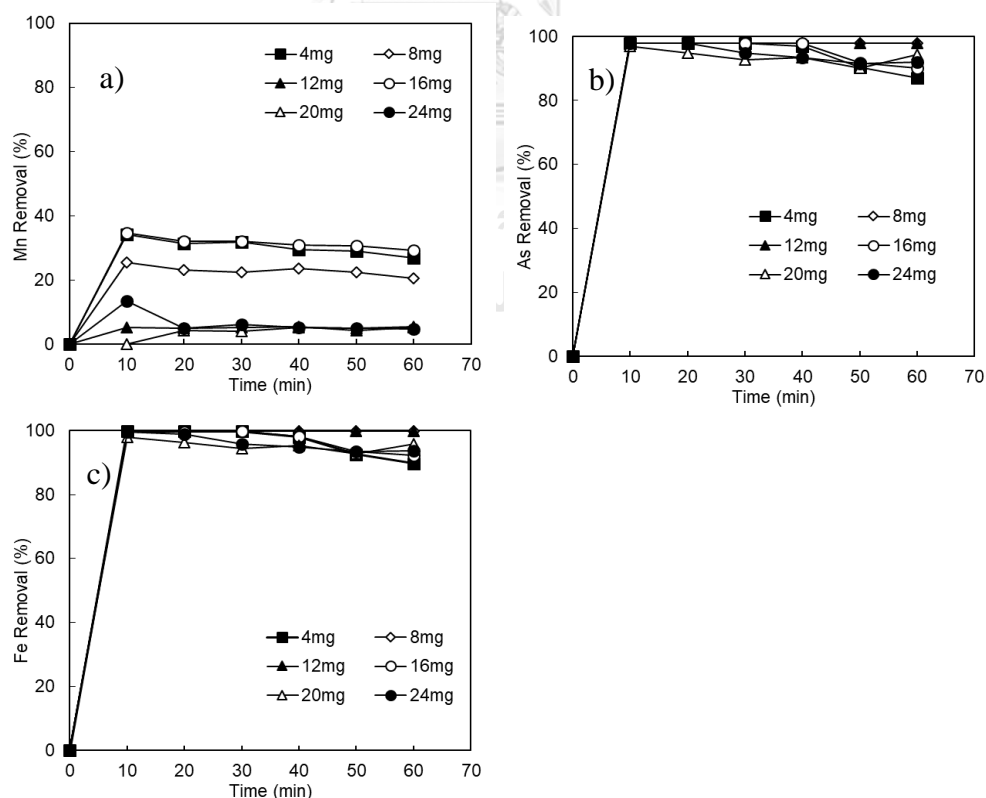
Figure 4.10 Removal efficiency at equilibrium on combined heavy metals removal by IOP a) Mn, b) As and c) Fe at pH = 8 ± 0.5 at 1 hr

4.3.2. Equilibrium on heavy metals adsorption by IOCS

The determination of equilibrium was chosen only the best IOCS dosages for heavy metals adsorption including 0.8, 1.2, 0.8 and 1.2 mg/L for single of Mn, As, Fe and combined heavy metals, respectively. This part was divided into two sub-parts as single and combined heavy metals.

    a.   Single heavy metals

The removal efficiency at equilibrium of single heavy metals related with time were illustrated in Figure 4.11. All single heavy metals achieved equilibrium at 10 min. Removal of Mn were increased from 0 to approximately 16% during the first 10 min of time. For As, the increasing of As removal changed slightly from 0 to about 5% in 10 min. However, the removal of Fe increased faster with removal efficiency about 99%. By comparing the capacities of removal with 10 min, the results suggested that Fe removal was highest at 99% and As was the lowest at 5%. Fe adsorbed faster than Mn and As in 10 min of time.
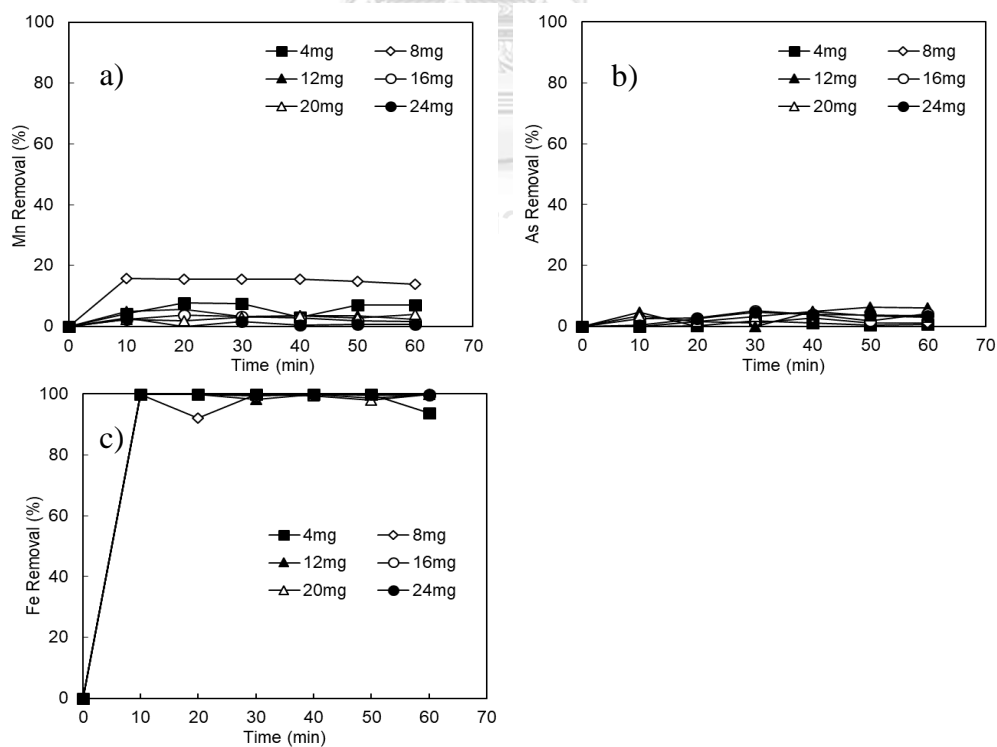
Figure 4.11 Removal efficiency at equilibrium on single heavy metals removal by IOCS a) Mn, b) As and c) Fe at pH = 8 ± 0.5 at 1 hr

b. Combined heavy metals

The removal efficiency at equilibrium on combined heavy metals removal using different IOCS dosages were represented in Figure 4.12 4.12. All heavy metals in combined condition reached equilibrium in 10 min of times. Moreover, the results showed that Mn removal increased from 0 to approximately 30 % during 10 min. As a result, As was removed faster in 10 min adsorption by the steep slope from graph. Hence, As was adsorbed well in 10 min of equilibrium with 99 % removal. Lastly, the removal of Fe raised from 0 to 99 % in 10 min. Therefore, the order of effect contact time in 10 min adsorption removal ranged by 99% of Fe > 99 %As > 30% of Mn removal.
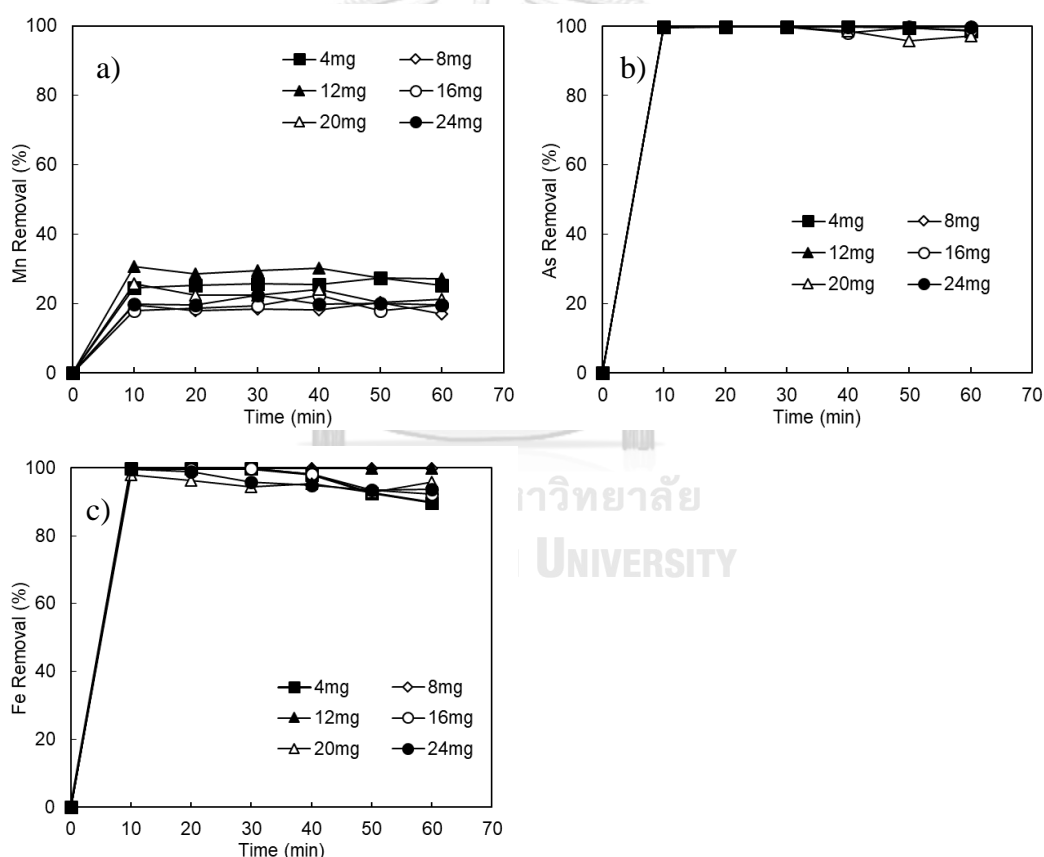
Figure 4.12 Removal efficiency at equilibrium on combined heavy metals removal by IOCS a) Mn, b) As and c) Fe at pH = 8 ± 0.5 at 1 hr

4.4. Effect of adsorbent capacities on heavy metals adsorption

The results of adsorption capacities of IOP and IOCS were varied all value ranges of IOP and IOCS dosages. Hence, the adsorption capacities of IOP or IOCS were calculated by Equation 4.11.

$$q_t = \frac{V}{M}(C_0 - C_t)$$ Eq. 4.11

Where qt is adsorption capacity of IOP or IOCS adsorbed heavy metals along the times (mg/mg Fe_2O_3), Co is the initial concentration of every metals (mg/L), Ct is is the initial concentration of every metals along the times (mg/L), V is the volume of water (L), and M is mass of Fe_2O_3 containing on IOP or IOCS (mg).

4.4.1. Effect of adsorption capacities on heavy metals removal by IOP

This part demonstrated about adsorption capacity of IOP on heavy metals Mn, As and Fe from 10 to 60 min as time adsorption interval. The results were selected only the optimal dosages to present in this case including 12, 12, 20, 16 mg/L of IOP for single heavy metal Mn, As, Fe and combined heavy metals, respectively.

a.   Single heavy metals

Equilibrium concentration and adsorption capacity of each heavy metals were exhibited in Figure 4.13. The results showed that maximum of adsorption capacities of single Mn, As and Fe on IOP were 0.586, 0.011 and 0.494 mg/mgFe_2O_3 at different contact time 20, 30 and 10 min, respectively. In detail, adsorption capacity of Mn on IOP gradually increased from 0.47 to 0.58 mg/mgFe_2O_3 corresponding to concentration of Mn are 9.58mg/L to 8.26 mg/L during 10 to 20 min. Then, it stopped rising by reaching equilibrium as mentioned in section above. In addition, As was adsorbed by IOP with 0.011 mg/mgFe_2O_3 with residual concentration of As approximately 0.348 mg/L in 30 min; however, a small declining of concentration As was from 0.348 to 0.334 mg/L while adsorption capacity of As increased from 0.011 to 0.012 mg/mgFe_2O_3 between times of 30 and 60 min. Furthermore, the adsorption capacities of Fe were pretty good about 0.494 mg/mgFe_2O_3 in 10 min with 0.1 mg/L

of effluent concentration of Fe. In contrast, the adsorption capacity of Fe decreased slightly from 0.494 to 0.487 mg/mgFe$_2$O$_3$ during 10 to 60 min. Due to decreasing adsorption capacity of IOP of Fe, concentration of Fe slightly increased from 0.10 to 0.25 mg/L. The decreasing of adsorption capacity IOP of Fe is caused by available active site of IOP which enhance the faster at initial shorter time. To sum up, IOP adsorbed Mn better than Fe and As due to high initial concentration of pollutants made higher adsorption capacity.
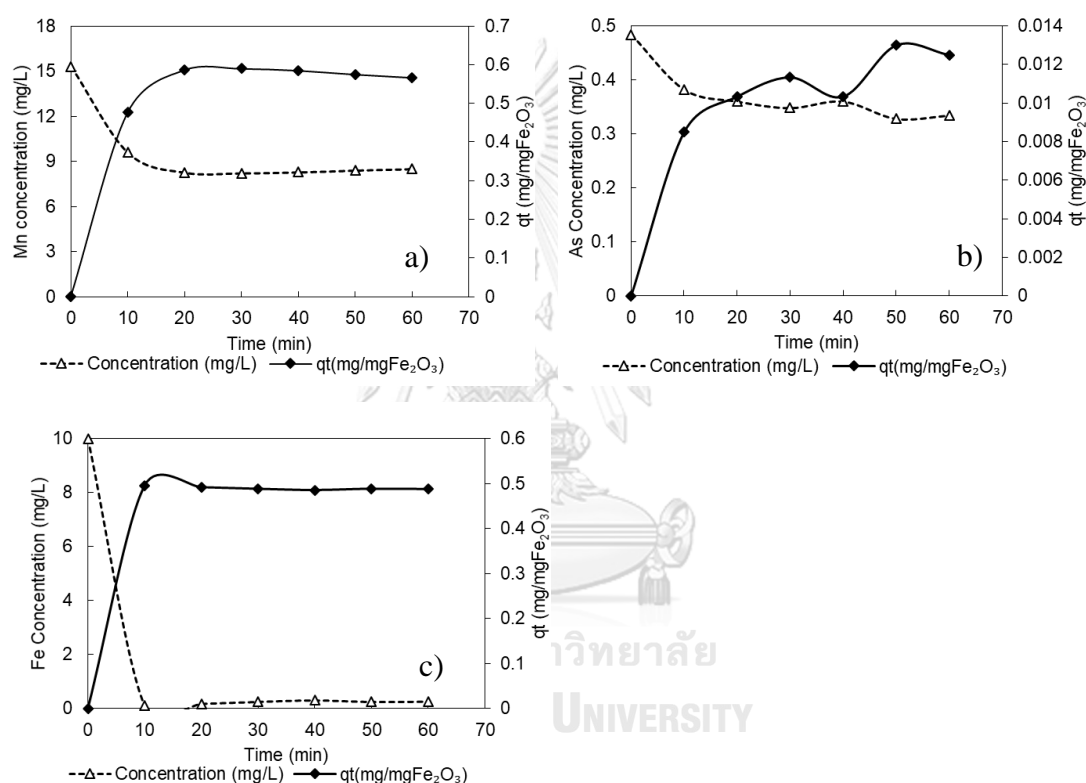
Figure 4.13 Effect of time on adsorption capacity by IOP for single heavy metals a) Mn, b) As and c) Fe at pH=8±0.5 in 1 hr

b.   Combined heavy metals

Equilibrium concentration and adsorption capacity of each heavy metals were exhibited in Figure 4.14. All the corresponding the maximum of adsorption capacities of Mn, As and Fe are 0.332, 0.0029 and 0.624 mg/mgFe$_2$O$_3$, respectively in 10 min of contact time, and concentration of Mn, As and Fe decreased to 9.97, 0.01 and 0.022 mg/L, respectively. However, adsorption capacities of Mn decreased slightly to 0.307 mg/mgFe$_2$O$_3$ at 20 min of equilibrium time and remained constant during 20 to 60

min. Furthermore, adsorption capacity of As gradually increased to 0.0029 mg/mgFe$_2$O$_3$ and then stable between 10 to 40 min. However, adsorption capacity of As decreased slowly from 0.0296 to 0.0273 mg/mgFe$_2$O$_3$ at the time between 40 to 60 min. Additionally, the concentration of Fe remained stable about 0.02 mg/L even at equilibrium. To sum up, the combined of heavy metals Mn, As and Fe initially adsorbed faster at short contact time. This reflects that larger numbers of adsorptive sites were available for adsorbate during the initial short contact times (Kitkaew et al., 2018). Removal efficiency of combined heavy metals reached equilibrium at 10 min.
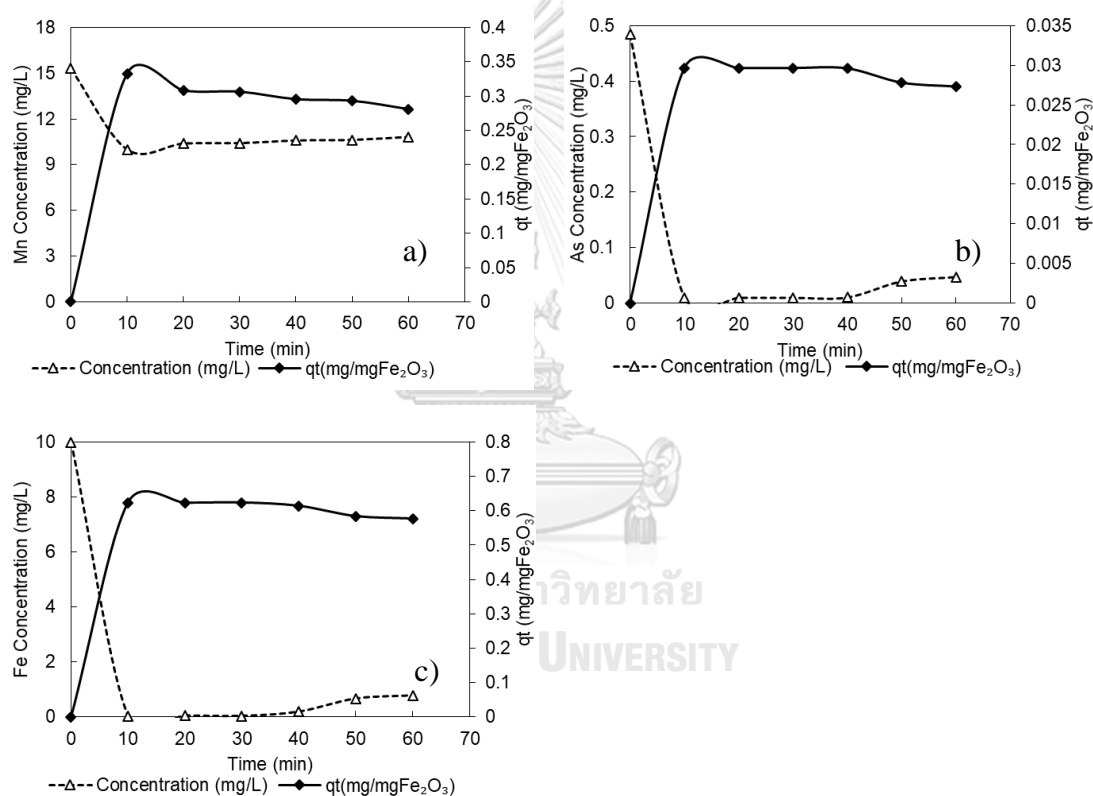
Figure 4.14 Effect of time on adsorption capacity by IOP for combined heavy metals a) Mn, b) As and c) Fe at pH=8 ± 0.5 in 1 hr

In addition, considering the order of maximum adsorption capacities of single heavy metals with combined heavy metals, results showed that single Mn (0.586 mg/mgFe$_2$O$_3$) higher than combined Mn (0.332 mg/mgFe$_2$O$_3$), single As (0.011 mg/mgFe$_2$O$_3$) lower than combined As (0.029 mg/mgFe$_2$O$_3$), and single Fe (0.494 mg/mgFe$_2$O$_3$) lower than combined Fe (0.624 mg/mgFe$_2$O$_3$). Hence, all IOP adsorption capacity of single heavy metal Mn was higher than those in combined

heavy metals because number of active sites were reduced by many pollutants contaminated in water. On the other hand, IOP adsorption capacity of single As and Fe was lower than combined As and Fe due to co-precipitation between As and Fe enhances the adsorptive capacity of As in combined system.

4.4.2. Effect of adsorption capacity on heavy metals removal by IOCS

In summarize, the results in the previous section of effect of IOCS dosages on heavy metals adsorption, the optimal dosages of IOCS discussed in this part include 0.8, 1.2, 0.8 and 1.2 mg/L of IOCS. There are two parts as single and combined heavy metals.

a.   Single heavy metals

Equilibrium concentration and adsorption capacity of each heavy metals were exhibited in Figure 4.15. The adsorption capacities IOCS of Mn, As and Fe were about 2.99, 0.02 and 12.48 mg/mgFe_2O_3, respectively occurred in 10 min at equilibrium. Based on adsorption capacity of single heavy metals, concentration of single Mn, As and Fe were minor decreased to 12.90, 0.489 and 0.01 mg/L from initial concentration, respectively. Adsorption capacities of Mn and Fe were remained constant during 10 to 60 min. However, adsorption capacities of As remained the same between in 10 to 60 min except during 20 and 30 min. The concentration of As remained as initial concentration about 500 mg/L and adsorption capacity of As was shown the lowest value during 20 and 30 min due to experimental error. However, V. Gupta et al. (2005) found that IOCS about 20 g/L adsorbed As well in 120 min of contact time and only 40 % of As removal happened in 20 min. Moreover, from previous studies, IOCS dosages were studied in 1.5 thousand times as high as IOCS doses in this study, but removal efficiency of As was not significantly effective in 20 to 40 min of contact time. Therefore, this reason could explain about the lowest value of adsorption capacity of As in 20 to 30 min of contact time. Additionally, As adsorption might be happened due to adsorption capacity IOCS started increasing to 0.02 mg/mgFe_2O_3 in contact time 10 min.
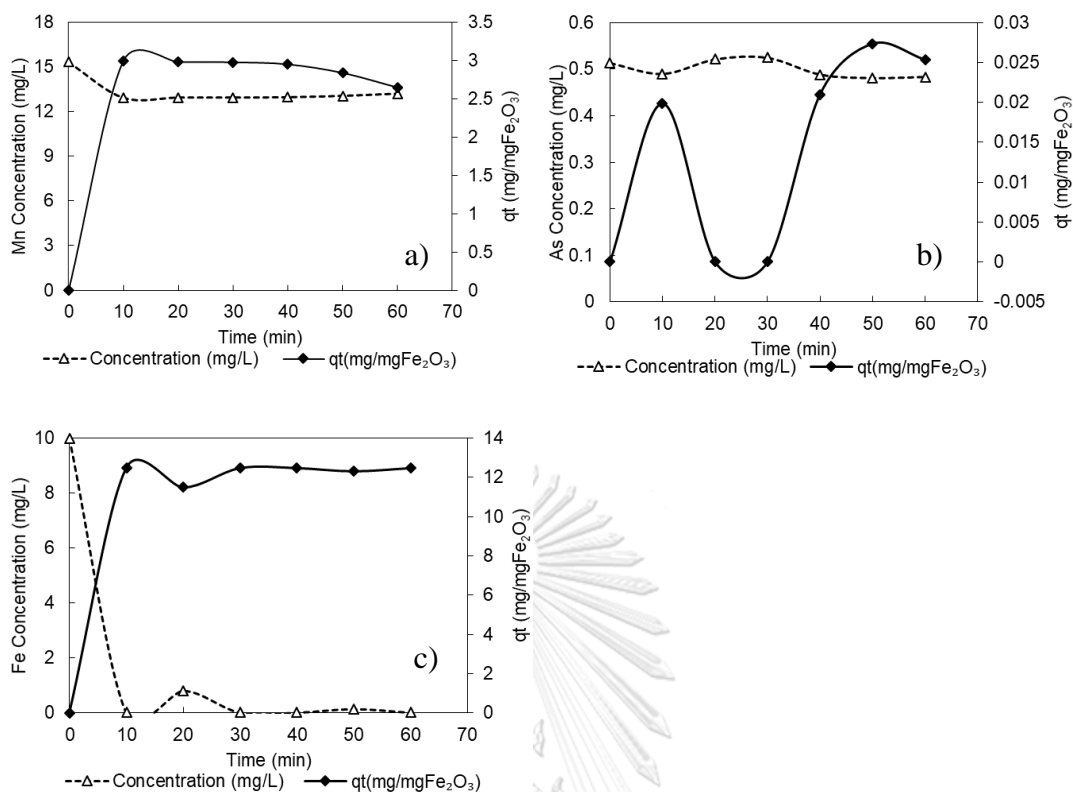
Figure 4.15 Effect of time on adsorption capacity by IOCS for single heavy metals a) Mn, b) As and c) Fe at pH=8 ± 0.5 in 1 hr

b.   Combined heavy metals

Equilibrium concentration and adsorption capacity of each heavy metals were exhibited in Figure 4.16, it demonstrated the maximum of adsorption capacity of combined Mn, As and Fe such as 3.903, 0.427 and 8.33 mg/mgFe$_2$O$_3$, and concentration was reduced to 10.61, 0.00001 and 0.01 mg/L, respectively in 10 min of time. In detail, the concentration Mn and As gradually declined to approximately 11.13 and 0.00001 mg/L during 10 and 60 min of time. Different from single Fe, adsorption capacity about 8.32 mg/mgFe$_2$O$_3$ possible reduced Fe to 0.01 mg/L during 10 to 60 min of time. Overall, in combined heavy metals equilibrium was reached in 10 min. The increasing of As adsorption capacity because of co-precipitation of As and Fe occurred around pH 6.5 to 8.5.
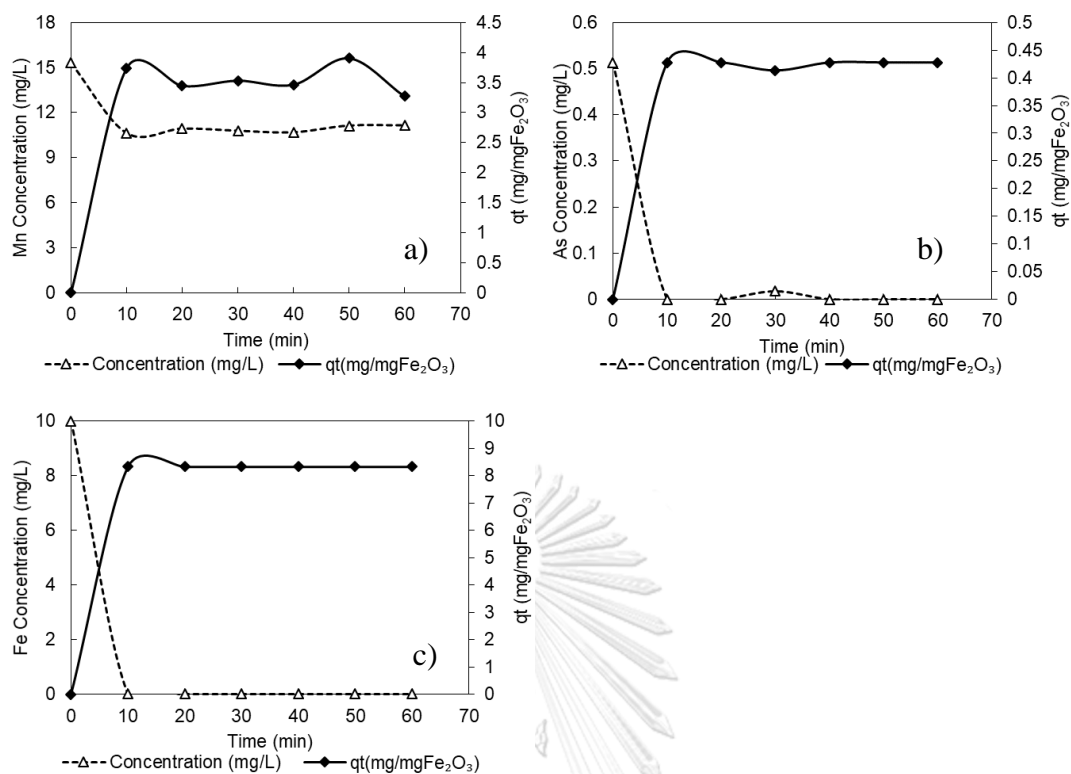
Figure 4.16 Effect of time on adsorption capacity by IOCS for combined heavy metals a) Mn, b) As and c) Fe at pH=8 ± 0.5 in 1 hr

Furthermore, considering the order of maximum adsorption capacities of IOP on single heavy metals with combined heavy metals, results showed that single Mn (2.99 mg/mgFe$_2$O$_3$) lower than combined Mn (3.90mg/mgFe$_2$O$_3$), single As (0.02 mg/mgFe$_2$O$_3$) lower than combined As (0.42 mg/mgFe$_2$O$_3$), and single Fe (12.48 mg/mgFe$_2$O$_3$) higher than combined Fe (8.33mg/mgFe$_2$O$_3$). Hence, all adsorption capacity of single heavy metal Mn and As were lower than combined heavy metals due to co-precipitation enhance As and Mn removal efficiency.

4.5. Summary

The best optimal values of heavy metals concentration, dosages, equilibrium, removal efficiency, adsorption capacity, WHO drinking water quality standard and Cambodia drinking water quality standard (CDWQS) were summarized in Table 4.4. The equilibrium concentration of single Mn, As, Fe and combined heavy metals were compared to the value of WHO drinking water standard and Cambodia drinking water quality standard. As a result, only As in combined heavy metals was lower than Cambodia drinking water standard. Final concentration is lower than WHO and Cambodia drinking water standard in both adsorbents except for Fe combined heavy metals using IOP.

Table 4.4 Summary result of final concentration of heavy metals with different adsorbent IOP and IOCS compared to WHO drinking water quality standard and Cambodia drinking water quality standard in 1 hr adsorption equilibrium

Adsorbent	Heavy metals	Dose mg/L	t min	C_t mg/L	q_{max} mg/mgFe$_2$O$_3$	R %	WHO standard mg/L	CDWQS mg/L
IOP	Single Mn	12	20	8.260	0.586	46	0.4	0.1
	Single As	12	30	0.348	0.011	28	0.01	0.05
	Single Fe	20	10	0.102	0.494	99	0.3	0.3
	Com Mn	16	10	9.970	0.332	34	0.4	0.1
	Com. As	16	10	0.010	0.003	98	0.01	0.05
	Com. Fe	16	10	0.022	0.624	99	0.3	0.3
IOCS	Single Mn	0.8	10	12.9	2.99	16	0.4	0.1
	Single As	1.2	10	0.489	0.02	5	0.01	0.05
	Single Fe	0.8	10	0.01	12.48	99	0.3	0.3
	Com. Mn	1.2	10	10.61	3.90	30	0.4	0.1
	Com. As	1.2	10	1E-05	0.42	99	0.01	0.05
	Com. Fe	1.2	10	0.01	8.33	99	0.3	0.3

4.6. Adsorption kinetic

The mechanisms of heavy metals adsorption along the time were studied by using two kinetic models including pseudo first-order and pseudo second-order. The pseudo first-order was used to explain adsorption in solid and liquid systems based on the sorption capacity of solids and understand the adsorption rate (Ho and McKay, 2000) following Equation 4.14.

$$\frac{dq_t}{dt} = k_1 \left(q_e - q_t \right)$$

Eq. 4.12

After integration
$$\ln \left(q_e - q_t \right) - \ln q_e = -k_1 t$$

Eq. 4.13

$$\log \left(q_e - q_t \right) = \log q_e - \frac{k_1}{2.303} t$$

Eq. 4.14

Where, qt represents the amount of heavy metals adsorbed on IOP and IOCS in every 10 min (mg/mg of Fe_2O_3), q_e represents the amount of heavy metals adsorbed on IOP at equilibrium (mg/mg of Fe_2O_3), k_1 is the pseudo-first order rate constant (/min). q_e and k_1 were calculated from intercept, and slop of plot between time as X axis and log (q_e-q_t) as Y axis, respectively.

The pseudo second-order rate was used to examine kinetic Equation 4.18 based on adsorption capacity from the concentration of a solution by analyzing the chemisorption in the solution (Ho, 2006).

$$\frac{dq_t}{dt} = k_2 \left(q_e - q_t \right)^2$$

Eq. 4.15

$$\frac{dq_t}{\left(q_e - q_t \right)^2} = k_2 dt$$

Eq. 4.16

$$\frac{1}{\left(q_e - q_t \right)} = \frac{1}{q_e} - k_2 t$$

Eq. 4.17

Linear regression is
$$\frac{t}{q_t} = \frac{1}{k_2 q_e^2} + \frac{t}{q_e}$$

q. 4.18

Where k_2 is the rate constant for pseudo second-order adsorption ($mgFe_2O_3$/mg.min), q_e and k_2 from pseudo second-order were obtained from slop and intercept of plot between time as X axis and t/qt as Y axis, respectively.

4.6.1. Heavy metals on kinetic model by IOP

a. Single heavy metals

Adsorption capacity of single heavy metals fitted as either first or pseudo second-order kinetics is presented in Figure 4.17. Table 4.5 describes parameters relating to the models. All detailed linear equation from graphs were shown in (Appendix.13). All adsorbent optimal dosages of single heavy metals adsorption, the correlation coefficient R^2 of pseudo first-order provided poor fitted. On the other hand, pseudo second-order of all single heavy metals a better fitted with value of R^2 closed to 1.000. The result is followed pseudo second- order as some researches (K. Gupta and Ghosh, 2009; Huang et al., 2007; Yoon et al., 2014). Because of the better fit of pseudo second-order, it could explain that chemical interaction between heavy metals on IOP surface layer involved valency forces through sharing or exchange of electrons between sorbent and sorbate (Ho and McKay, 2000).

The adsorption capacity of single Mn, As and Fe at 1 hr was 0.566, 0.013 and 0.487 mg/mgFe$_2$O$_3$, respectively. These values were approximately closed very well by pseudo second-order kinetic model calculation. Based on these model results, the assumption of heavy metals adsorption is followed a monolayer regime on the adsorbent surface and the rate of adsorption occurred faster at the initial step of adsorption (Phuengprasop et al., 2011).The models were repeated as the effect of times on heavy metals removal during 0 to 20 min of adsorption process. So, the reactions coefficient of heavy metals were determined by k_2 with its dosage optimal. Pseudo second-order adsorption rate of heavy metals from highest to lowest was that (22.752 $mgFe_2O_3$/mg.min for Fe), (20.766 $mgFe_2O_3$/mg.min for As) and (4.958 $mgFe_2O_3$/mg.min for Mn). Moreover, based on Figure 4.17f. the intercept is negative value -22.752 $mgFe_2O_3$/mg.min due to precipitation happened with adsorption process that removal mechanism start happened as a form of Fe(OH)$_3$.

Figure 4.17 Pseudo first-order and pseudo second-order kinetic models of single heavy metal a),b) Mn, c),d) As and e),f)Fe by using optimal dosages of IOP, respectively

Table 4.5 Kinetic pseudo first order and pseudo second-order adsorption models with different IOP doses and amount of adsorption capacity from experimental data for single heavy metals

Heavy Metals	Dosage (mg)	$q_{e, exp}$ (mg/mg Fe$_2$O$_3$)	Pseudo first-order			Pseudo second-order		
			$q_{e,Cal}$ (mg/mgFe$_2$O$_3$)	K_1(/min)	R^2	$q_{e,Cal}$ (mg/mgFe$_2$O$_3$)	K_2(mg Fe$_2$O$_3$/mg.min)	R^2
Mn	4	0.025	0.180	-0.040	0.375	0.038	-2.879	0.469
	8	0.423	0.027	-0.022	0.035	0.422	10.512	1.000
	12	0.566	0.324	-0.023	0.313	0.579	4.958	0.998
	16	0.098	0.032	-0.055	0.230	0.105	8.029	0.988
	20	0.205	0.203	-0.029	0.223	0.215	8.629	0.986
	24	0.234	0.510	-0.016	0.375	0.238	-10.539	0.999
As	4	0.003	0.008	-0.014	0.094	0.004	5.056	0.093
	8	0.004	0.001	-0.056	0.131	0.004	153	0.946
	12	0.013	0.001	-0.086	0.410	0.013	20.766	0.973
	16	0.003	0.001	-0.055	0.239	0.002	4370	0.609
	20	0.003	0.001	-0.041	0.097	0.003	16.654	0.735
	24	0.003	0.001	-0.048	0.183	0.006	2.642	0.217
Fe	4	2.428	1.509	0.009	0.375	2.434	-1.818	1.000
	8	1.107	1.358	0.027	0.179	1.076	-0.731	0.997
	12	0.766	0.884	-0.003	0.375	0.767	-1.711	0.999
	16	0.549	0.757	-0.006	0.375	0.563	-1.279	0.994
	20	0.487	0.576	0.014	0.018	0.486	-22.752	1.000
	24	0.349	0.613	-0.011	0.375	0.349	-1.827	0.997

b. Combined heavy metals

The parameters of pseudo first-order and pseudo second-order calculated from data of combined heavy metals adsorption by IOP are summarized in Table 4.6. Results expressed that the pseudo first-order were poorly fitted with R^2 of 0.375. In comparison, the pseudo second-order fitted better than pseudo first-order with R^2 closed to 1.000 (Figure 4.18). According to the corresponding well fitted results by pseudo second-order, the combined heavy metals Mn, As and Fe were adsorbed by chemisorption as in single heavy metals condition. Pseudo second-order is also a pointer to the dominance of chemisorption as a mechanism of heavy metals interaction with the sorbent surface (Oladoja et al., 2013). Moreover, the adsorption capacities of combined heavy metals were closed to the adsorption capacities of IOP calculated from experimental data. Because of the well fitted of second order, the consistency of adsorption capacity IOP of combined Mn, As and Fe at 1 hr equilibrium obtained from kinetic model include 0.282, 0.027 and 0.578 mg/mgFe$_2$O$_3$, respectively.

The mechanism of this adsorption process was chemisorption. Moreover, in chemical adsorption, it is assumed that the adsorption capacity is proportional to the number of active sites occupied on the adsorbent surface (Tofighy and Mohammadi, 2011). Pseudo second-order adsorption rate constant from (34.21 mg Fe$_2$O$_3$/mg.min for As), (1.72 mg Fe$_2$O$_3$/mg.min for Fe) and Mn (0.027 mg Fe$_2$O$_3$/mg.min for Mn).

In comparison, the rate of adsorption in pseudo second order kinetic between single heavy metals and combined heavy metals adsorption by IOP, the sequences are k_2 of Mn and Fe in single are higher than k_2 of Mn and Fe in combined heavy metals. In contrast, k_2 of As in single adsorption is lower than k_2 of As in combined heavy metals adsorption. Due to the fact that As was adsorbed well and faster only in 10 min at initial adsorption in combined condition.
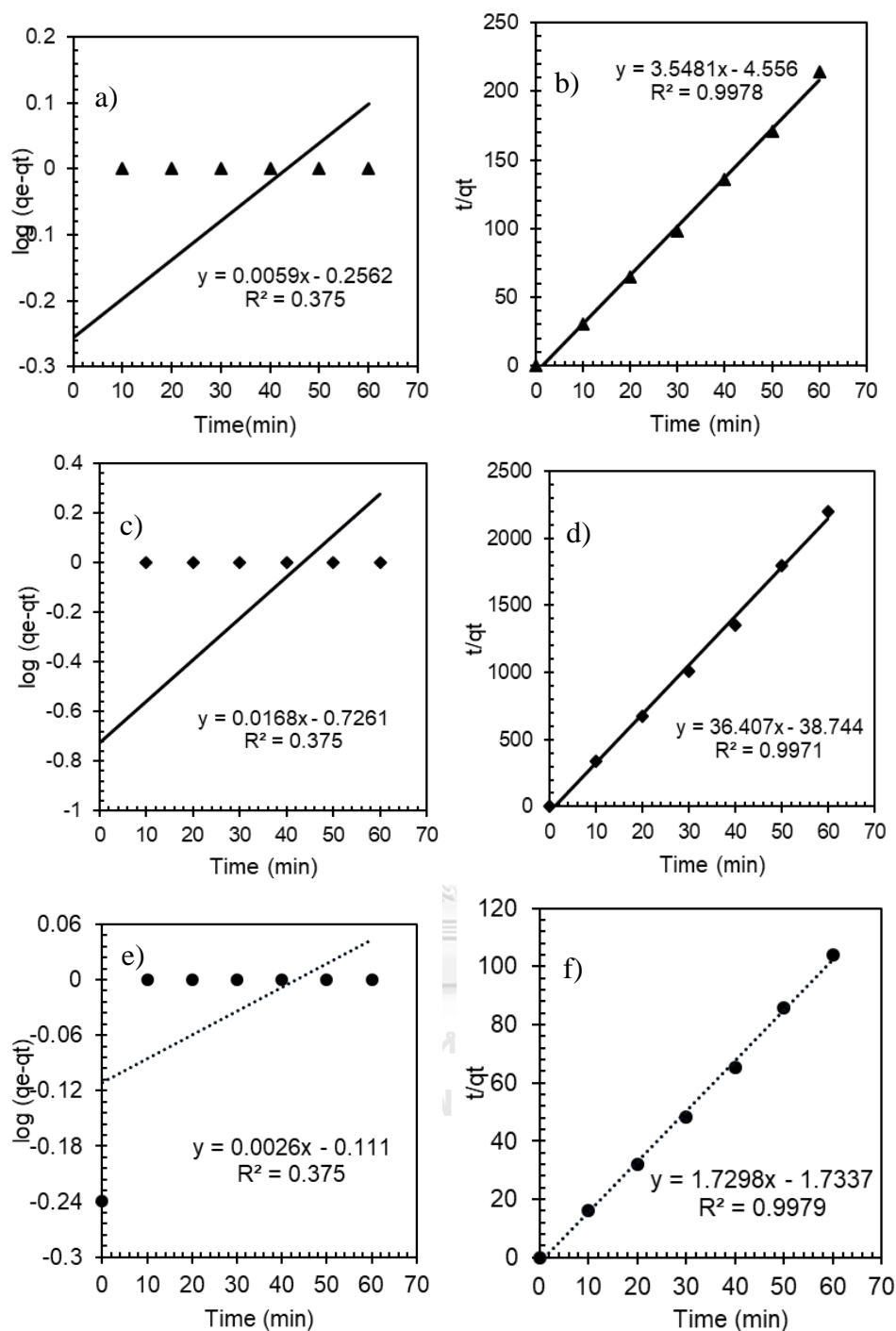
Figure 4.18 Pseudo first-order and pseudo second-order kinetic models of combined heavy metal a),b) Mn, c),d) As and e),f)Fe by using optimal dosages of IOP, respectively

Table 4.6 Kinetic pseudo first order and pseudo second-order adsorption models with different IOP doses and amount of adsorption capacity from experimental data for combined heavy metals

Heavy Metals	Dosage (mg)	$q_{e,exp}$ (mg/mg Fe_2O_3)	Pseudo first-order			Pseudo second-order		
			$q_{e,Cal}$ (mg/mgFe_2O_3)	K_1(/min)	R^2	$q_{e,Cal}$ (mg/mgFe_2O_3)	K_2(mg Fe_2O_3/mg.min)	R^2
Mn	4	1.029	1.013	0.0002	0.375	1.043	-0.463	0.993
	8	0.395	0.650	-0.010	0.375	0.404	-1.646	0.993
	12	0.066	0.088	-0.018	0.024	0.062	-23.782	0.975
	16	0.281	0.554	-0.014	0.375	0.282	-2.763	0.998
	20	0.042	0.014	-0.007	0.005	0.039	-31.455	0.938
	24	0.031	0.198	-0.037	0.375	0.030	-10.018	0.982
As	4	0.105	0.352	-0.024	0.375	0.107	-6.389	0.995
	8	0.059	0.269	-0.030	0.375	0.059	1.424E+15	1.000
	12	0.040	0.223	-0.035	0.375	0.040	1.602E+15	1.000
	16	0.027	0.188	-0.039	0.375	0.027	-34.00	0.997
	20	0.023	0.069	0.038	0.046	0.022	-229.266	0.999
	24	0.019	0.315	0.027	0.024	0.018	-88.543	0.999
Fe	4	2.244	1.455	0.009	0.375	2.263	-0.337	0.996
	8	1.247	0.028	-0.016	0.007	1.247	123.662	1.000
	12	0.831	0.918	0.002	0.375	0.831	-216.109	1.000
	16	0.577	0.774	-0.006	0.375	0.578	-1.726	0.998
	20	0.479	0.385	0.043	0.124	0.472	-15.177	0.999
	24	0.390	1.089	0.042	0.112	0.388	-4.308	1.000

4.6.2. Heavy metals on kinetic model by IOCS

a. Single heavy metals

Adsorption capacity of single heavy metals fitted as either first or pseudo second-order kinetics is presented in Figure 4.19. Table 4.7 describes parameters relating to the models. All detailed linear equations were shown in (Appendix.15). For all optimal dosages of single heavy metals Mn and Fe adsorption, the correlation coefficient R^2 of pseudo first-order provided poor fitted. However, 12 mg/L of IOCS for As adsorption were shown a better agreement with pseudo second-order than pseudo first-order after cutting the two errors data points at 20 to 30 min adsorption time with R^2 equal 0.970. Furthermore, the results indicated the best fit for pseudo second-order nearly to 1.000 with all adsorbents dosages except for some dosages of single As (24 mg/L). So, As and Fe was adsorbed on surface layer of IOCS by chemisorption.

According to the adsorption capacity IOCS of single Mn, As and Fe at 1 hr equilibrium obtained from kinetic models include 2.703, 0.026 and 12.506 mg/mgFe$_2$O$_3$, respectively. Based on Table 4.7, the order of rate adsorption capacity of optimal adsorbent dosages corresponding to kinetic model fitted include As (17.137 mg Fe$_2$O$_3$/mg.min) , Mn (0.266 mg Fe$_2$O$_3$/mg.min) and Fe (0.208 mg Fe$_2$O$_3$/mg.min) of pseudo second-order.
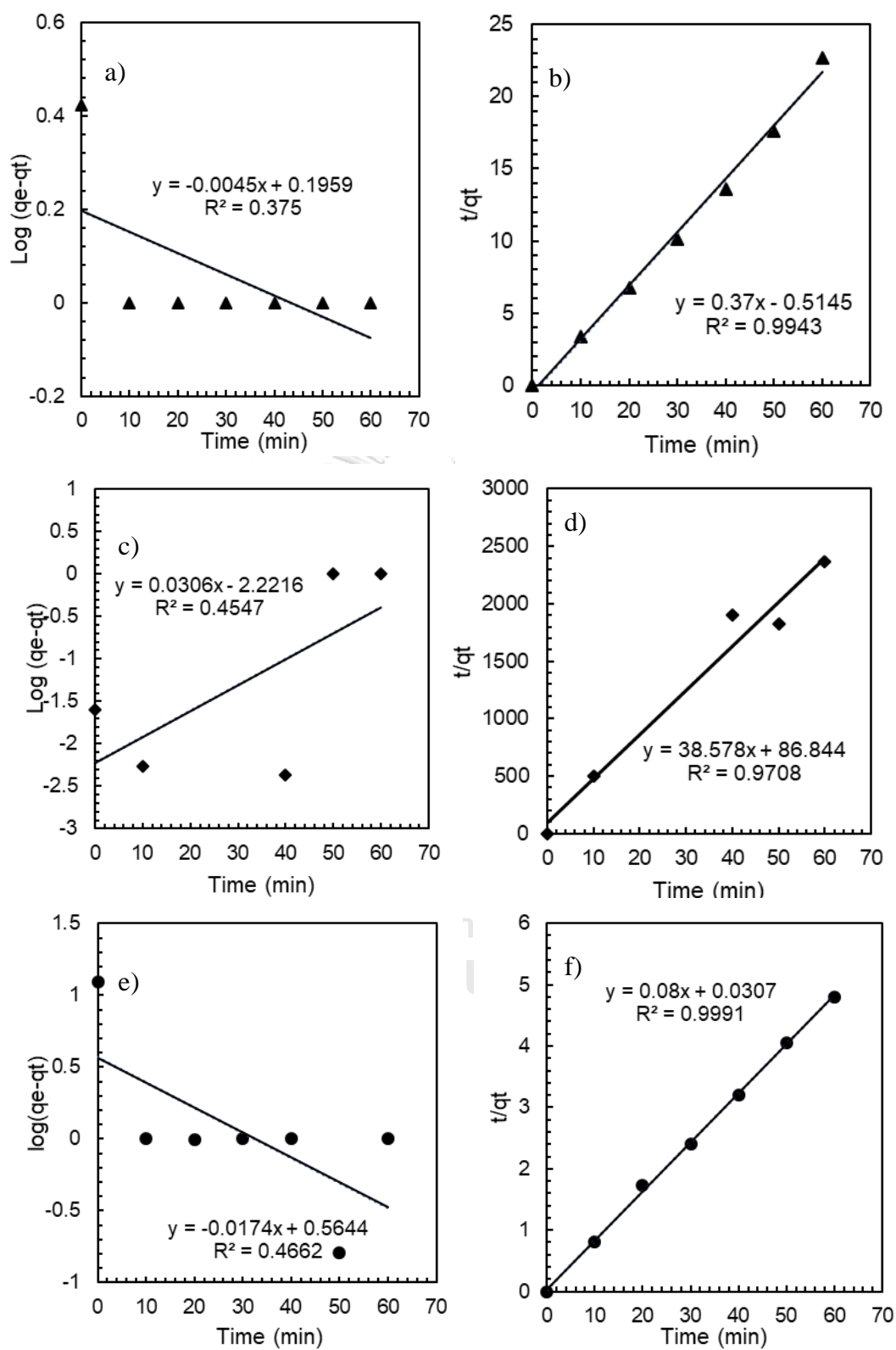
Figure 4.19 Pseudo first-order and pseudo second-order kinetic models of combined heavy metal a),b) Mn, c),d) As and e),f)Fe by using optimal dosages of IOCS, respectively

Table 4.7 Kinetic pseudo first order and pseudo second-order adsorption models with different IOCS doses and amount of adsorption capacity from experimental data for single heavy metals

Heavy Metals	Dosage (mg)	$q_{e,exp}$ (mg/mg Fe_2O_3)	Pseudo first-order			Pseudo second-order		
			$q_{e,Cal}$ (mg/mgFe_2O_3)	K_1(/min)	R^2	$q_{e,Cal}$ (mg/mgFe_2O_3)	K_2(mg Fe_2O_3/mgmin)	R^2
Mn	0.4	2.695	2.254	0.040	0.048	2.353	0.130	0.616
	0.8	2.642	1.570	0.010	0.375	2.703	0.266	0.994
	1.2	0.303	0.575	-0.013	0.375	0.331	0.535	0.915
	1.6	0.155	248.142	0.363	0.375	0.159	0.998	0.904
	2.0	0.309	0.137	-0.005	0.132	0.298	0.364	0.826
	2.4	0.045	0.139	0.004	0.001	0.023	1.552	0.236
As	0.4	0.008	0.012	-0.056	0.246	0.007	-527.088	0.481
	0.8	0.007	0.020	-0.084	0.632	0.007	-13.582	0.814
	1.2	0.025	0.006	-0.069	0.527	0.026	17.137	0.970
	1.6	0.013	0.005	-0.043	0.142	0.010	-236.008	0.682
	2.0	0.007	0.026	-0.072	0.381	0.009	19.179	0.752
	2.4	0.007	0.004	-0.110	0.702	0.020	0.648	0.079
Fe	0.4	23.44	4.326	0.034	0.375	23.969	-0.062	0.997
	0.8	12.487	3.841	0.040	0.092	12.506	0.208	0.999
	1.2	8.325	2.773	-0.054	0.130	8.320	1.670	1.000
	1.6	6.243	1.392	0.020	0.002	6.244	8.845	1.000
	2.0	4.995	2.182	0.048	0.156	4.959	-3.372	1.000
	2.4	4.1475	1.899	0.015	0.375	4.153	-0.496	1.000

b. Combined heavy metals

Adsorption capacity of single heavy metals fitted as either first or pseudo second-order kinetics is presented in Figure 4.20. Table 4.8 describes parameters relating to the models. All detailed linear equations were shown in (Appendix.16). According to the R^2 value, results indicated all adsorbents dosages of all combined heavy metals fitted better with pseudo-second order rather than pseudo first-order. Specifically, R^2 for pseudo first-order and pseudo second-order was 0.375, 0.375, 0.375 and 0.997, 0.997 and 0.997, for Mn, As and Fe, respectively. A good correlation of R^2 very close to 1.00 of pseudo second-order was explained the chemical adsorption. All adsorption capacities of combined heavy metals generated from calculated from pseudo second-order kinetic model provided a good agreement with adsorption capacities IOCS of combined heavy metals obtained from experimental data.

According to the adsorption capacity IOCS of combined Mn, As and Fe at 1hour equilibrium obtained from pseudo second order kinetic model include 3.483, 0.427 and 8.325 mg/mgFe_2O_3, respectively. Because of all heavy metals were adsorbed by IOCS following pseudo second-order, thus the order of pseudo second order adsorption rate from As (15.669 mg Fe_2O_3/mg.min for As), (-0.255 mg Fe_2O_3/mg.min for Mn) and (-1.442E+13 mg Fe_2O_3/mg.min for Fe). The negative value of k_2 is from the intercept of equation that it could be happened by Mn and Fe precipitation mechanism before adsorption happened.

As comparison, the adsorption rate capacity between single heavy metals and combined heavy metals are k_2 of single Mn is higher than k_2 of Mn in combined and k_2 of Fe in single condition is larger than k_2 of Fe in combined heavy metals of pseudo second-order. Anyway, the rate of adsorption of As was hardly comparative between single and combined cases depending on co-precipitation existing.
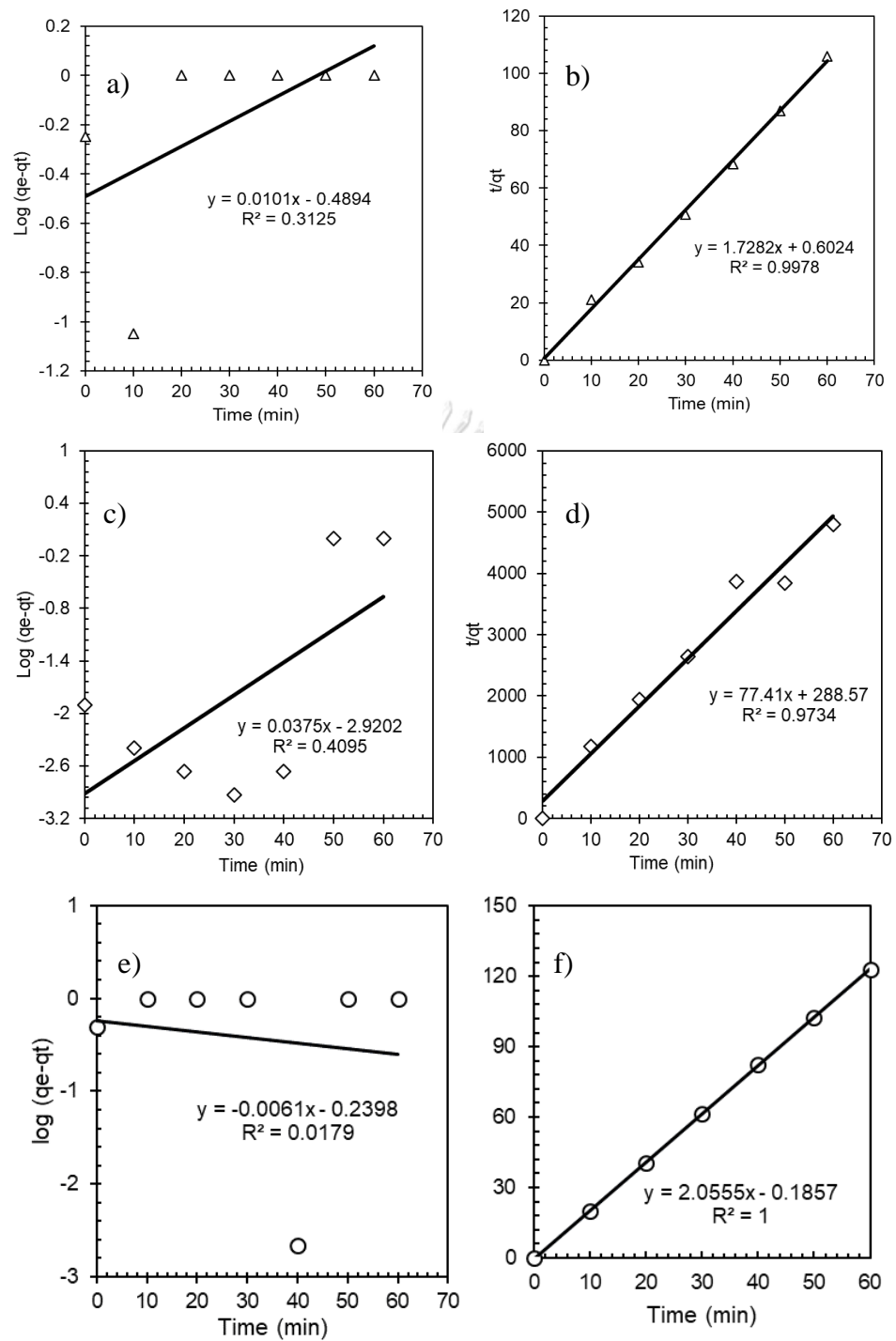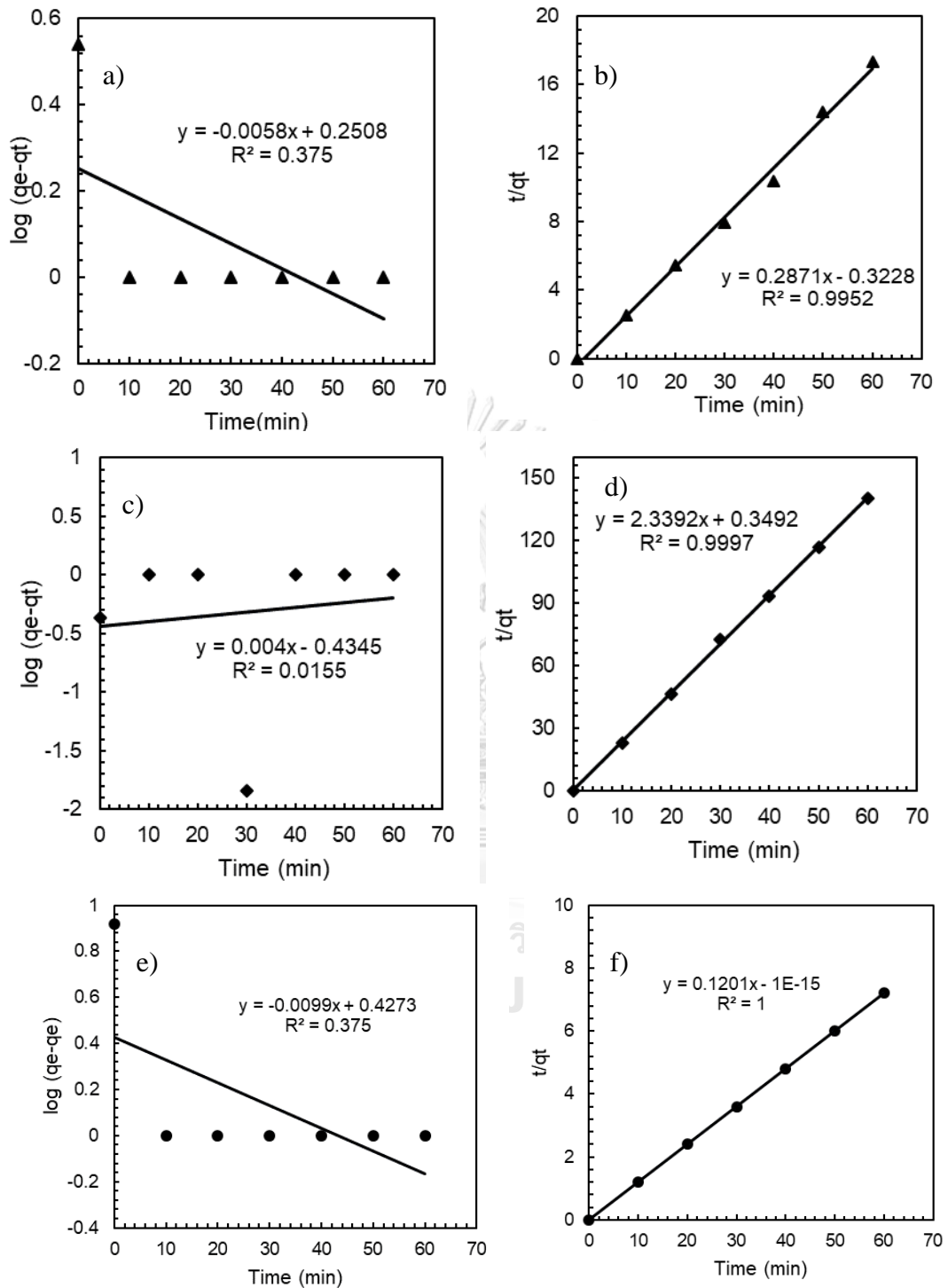
Figure 4.20 Pseudo first-order and pseudo second-order kinetic models of combined heavy metal a),b) Mn, c),d) As and e),f)Fe by using optimal dosages of IOCS, respectively

Table 4.8 Kinetic pseudo first order and pseudo second-order adsorption models with different IOCS doses and amount of adsorption capacity from experimental data for combined heavy metals

Heavy Metals	Dosage (mg)	$q_{e,exp}$ (mg/mg Fe$_2$O$_3$)	Pseudo first-order			Pseudo second-order		
			$q_{e,Cal}$ (mg/mgFe$_2$O$_3$)	K$_1$(/min)	R^2	$q_{e,Cal}$ (mg/mgFe$_2$O$_3$)	K$_2$(mg Fe$_2$O$_3$/mg.min)	R^2
Mn	0.4	9.665	0.689	0.001	0.181	9.982	0.336	0.996
	0.8	3.270	1.733	0.012	0.375	3.455	-0.526	0.985
	1.2	3.468	1.781	0.013	0.375	3.483	-0.255	0.995
	1.6	1.865	0.201	-0.002	0.080	1.872	11.786	0.915
	2.0	1.632	1.511	0.024	0.033	1.606	-0.452	0.991
	2.4	1.255	0.295	-0.016	0.140	1.266	-1.858	0.996
As	0.4	1.263	1.115	0.003	0.375	1.267	-4.723	1.000
	0.8	0.640	0.389	0.018	0.000	0.641	7.747	0.999
	1.2	0.427	0.368	-0.009	0.081	0.427	15.669	1.000
	1.6	0.316	0.467	0.010	0.002	0.317	-24.981	1.000
	2.0	0.240	0.781	0.025	0.014	0.247	-9.837	1.000
	2.4	0.213	0.122	-0.017	0.039	0.214	-520.857	1.000
Fe	0.4	24.650	4.427	0.034	0.375	24.728	-0.266	1.000
	0.8	12.487	2.819	0.041	0.051	12.484	30.552	1.000
	1.2	8.325	2.674	0.022	0.375	8.325	-1.442E+13	1.000
	1.6	6.176	2.084	0.031	0.023	6.174	1.535	1.000
	2.0	4.863	2.505	0.035	0.375	4.828	0.521	1.000
	2.4	4.162	1.939	0.015	0.373	4.163	1.923E+13	1.000

4.7. Adsorption isotherm

In order to study the adsorption behavior of the heavy metals using IOP and IOCS, the experiment for adsorption isotherm was carried out by varied IOP and IOCS dosages in range 4, 8, 12, 16, 20 and 24 mg/L with initial concentration of heavy metals in 1hour equilibrium time. This work uses two well-known isotherm models including Langmuir and Freundlich. Basically, Langmuir model was employed to understand behavior of heavy metals on the IOP or IOCS which is described the monolayer adsorption (Dada et al., 2012) . Other model is Freundlich, it was applied to explain the non-ideal, reversible and multilayer adsorption with non-uniform distribution of adsorption heat and the heterogeneous nature of adsorbents (Dada et al., 2012). The Langmuir and Freundlich models are obtained by linear form in Equation 4.20 and 4.22, respectively.

$$q_e = \frac{q_m K_L C_e}{1 + K_L C_e} \qquad\qquad \text{Eq. 4.19}$$

$$\frac{C_e}{q_e} = \frac{1}{q_m} + \frac{1}{q_m K_L} \qquad\qquad \text{Eq. 4.20}$$

Where q_{max} is maximum adsorption capacity (mg/mg Fe_2O_3), K_L is Langmuir coefficient constant (L/mg), the value of q_{max} , K_L is computed from the slope and intercept of the Langmuir plot of Ce/qe (as Y axis) versus Ce (as X axis),

$$q_e = K_F C_e^{\frac{1}{n}} \qquad\qquad \text{Eq. 4.21}$$

$$\log q_e = \log K_F + \frac{1}{n} \log C_e \qquad\qquad \text{Eq. 4.22}$$

Where K_F indicates the Freundlich isotherm capacity constant (mg/mg IO.Fe_2O_3g/L)-1/n and 1/n is an intensity of adsorption of heavy metals on multilayer of IOP and obtained by intercept and slope of Freundlich linear plot of Log Ce (as X axis) and Log qe (as Y axis), respectively.

4.7.1. Adsorption isotherm for IOP

The linear plotted of Langmuir and Freundlich models of single and combined heavy metals by using different IOP dosages were presented in Figure 4.21 and Figure 4.22. Specifically, R^2 for Langmuir and Freundlich was 0.62, 0.77, 0.75 and 0.70, 0.78 and 0.2007, for Mn, As and Fe respectively. Regarding the correlation coefficients R^2, the experimental data of single heavy metals Mn, As fitted with Freundlich better than Langmuir isotherm for the adsorption. The better fitted of Freundlich model described a heterogeneous multilayer adsorption of single Mn and As on IOP surface. Moreover, the intensity of Freundlich adsorption was lower than 1, which indicated the normal adsorption (n<1) (Foo and Hameed, 2010). The K_F of Mn was 8,139 as higher value of K_F indicated IOP has high affinity toward heavy metals which is consistence with experimental observation. Conversely, for single heavy metal Fe, Langmuir isotherm fitted better than Freundlich isotherm Therefore, the adsorption of single metal Fe onto the IOP occurred in monolayer. Because of the values of q_m of single heavy metals generated by its better fit model results, the order of the highest adsorption capacity was (0.656 mg/mgFe_2O_3 for Mn), (0.377 mg/mgFe_2O_3 for Fe) and (0.010 mg/mgFe_2O_3 for As) are presented in Table 4.9.

Specifically, R^2 for Langmuir and Freundlich was 0.779, 0.227, 0.362 and 0.811, 0.0008 and 0.030, for Mn, As and Fe respectively. According to the correlation coefficients R^2, the experimental data of combined heavy metals Mn was fitted with Freundlich isotherm better than Langmuir isotherm for the adsorption. The better fitted of Freundlich model described a heterogeneous multilayer adsorption of IOP surface for Mn. However, As and Fe adsorption of IOP was followed the Langmuir isotherm model based on R square is higher and better fitted than Freundlich model. The lower R^2 of As and Fe using Langmuir could explain the mechanism of adsorption because low R^2 values just show about the fitted model equation to data obtained from experiment. Furthermore, the reason R^2 of As and Fe, it may be fitted well with other adsorption isotherm models. Therefore, it indicated that As and Fe was adsorbed on monolayer of IOP during combined heavy metals adsorption. The maximum adsorption capacities of Mn, As and Fe at equilibrium were generated from the better fitted models include 0.699, 0.055 and 1.030 mg/mgFe_2O_3, respectively.

Because of Mn following Freundlich, adsorption intensity 1/n is -9.098 which is lower than 1 (Table 4.10). As a result, it was pointed the fact that Mn adsorption on IOPS is normal adsorption (n<1)(Dada et al., 2012) .
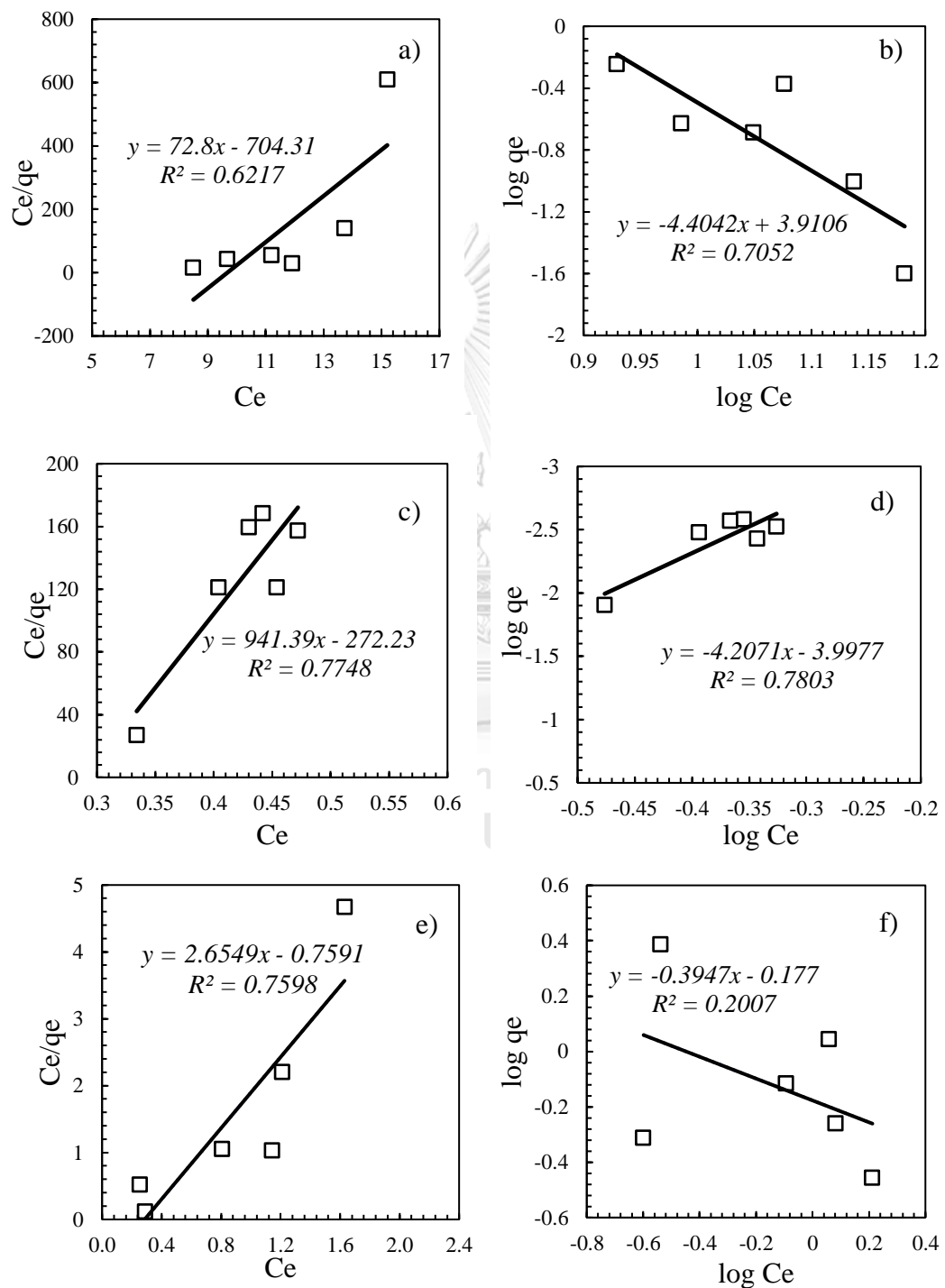
Figure 4.21 Adsorption isotherm Langmuir and Freundlich models for single heavy metals adsorption a),b)Mn, c),d) As, e),f) Fe, at pH 8 ±0.5, respectively by IOP
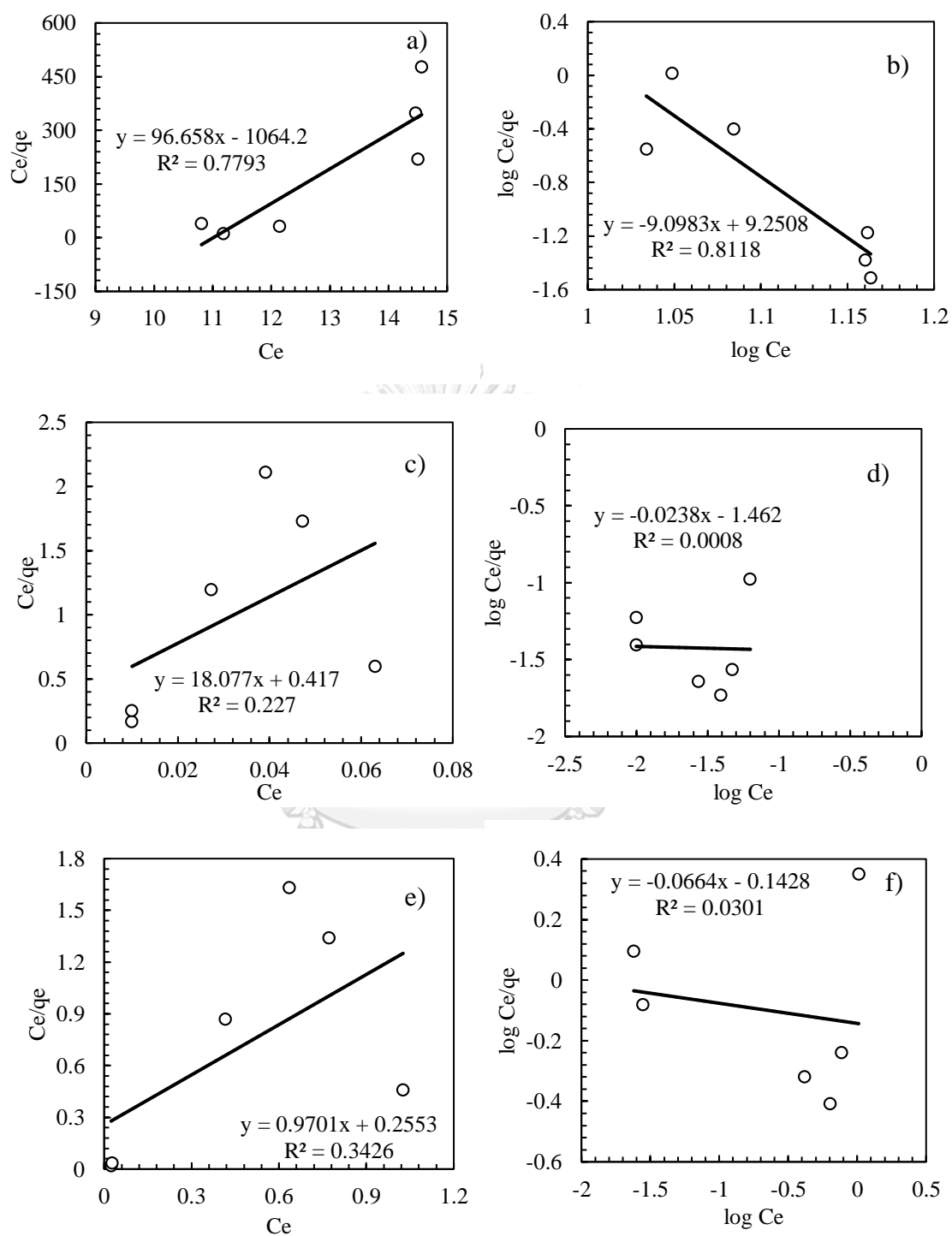
Figure 4.22. Adsorption isotherm Langmuir and Freundlich models for combined heavy metals adsorption a),b)Mn, c),d) As, e),f) Fe, at pH 8 ±0.5, respectively by IOP

Table 4.9. Langmuir and Freundlich isotherm models parameters with single heavy metal from different IOP dosages in 1hr equilibrium

Isotherm parameters	Mn	As	Fe
Langmuir isotherm			
q_{max} (mg/mg Fe_2O_3)	0.0137	0.0011	0.3766
K_L (L/mg)	1.950E-05	3.902E-06	0.496
R_L	0.278	0.268	0.116
R^2	0.621	0.774	0.7591
Freundlich isotherm			
$q,_{model}$(mg/mgFe_2O_3)	0.656	0.0101	1.14
K_F (mg/mg Fe_2O_3)	8139	0.0001	0.665
$1/n$	-4.404	-4.207	-0.394
R^2	0.705	0.780	0.201

Table 4.10 Langmuir and Freundlich isotherm models parameters with combined heavy metal from different IOP dosages in 1 hr equilibrium

Isotherm parameters	Mn	As	Fe
Langmuir isotherm			
q_{max} (mg/mg Fe_2O_3)	0.0103	0.055	1.030
K_L (L/mg)	9.72E-06	0.133	4.037
R_L	0.061	0.618	0.066
R^2	0.779	0.227	0.343
Freundlich isotherm			
$q,_{model}$ (mg/mgFe_2O_3)	0.699	0.037	0.7322
K_F (mg/mgFe_2O_3)	1.78E+08	0.0345	0.720
$1/n$	-9.098	-0.024	-0.066
R^2	0.812	0.0008	0.030

4.7.2. Adsorption isotherm for IOCS

The linear plotted of Langmuir and Freundlich models of single heavy metals by using different IOCS dosages were presented in Figure 4.23. Specifically, R^2 for Langmuir and Freundlich was 0.369, 0.682, 0.894 and 0.733, 0.670 and 0.367, for Mn, As and Fe respectively. The corresponding R^2 of 0.682 for As and 0.894 for Fe were better fitted with Langmuir models while R^2 of Freundlich are 0.670 and 0.367 for As and Fe, respectively. Additionally, the better fitted of R^2 of 0.733 from Freundlich model is only Mn which described a heterogeneous multilayer adsorption of single Mn on IOCS surface layer. Moreover, the intensity of Freundlich adsorption was -26.071 lower than 0, which is indicated the normal adsorption. Therefore, the adsorption of As and Fe metals onto the IOCS occurred in monolayer with the maximum adsorption capacity of 0.00006 mg/mg Fe_2O_3 of As, 2.554 mg/mgFe_2O_3 of Fe. Because of the values of q_m of single heavy metals generated by its better fit model, the order of the highest adsorption capacity was from (25.542 mg/mgFe_2O_3 for Fe), (0.16 mg/mgFe_2O_3 for Mn) and (0.0006 mg/mgFe_2O_3 for As) are presented in Table 4.11.

The linear plotted of Langmuir and Freundlich models of combined heavy metals by using different IOCS dosages were presented in Figure 4.24. The corresponding R^2 of 0.68 for As and 0.89 for Fe were better fitted with Langmuir models while R^2 of Freundlich are 0.67 and 0.36 for As and Fe, respectively. Based on the correlation coefficients R square from graphs, the As and Fe was better fitted with Langmuir models. However, Mn still be the same as single case that Mn was fitted with Freundlich model ($R^2 = 0.29$) which described a heterogeneous multilayer adsorption of IOCS surface for Mn. The R^2 does not well fit, it has no effect to mechanism explanation of Mn, but it could be effect to model parameters prediction, and it happened by Mn (IV) precipitation occurrence. Moreover, the intensity of Freundlich adsorption was -8.112 lower than 1, which is indicated the normal adsorption. Therefore, the adsorption of As and Fe metals onto the IOCS occurred in monolayer. The corresponding values of q_{max} at different heavy metals calculated based on its better fit model, the order of the highest adsorption capacity was from (5.347

mg/mgFe$_2$O$_3$ for Fe), (4.908 mg/mgFe$_2$O$_3$ for Mn) and (0.28 mg/mgFe$_2$O$_3$ for As) are presented in Table 4.12.
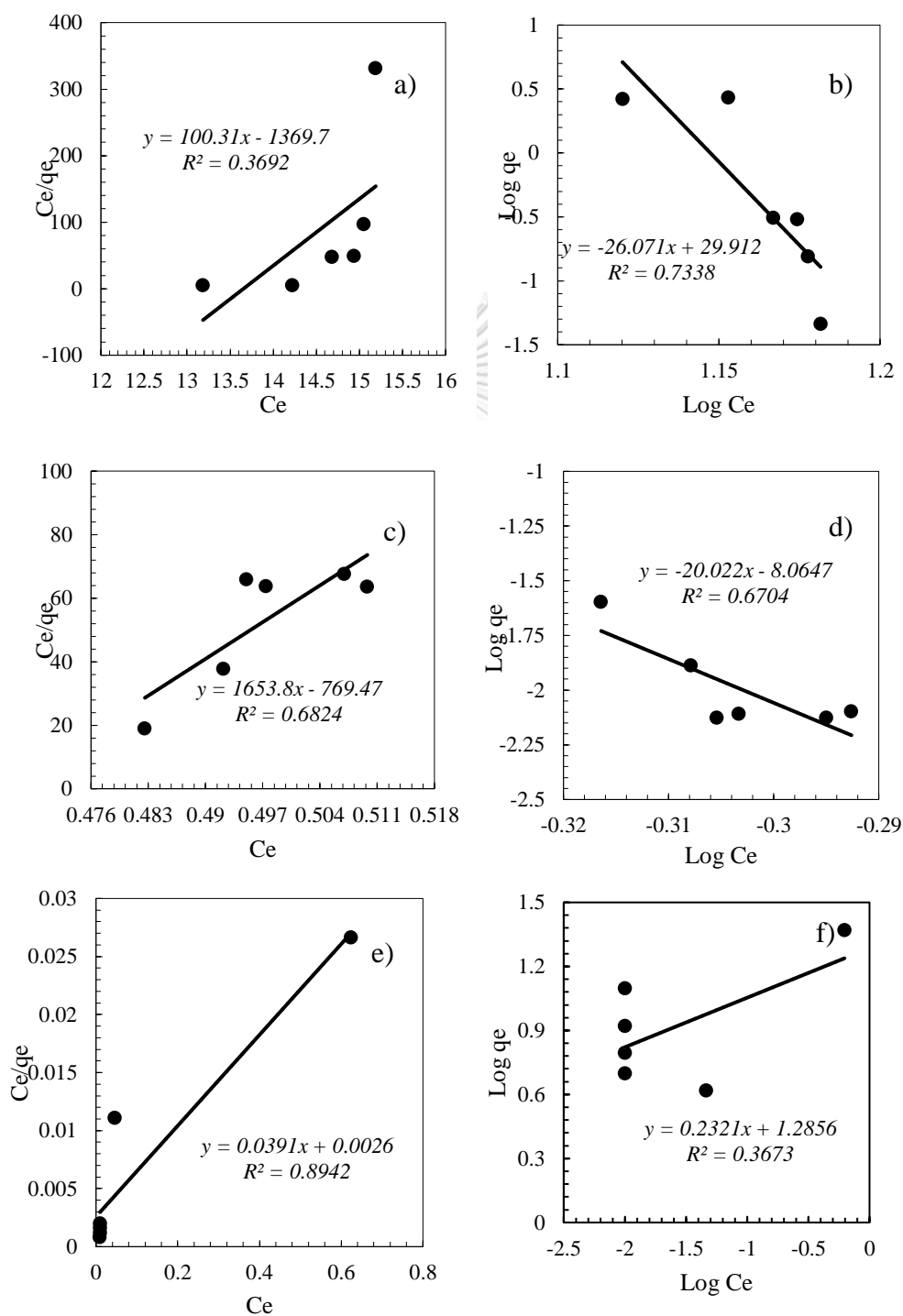
Figure 4.23 Adsorption isotherm Langmuir and Freundlich models for single heavy metals adsorption a),b)Mn, c),d) As, e),f) Fe, at pH 8 ±0.5, respectively by IOCS
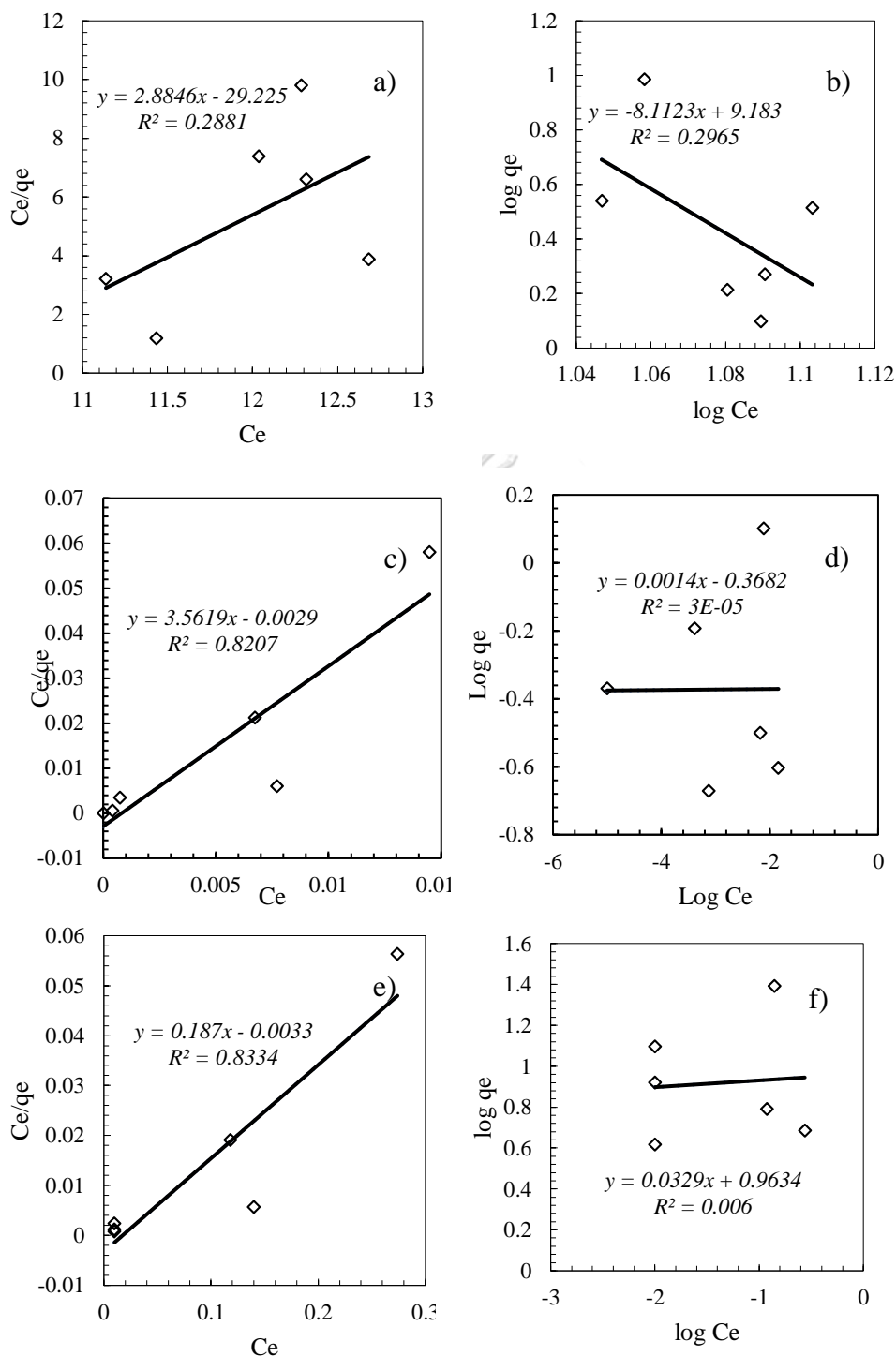
Figure 4.24 Adsorption isotherm Langmuir and Freundlich models for combined heavy metals adsorption a),b)Mn, c),d) As, e),f) Fe, at pH 8 ±0.5, respectively by IOCS

Table 4.11 Langmuir and Freundlich isotherm models parameters with single heavy metal from different IOCS dosages in 1hr equilibrium

Isotherm parameters	Mn	As	Fe
Langmuir isotherm			
q_{max} (mg/mg Fe_2O_3)	0.009	0.0006	25.542
K_L (L/mg)	7.27E-06	7.88E-08	982,4
R_L	0.999	1.000	1.02E-05
R^2	0.369	0.682	0.894
Freundlich isotherm			
q,model (mg/mgFe_2O_3)	0.16	0.018	0.525
K_F (mg/mg Fe_2O_3)	8.16E+29	8.61E-09	1.533
1/n	-26.071	-20.022	0.232
R^2	0.734	0.670	0.367

Table 4.12 Langmuir and Freundlich isotherm models parameters with combined heavy metal from different IOCS dosages in 1hr equilibrium

Isotherm parameters	Mn	As	Fe
Langmuir isotherm			
q_{max} (mg/mg Fe_2O_3)	0.35	0.28	5.347
K_L (L/mg)	0.001	9.614	164.03
R_L	0.982	0.168	0.0006
R^2	0.288	0.821	0.833
Freundlich isotherm			
q, model(mg/mg Fe_2O_3)	4.908	0.421	7.899
K_F (mg/mg Fe_2O_3)	1.52E+09	0.428	9.191
1/n	-8.112	0.001	0.033
R^2	0.297	3E-05	0.006

4.8. Comparison between IOP and IOCS on heavy metals adsorption

4.8.1. Comparison between IOP and IOCS

In summary, the removal efficiency of heavy metals in single heavy metal adsorption condition using optimal IOP dosages at equilibrium times are approximately 44, 30, 97 % of removal Mn, As and Fe, respectively (Table 4.13). In combined heavy metals adsorption condition, Mn, As and Fe were removed with about 29, 90, 92 % of initial concentration. In comparison, Mn removal efficiency slightly decreased about 15% removal from single to combined heavy metals process. However, in combined heavy metals As removal efficiency was dramatically increased to 90% compared to single As process about 30 % of removal. For Fe removal efficiency decreased from 97 to 92 % between single and combined heavy metals adsorption process.

Moreover, using IOCS optimal dosages, the removal efficiency of single metals (Mn, As and Fe) was about 14, 6 and 99 % of removal, respectively. On other hand, in combined heavy metals adsorption process, the removal efficiency of heavy metals increased together such as 27, 99 and 99% of removal Mn, As and Fe, respectively. Due to the fact of removal efficiency results, the performance of IOCS was better adsorbed heavy metals in combined process than single condition except only Fe adsorption. Basically, smaller particles size of adsorbents increased removal efficiency of pollutants through high active sites (Mondal et al., 2008). Since mean diameters of IOP about 0.85 mm smaller than 2.30 mm, so IOP adsorbed heavy metals higher than IOCS.

In contrast, the adsorption capacity IOP of heavy metals reveals a greater capacity than adsorption capacity IOCS of heavy metals in single heavy metals adsorption based on higher removal efficiency. Although, in combined IOCS was perform more effective than IOP. In addition, the removal of heavy metals using IOP in combined condition still is lower than CDWQS standard for As. So, in combined IOP and ICOS are suitable for heavy metals removal. Lastly, the cost estimation of IOP and IOCS are 1,600 Bahts and 1,643 Bahts. The price was quite the same in order to synthesize these both adsorbents (Appendix 19).

Table 4.13 Summary results of removal efficiency of optimal dosages at equilibrium time and adsorption capacity of IOP and IOCS in single and combined heavy metals pollutants

Adsorbent types	Groundwater pollution types	Heavy metals pollution	Removal Efficiency (%)	Final concentration (mg/L)	Adsorption capacity
IOP	Single	Mn	44.44	8.5	0.566
		As	30.99	0.334	0.012
		Fe	97.48	0.252	0.487
	Combined	Mn	29.34	10.81	0.280
		As	90.23	0.047	0.027
		Fe	92.28	0.772	0.576
IOCS	Single	Mn	13.81	13.18	2.64
		As	5.92	0.482	0.02
		Fe	99.99	0.01	12.48
	Combined	Mn	27.20	11.13	3.46
		As	99.99	0.00001	0.42
		Fe	99.99	0.01	8.32

4.8.2. Mechanisms of heavy metals adsorption

a. Single heavy metals adsorption

In single heavy metals condition, the heavy metals were adsorbed following the chemisorption. Therefore, chemical interaction was occurred on the surface charges of IOP and IOCS which enhanced the heavy metals removal efficiency based on PZC. Generally, the point zero charge of iron oxide was around 6 to 10. The point zero charge of IOP which highly contained Fe_2O_3 was approximately 6.20 (Mustafa, Tasleem, and Naeem, 2004)and IOCS was about 9.8 (Thirunavukkarasu et al., 2003). The pH of water was maintained around 8 ± 0.5 by $NaHCO_3$ as buffer, so there are two interaction on both adsorbents. Due to the fact of PZC of IOP is lower than pH of water, so there are negatively charge of surface IOP with positive charge of heavy metals (Mn^{2+}, As^{5+} and Fe^{2+} with hydroxide of surface IOP. Based on Smith (1999) the chemical stoichiometry could be demonstrated by Equation 4.23.

$$Fe^sOH^o + M^{2+} \leftrightarrow Fe^sOM^+ + H^+ \qquad \text{Eq. 4.23}$$

Where, M is heavy metals ions and s is surface.

In addition, PZC value of IOCS was higher than pH of water, so the adsorption on surface IOCS occurs positively charges which in turn attached negatively charge of heavy metals group (Genç-Fuhrman, Mikkelsen, and Ledin, 2007) such as $MnOO^-$, $H_2AsO_4^{2-}$ and $FeOO^-$. However, Mn was hardly to produce negatively moiety group in pH higher than neutral (Mondal et al., 2008). Hence, it leaded Mn removal of IOCS was lower than Mn removal by IOP in single adsorption. According to Thirunavukkarasu et al. (2003) As adsorption removal, the chemical reaction could follow the Equation 4.24.

$$\alpha\text{-FeOOH} + H_2AsO_4^{2-} + 3\,H^+ \rightarrow FeH_2AsO_4 + 2\,H_2O \qquad \text{Eq. 4.24}$$

Based on Katsoyiannis and Zouboulis (2002), during this procedure the responsible mechanism for the removal of arsenic was adsorption on iron oxides, which refers to the formation of surface complexes between soluble arsenic species and the solid hydroxide surface sites, as As gets in contact with the deposited iron oxides. Ferric arsenate was produced, as indicated schematically in the following Equation 4.25.

$$M\text{-FeOH} + H_3AsO_4 \rightarrow M\text{-Fe-}H_2AsO_4 + H_2O \qquad \text{Eq. 4.25}$$

On the basis molecular scale, the binding of As species can be described using spectroscopic techniques. Spectroscopic studies of As sorption on goethite and Ferric hydride, using EXAFS and XANES have indicated that arsenate was strongly bounded on these surfaces as inner sphere complexes, which are attached predominantly as binuclear bidentate linkages, whereas at low surface coverage, monodentate linkages can be formed Goldberg and Johnston (2001). Therefore, a more detailed mechanism for As(V) sorption on surface of HFO can be proposed, according to the following Equation4.26, 4.27 and 4.28 (Hiemstra and Van Riemsdijk, 1999).

$$FeOH^{1/2} + H^+(aq) + AsO_4^3(aq) \rightarrow FeOAsO_3 + H_2O \; k_1(\text{monodentate}) \quad \text{Eq. 4.26}$$

$$2FeOH^{1/2} + 2H^+(aq) + AsO_4^3(aq) \rightarrow Fe_2O_2AsO_2 + 2H_2O \; k_2(\text{bidentate}) \quad \text{Eq. 4.27}$$

$$2FeOH^{1/2} + 3H^+ + AsO_4^3(aq) \rightarrow Fe_2O_2AsOOH + 2H_2O \; k_3(\text{protonated bidentate}) \text{Eq. 4.28}$$

The aforementioned reactions suggest that arsenic was mainly sorbed on iron oxides through specific adsorption (chemisorption), where the adsorbing (arsenic) is bounded directly with the surface functional group (Cornell and Schwertmann, 2003).

Moreover, in terms of Fe removal based on observation, there also has some agglomeration of iron occurred in water after adsorption process (Figure 17.A and B). According to Fu, Dionysiou, and Liu (2014) iron possible precipitated based on this Equation 4.29 and 4.30.

$$Fe^{2+} + 2OH^- \rightarrow Fe(OH)_2 \qquad\qquad \text{Eq. 4.29}$$

$$4Fe(OH)_2 + 2H_2O + O_2 \rightarrow 4Fe(OH)_3 \qquad\qquad \text{Eq. 4.30}$$
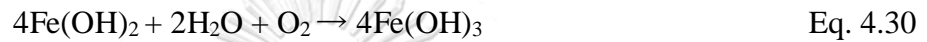
b. Combined heavy metals adsorption

In combined heavy metals adsorption process also adsorbed via similar mechanism as single heavy metals, but there also has co-precipitation As with Fe. It was considered as more mechanism that improve As removal efficiency. By Roberts et al. (2004) found that 3.8 mg/L of Ferrous concentration in water could amply sufficient for 90 % of As removal at initial concentration 500 μg/L. The mechanism of removal due to co-precipitation of As reaction followed the chemical reaction Equation 4.32 and 4.32.

$$Fe^{II}(OH)_x^{(2-x)+} + 1/4O_2 + H^+ \rightarrow Fe^{II}(OH)_x^{(3-x)+} + 1/2H_2O \qquad\qquad \text{Eq. 4.31}$$

$$Fe^{II}(OH)_x^{(3-x)+} + (3-x)H_2O \rightarrow Fe^{III}(OH)_3 + (3-x)H^+ \qquad\qquad \text{Eq. 4.32}$$
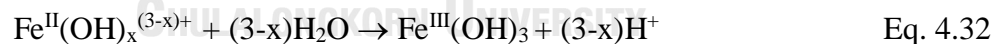
At pH around (6.5 to 8.5), co-precipitation of As was happened based on Equation 4.33 and 4.34.

$$Fe^{III}(OH)_3 \rightarrow Fe\text{-}OH \qquad\qquad \text{Eq. 4.33}$$

$$Fe\text{-}OH + As(V) \leftrightarrow Fe\text{-}As(V) \qquad\qquad \text{Eq. 4.34}$$
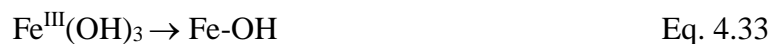
4.9. Effect of sulfate on heavy metals adsorption

Highly existing of sulfate concentration are present in groundwater sources in the range from 0 to 150 mg/L. This anion can compete with heavy metals for available surface binding sites and interfere in the removal of heavy metals by alteration of the

electrostatic charge on the surface of adsorbent (Yu et al., 2013). This part explained about the effect of sulfate in water on heavy metals removal adsorption by IOP and IOCS in equilibrium which is responded to the second objective of this study. The variation of SO_4^{2-} ranged from 0 to 150 mg/L. Removal efficiency were compared to only the dosages optimal for single and combined heavy metals condition. The optimal dosage was obtained from first objective such as 12, 12, 20 and 16 mg of IOP and 8, 12, 8 and 12 of IOCS for single Mn, As and Fe and combined these heavy metals, respectively.

4.9.1. Effect of sulfate on heavy metals adsorption by IOP

a. Single heavy metals

The optimal IOP dosages 12, 12, 20 mg/L was taken to study the effect of sulfate on single Mn, As and Fe removal in adsorption process since sulfate concentration has highly value range presence in groundwater. The removal efficiency along the time of single heavy metals by adding different concentration of sulfate were presented in the Figure 4.25. At equilibrium, without sulfate in water, 12 mg/L of IOP adsorbed Mn and As about 46.10 % and 28 %, respectively. However, by adding the concentration of sulfate 50, 100 and 150 mg/L to water, the removal efficiency of single Mn, and As gradually reduced to 7.18, 5.24 and 6.09 % of Mn removal and no removal of As, respectively. The removal Fe at equilibrium of Fe presence with 0, 50, 100 and 150 mg/L of sulfate were approximately 98.98, 99.9, 99.2 and 99.9% of removal, respectively.

Therefore, the concentration of sulfate in water are negatively significant effect on single Mn and As removal. The removal efficiency of Mn and As reduction when adding sulfate. This was because sulfate coated on the surface layer of iron oxide particles with reducing surface active site by producing more anion on surface layer. The result of Mn removal decreased when sulfate increased is similar to result from this (Pulsawat et al., 2003). They found that adsorption capacity of adsorbents on Mn was reduced after adding sulfate. Therefore, sulfate concentration in water insignificantly affect single Fe removal in adsorption since it had precipitation

mechanism between Fe, hardness and sulfate in water. Based on Mouton, van Deventer, and Vaarno (2007) the oxidation of Fe with sulfate occurred by chemical reaction in Equation 4.35.

$$2FeSO_{4(aq)} + O_{2(g)} + SO_{2(g)} + 3Ca(OH)_{2(aq)} \rightarrow 3CaSO_{4(s)} + 2Fe(OH)_{3(s)} \qquad \text{Eq. 4.35}$$
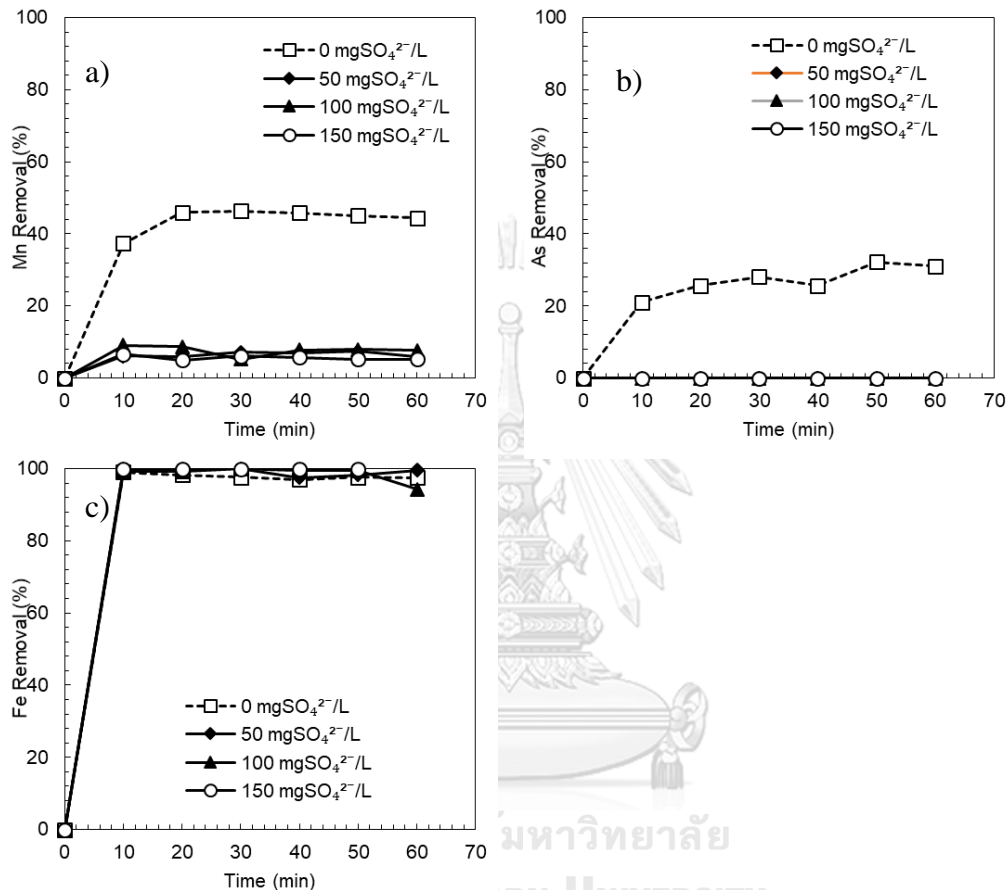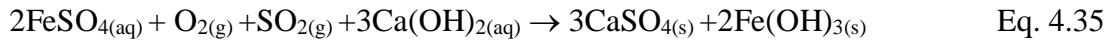
Figure 4.25 Effect of sulfate concentration on single heavy metals adsorption a)Mn, b)As and c)Fe by using optimal dosages IOP

    b. Combined heavy metals

The optimal IOP dosages 16 mg/L was used to study effect of sulfate on combined Mn, As and Fe removal in adsorption process. Removal efficiency along the times of combined heavy metals sulfate were shown in the Figure 4.26. When concentration of sulfate increased from 50, 100 and 150 mg/L, the removal efficiency of combined heavy metals at equilibrium dramatically decrease to 19.54, 20.49 and 21.28 % of Mn removal, respectively. However, after adding more sulfate into water, the removal of

As and Fe were slightly increased to 98.90, 99.51 and 100% of As removal and about 99.2, 99.6 and 99.9% of Fe removal, respectively.

Mn removal of all sulfate adjustment variation, It indicated that sulfate had negatively effect on Mn removal. Even though, SO_4^{2-} insignificantly affect As removal. The effect at lower concentration of SO_4^{2-} had a negligible on As removal because of the sulfate binding affinity for the adsorbent is weaker than arsenic (Jeong, Maohong, et al., 2007). Moreover, Fe removal of all influence various concentration of sulfate in water remained constant, it revealed that sulfate insignificantly affect Fe adsorption. The results has similar to Meng, Bang, and Korfiatis (2000) ranged 0 to 300 mg/L of sulfate insignificantly affect on As removal while Fe presence in water 1 mg/L.
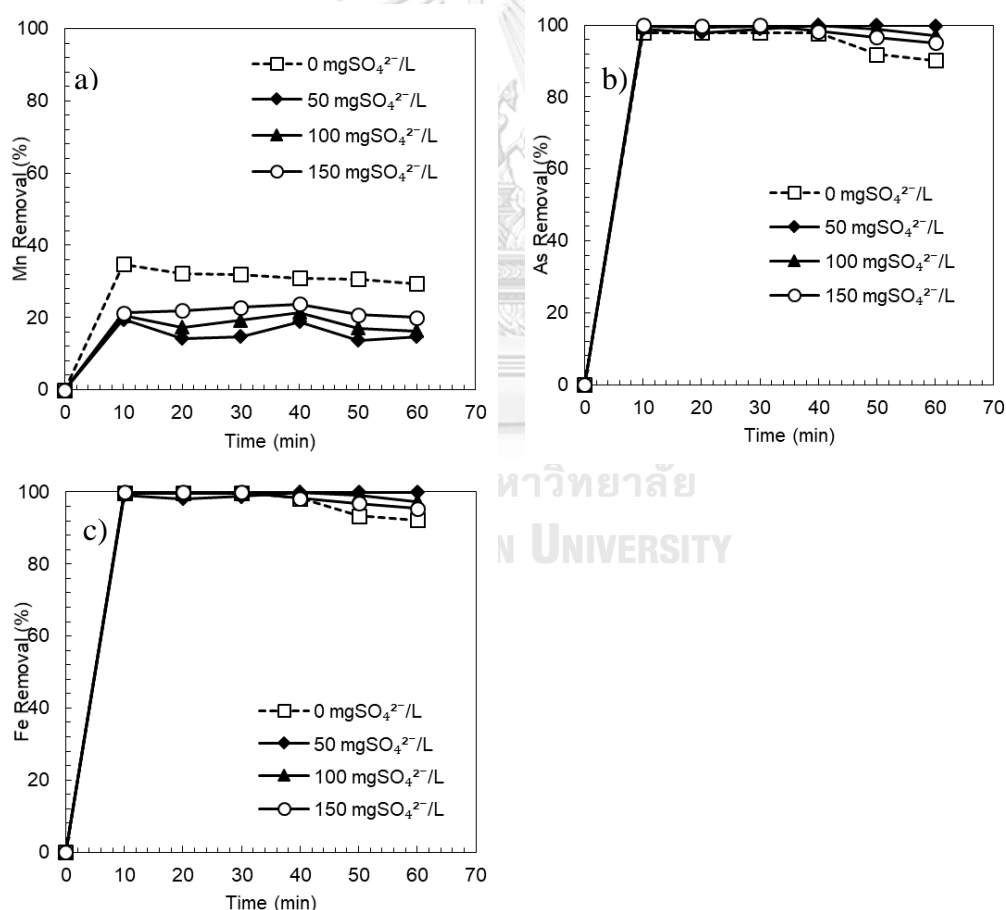
Figure 4.26 Effect of sulfate concentration on combined heavy metals adsorption a)Mn, b)As and c)Fe by using optimal dosages IOP

4.9.2. Effect of sulfate on heavy metals adsorption by IOCS

a. Single heavy metals

Based on the result from first objective, the optimal IOCS dosages 0.8, 1.2, 0.8 mg/L was taken to study effect of sulfate on single Mn, As and Fe removal in adsorption process. The removal efficiency along the time of single heavy metals by adding different concentration of sulfate were presented in the Figure 4.27. When concentration of sulfate increased from 50, 100 and 150 mg/L, the removal efficiency of Mn gradually decreased to 0.07, 10.41 and 13.37 % of removal, respectively at equilibrium. In contrast, the removal of adsorption As and Fe by adding sulfate in influence were approximately remained constant including 8.65, 4.44, and 9.70 % of As removal and 99.9, 99.9, and 97.10 % of Fe removal, respectively. Therefore, influences of sulfate significantly affect Mn adsorption of IOCS. However, presences of sulfate in water insignificantly affect As and Fe removal.
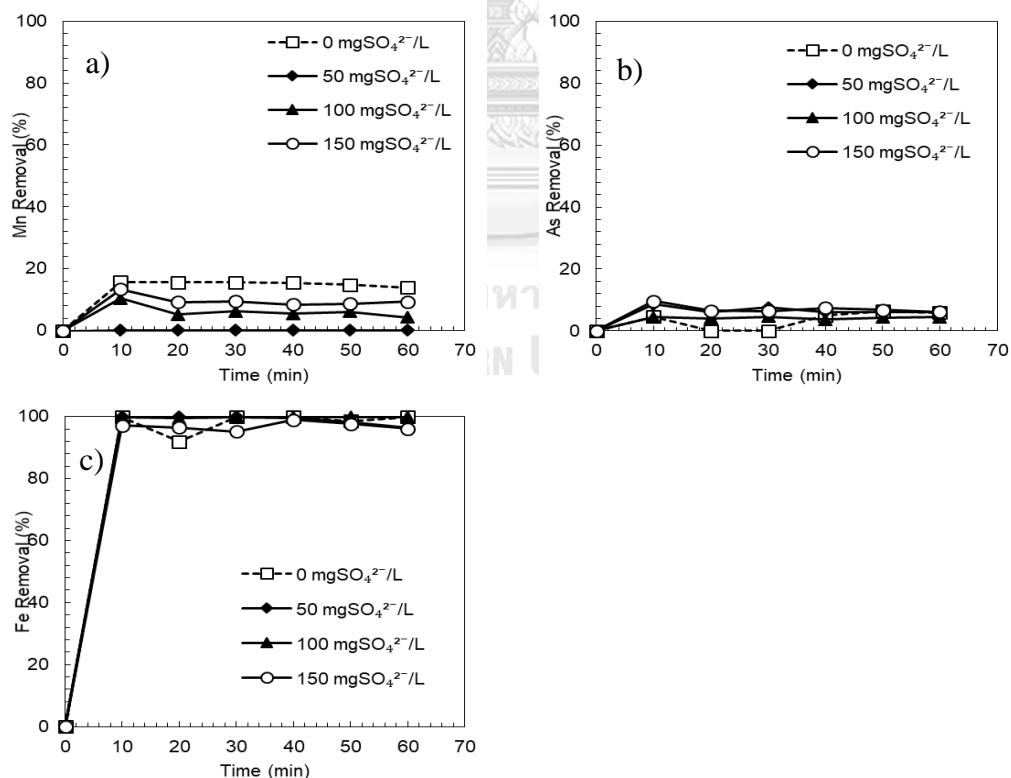
Figure 4.27 Effect of sulfate concentration on single heavy metals adsorption a)Mn, b)As and c)Fe by using optimal dosages IOCS

b. Combined heavy metals

In combined heavy metals adsorption by IOCS case, the optimal IOCS dosages as 1.2 mg/L. This dosage was used to study the effect sulfate on heavy metals adsorption removal. The relationship between removal efficiency of combined heavy metals by adding different concentration of sulfate is presented in Figure 4.28. When concentration of sulfate increased from 50 to 150 mg/L, the removal efficiency of Mn was fluctuated in the range of 21.41, 16.95 and 21.45 %, respectively while no presence of sulfate in water Mn removed 30.61%. Even though, adding sulfate in water, the removal of As and Fe removal were stable as without sulfate presence in 99 % of As and Fe removal at equilibrium. Furthermore, the value of removal efficiency of Mn indicated that sulfate significantly affects Mn adsorption through adding sulfate concentration. Additionally, As and Fe at all sulfate concentration ranges remained stable, thus sulfate presences in water has no significant effect on As and Fe removal.
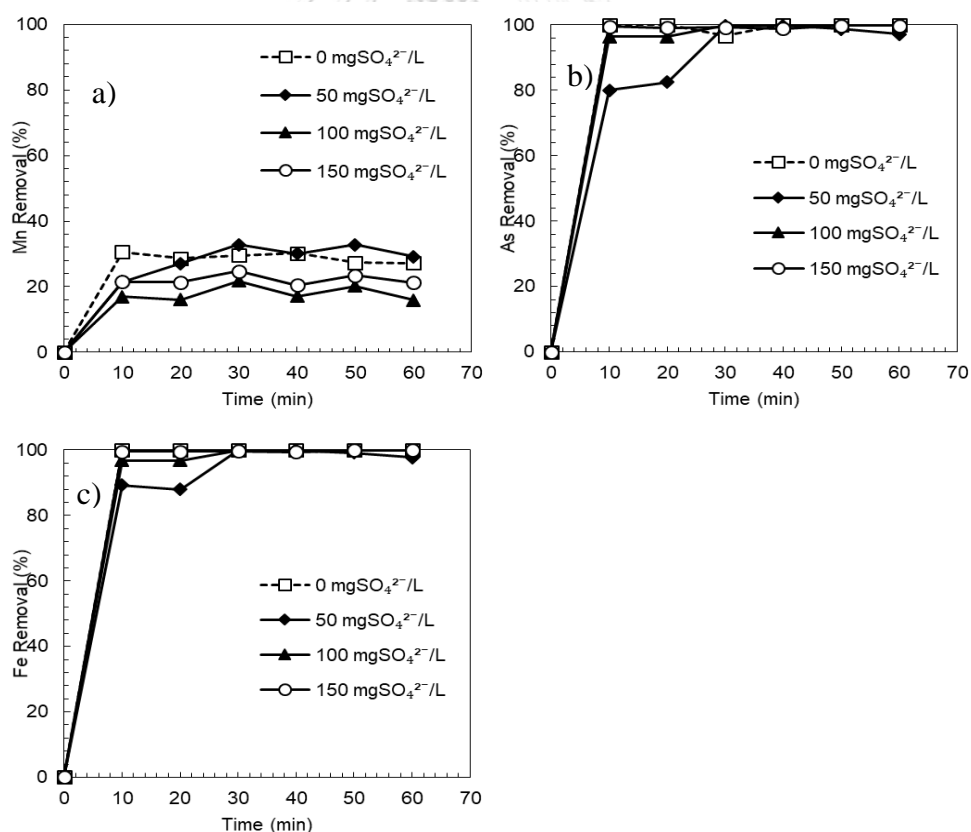
Figure 4.28 Effect of sulfate concentration on combined heavy metals adsorption a)Mn, b)As and c)Fe by using optimal dosages IOCS

4.10. Leaching heavy metals adsorption

This part described and discuss about the waste characteristic results of IOP and IOCS after adsorption process that is responded to the third objective of this study. Toxicity Characteristic Leaching Procedure (TCLP) is an EPA standard method 1311 was used to leach heavy metals from IOP and IOCS in 18 hours. The results of loading concentration of IOP and IOCS showed in Figure 4.29. Heavy metals concentration constituents on IOP was 3.050, 0.0012, 32.361 μg/mgIOP of Mn, As and Fe, respectively in single heavy metals condition and 4.002, 0.000021 and 45.486 μg/mgIOP of Mn, As and Fe, respectively in combined heavy metals condition. In addition, based on the bar chart, heavy metals concentration composition on IOCS included 0.0079, 0.00021, 0.0179 μg/mg IOCS of Mn, As and Fe, respectively in single heavy metals condition and 0.003, 0.00007 and 0.031 μg/mgIOCS of Mn, As and Fe, respectively in combined heavy metals condition. The highest of concentration Mn and Fe leached from IOP was obtained from its composition via XRF results. However, in leachate, As had lower concentration due to As has higher chemical bound with iron oxide (Goldberg and Johnston, 2001).
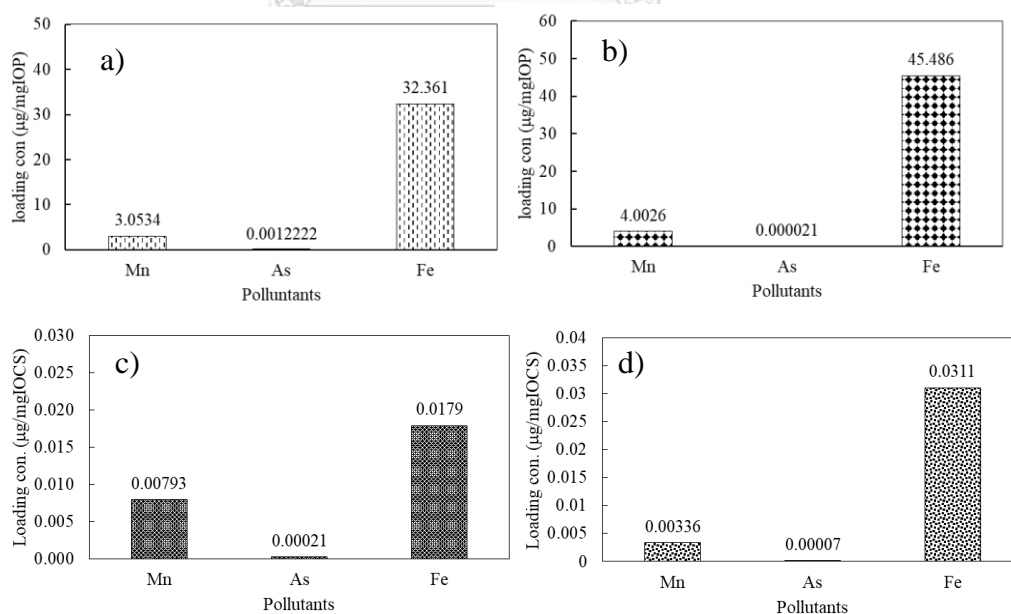
Figure 4.29 Concentration of heavy metals leachates from a),b)IOP and c), d) IOC after adsorption in a), c) single heavy metals adsorption and b), d) combined heavy metals adsorption.

Beside concentration heavy metals loading on IOP and IOCS, the concentration of heavy metals Mn, As and Fe in leaching were compared to EPA regulatory (E.P.A., 1990) and summarized in Table 4.13. Concentration of Mn, As and Fe in leachates was 145.4, 0.058, 1541 mg/L in single condition and 190.6, 0.001 and 2166 mg/L in combined condition, respectively. According to table 4.18, concentration of Mn, As and Fe in leachates are 0.378, 0.01, 0.85 mg/L in single condition and 0.160, 0.0033 and 1.480 mg/L in combined condition, respectively obtained from optimal dosages of IOCS. The EPA toxicity characteristic limits mean that wastes contain extract constituents on the list at concentrations that equal or exceed the value concentrations are identified hazardous waste characteristic (Olcay YILMAZ, Erdal COKCA, and ¨UNL¨U, 2002). By compared to the EPA regulatory standard characteristic limits, given in Table 4.14, it was observed that only Fe concentrations in the leachate from IOP in both conditions exceeded the permitted level. Therefore, only IOP adsorbed Fe are identified hazardous waste.

Table 4.14 Summary results of leaching heavy metals from IOP and IOCS compare to TCLP hazardous standard limit and WHO drinking water standard

Adsorbents types	Groundwater types	Adsorbents mass (mg)	Metals	Leaching Con. (mg/L)	Loading con. (μg/mg)	WHO drinking water standard (mg/L)	TCLP standard (mg/L)
Iron oxide particles	Single	10	Mn	145.40	3.053	0.4	-
		6.7	As	0.058	0.00122	0.01	5
		23	Fe	1541	32.361	0.3	30
	Combined	15.5	Mn	190.60	4.003	0.4	-
		15.5	As	0.0010	21.E-06	0.01	5
		15.5	Fe	2166	45.486	0.3	30
Iron oxide coated sand	Single	43.3	Mn	0.378	0.008	0.4	-
		64.4	As	0.010	0.00021	0.01	5
		42.6	Fe	0.850	0.018	0.3	30
	Combined	64.4	Mn	0.160	0.0034	0.4	-
		64.4	As	0.0033	0.0001	0.01	5
		64.4	Fe	1.480	0.031	0.3	30

CHAPTER 5
CONCLUSION AND RECOMMENDATION

5.1. Conclusion

In conclusion, this study aims to understand 1) adsorption mechanisms of Mn, As and Fe on iron oxide particles and iron oxide coated sand; 2) the effect of anion (SO_4^{2-}) on heavy metal removal efficiency, and 3) the leachability of both adsorbents after use. In summary, the results of this study include:

- Both adsorbents, IOP and IOCS were synthesized successfully based on XRF and SEM-EDS result.
- At equilibrium, based on removal efficiency of heavy metals adsorption the optimal dosages were 12, 12, 20 and 16 mg/L of IOP corresponding to 44, 30, 97 % of removal of Mn, As and Fe in single adsorption, and 29, 90, 92 % of removal of Mn, As and Fe in combined process, respectively. Moreover, for IOCS optimal dosages were 0.8, 1.2, 0.8 and 1.2 mg/L of IOCS. Removal efficiency of Mn, As and Fe for single and combined process is 14, 6 and 99 % (for single), and 27, 99 and 99% (for combined).
- Considering on optimal dosages, the equilibrium of single heavy metals adsorption process of Mn, As and Fe, and a combined heavy metal were initially fast and reached at 20, 30, 10 and 10 min, respectively. For IOCS, all of condition was faster than 10 min.
- For single heavy metal adsorption, IOP was found to have a greater adsorption capacity than IOCS. In addition, both adsorbents removed As to the level that was lower than CDWQS and WHO Standard due to co-precipitation between As and Fe happened in combined process. Therefore, IOP an IOCS were effective adsorbents to remove heavy metals from simulated groundwater.
- Heavy metals adsorbed on IOP and IOCS via chemisorption on surface layer following pseudo second-order kinetic model.
- Mn followed only Freundlich isotherm models in both adsorbents and adsorption condition. The high K_F indicated the large affinity toward Mn which is in

consistent with q_{exp} and $1/n$, which is lower than 1. This indicated that normal adsorption. However, As followed Langmuir models with the maximum adsorption capacity of 0.055, 0.28 and 0.0006 mg/mgFe_2O_3 in combined process of IOP, IOCS system and single heavy metals adsorption in IOCS system, respectively. For Fe adsorption by IOP followed Langmuir mode l with q_m about 0.376 and 1.030 mg/mgFe_2O_3 (for single and combined adsorption). For IOCS, q_m was about 25.54 and 5.35 mg/mgFe_2O_3 in single and combined heavy metals adsorption, respectively.

- For IOP in single heavy metals adsorption process, sulfate present in water significantly reduced adsorption removal of Mn and As in single and combined process. However, it insignificantly affected Fe adsorption.

- For IOCS in single heavy metals Mn adsorption was affected by the presence of SO_4^{2-}. Moreover, As and Fe removal were insignificantly affected by SO_4^{2-} in any ranges. On the other hand, in combined heavy metals process, SO_4^{2-} present in water had no effect on Mn, As and Fe removal.

- TCLP results of IOP were 3.05, 0.0012, 32.361 µg/mgIOP of Mn, As and Fe, respectively in single heavy metals condition and 4.002, 0.000021 and 45.486 µg/mgIOP of Mn, As and Fe, respectively in combined heavy metals condition.

- For IOCS, TCLP results suggested 0.0079, 0.00021, 0.0179 µg/mg IOCS of Mn, As and Fe, respectively in single heavy metals condition and 0.00336, 0.00007 and 0.0311 µg/mgIOCS of Mn, As and Fe, respectively in combined heavy metals condition.

- According to TCLP Standard, IOCS was considered non-hazardous waste, while IOP was identified to have higher Fe than the standard.

5.2. Recommendation

Based on the capacity of both adsorbents and due to this study was conducted in batch adsorption experiment, so there are three recommendation parts such as water treatments and waste management part and technical part.

• Based on the effectiveness of IOP and IOCS in terms of heavy metals removal, both adsorbents should be good adsorbents for rural water treatment in the case study, and it would be a part to reach the nation targets in accessing of safe

drinking water in Cambodia. The further research should conduct experiment in column test (Lab scale or pilot scale) in order to determine the bed volume depth before going to apply to real situation.

• If both adsorbents are applied in the real application, for single metals condition IOP should be chosen for adsorbents. For combined heavy metals case, either adsorbents can work depending on the raw materials available in the area.

• Based on results of effect sulfate on heavy metals removal, there has insignificantly effect SO_4^{2-} on heavy metals. Only Mn adsorption affects in both adsorbents, so when Mn contaminated in water, IOP and IOCS could not to remove.

• Therefore, in real application, before applying either adsorbents for Mn removal, analysis of SO_4^{2-} in raw water should be conducted. Furthermore, other anions and cations in raw water should be studied to understand the effect of ligands on IOP and IOCS adsorption process.

• For waste management, TCLP results suggested that IOP was a solid hazardous waste according to exceeding level of Fe. Therefore, this waste should be disposed of to secure landfill. However, Mn- or As-adsorbed IOP, or IOCS should be regenerated for a reuse, or can be used for construction materials such as mortar.

• Due to there has some fluctuated results in case of varied dosages, the next research should vary adsorbents doses in replication in order to find a statistic error bar for results explanation.

• Since As leachate concentration in single case of As-adsorbed IOP, or IOCS exceed WHO drinking water standard, therefore the wastes after adsorption should take attention to dispose of to secure landfill.

• Due to this study cannot separate between heavy metals that remove by adsorption and co-precipitation, thus further research should exactly consider on real adsorption capacity adsorbed by IOP or IOCS and co-precipitation.

REFERENCES

Abuh, M., et al. 2013. Kinetic rate equations application on the removal of copper (II) and zinc (II) by unmodified lignocellulosic fibrous layer of palm tree trunk-single component system studies. International Journal of Basic and Applied Science 50(4), 800-809.

Agarwal, M., and Singh, K. 2017. Heavy metal removal from wastewater using various adsorbents: a review. Journal of Water Reuse and Desalination 7(4), 387-419.

Al Rmalli, S., Haris, P. I., Harrington, C. F., and Ayub, M. 2005. A survey of arsenic in foodstuffs on sale in the United Kingdom and imported from Bangladesh. Science of the Total Environment 337(1-3), 23-30.

Alexandar S, and Pharm M. (2015). Pin:636008 AdsorptionAdsorption.

Ali, I., and Gupta, V. 2006. Advances in water treatment by adsorption technology. Nature protocols 1(6), 2661.

Asmel, N. K., Yusoff, A. R. M., Krishna, L. S., Majid, Z. A., and Salmiati, S. 2017. High concentration arsenic removal from aqueous solution using nano-iron ion enrich material (NIIEM) super adsorbent. Chemical engineering journal 317, 343-355.

ASTM. Standard Practice for Classification of Soils for Engineering Purposes (Unified Soil Classification System) 1D2487. ASTM international, 2017.

Babaee, Y., Mulligan, C. N., and Rahaman, M. S. 2018. Removal of arsenic (III) and arsenic (V) from aqueous solutions through adsorption by Fe/Cu nanoparticles. Journal of Chemical Technology & Biotechnology 93(1), 63-71.

Baig, S. A., Sheng, T., Hu, Y., Lv, X., and Xu, X. 2013. Adsorptive removal of arsenic in saturated sand filter containing amended adsorbents. Ecological engineering 60, 345-353.

Barakat, M. 2011. New trends in removing heavy metals from industrial wastewater. Arabian Journal of Chemistry 4(4), 361-377.

Benjamin, M. M., Sletten, R. S., Bailey, R. P., and Bennett, T. 1996. Sorption and filtration of metals using iron-oxide-coated sand. water research 30(11), 2609-2620.

Berg, M., et al. 2007. Magnitude of arsenic pollution in the Mekong and Red River Deltas—Cambodia and Vietnam. Science of the Total Environment 372(2-3), 413-425.

bin Jusoh, A., Cheng, W., Low, W., Nora'aini, A., and Noor, M. M. M. 2005. Study on the removal of iron and manganese in groundwater by granular activated carbon.

Desalination 182(1-3), 347-353.

Bradley, I., Straub, A., Maraccini, P., Markazi, S., and Nguyen, T. H. 2011. Iron oxide amended biosand filters for virus removal. water research 45(15), 4501-4510.

Buschmann, J., Berg, M., Stengel, C., and Sampson, M. L. 2007. Arsenic and manganese contamination of drinking water resources in Cambodia: coincidence of risk areas with low relief topography. Environmental science & technology 41(7), 2146-2152.

Buschmann, J., et al. 2008. Contamination of drinking water resources in the Mekong delta floodplains: Arsenic and other trace metals pose serious health risks to population. Environment International 34(6), 756-764.

Carolin, C. F., Kumar, P. S., Saravanan, A., Joshiba, G. J., and Naushad, M. 2017. Efficient techniques for the removal of toxic heavy metals from aquatic environment: A review. Journal of environmental chemical engineering 5(3), 2782-2799.

CDIC. (2012). Resource Development International Cambodia , groundwater arsenic in Cambodia. .

Chaudhry, S. A., Zaidi, Z., and Siddiqui, S. I. 2017. Isotherm, kinetic and thermodynamics of arsenic adsorption onto iron-zirconium binary oxide-coated sand (IZBOCS): modelling and process optimization. Journal of Molecular Liquids 229, 230-240.

Cornell, R. M., and Schwertmann, U. The iron oxides: structure, properties, reactions, occurrences and uses. John Wiley & Sons, 2003.

Crittenden, J. C., Trussell, R. R., Hand, D. W., Howe, K. J., and Tchobanoglous, G. MWH's water treatment: principles and design. John Wiley & Sons, 2012.

Dada, A., Olalekan, A., Olatunya, A., and Dada, O. 2012. Langmuir, Freundlich, Temkin and Dubinin–Radushkevich isotherms studies of equilibrium sorption of Zn2+ unto phosphoric acid modified rice husk. IOSR Journal of Applied Chemistry 3(1), 38-45.

Deka, L., and Bhattacharyya, K. G. 2018. Adsorption of As (III) from aqueous solutions by iron oxide-coated sand.

E.P.A. (1990). Hazardous Waste Management System; Identification and Listing of Hazardous Waste; Toxicity Characteristics Revisions

 (Vol. Rules and Regulations, pp. Vol. 55, No. 61). Office of Solid Waste.

Ellis, D., Bouchard, C., and Lantagne, G. 2000. Removal of iron and manganese from groundwater by oxidation and microfiltration. Desalination 130(3), 255-264.

EPAmethod1311. (1992). METHOD 1311 TOXICITY CHARACTERISTIC LEACHING PROCEDURE (pp. 33).

Faraji, M., Yamini, Y., and Rezaee, M. 2010. Magnetic nanoparticles: synthesis, stabilization, functionalization, characterization, and applications. Journal of the Iranian Chemical Society 7(1), 1-37.

Ferguson, J. F., and Gavis, J. 1972. A review of the arsenic cycle in natural waters. water research 6(11), 1259-1274.

Foo, K. Y., and Hameed, B. H. 2010. Insights into the modeling of adsorption isotherm systems. Chemical engineering journal 156(1), 2-10.

Freundlich, H. 1906. Over the adsorption in solution. J. Phys. Chem 57(385471), 1100-1107.

Fu, F., Dionysiou, D. D., and Liu, H. 2014. The use of zero-valent iron for groundwater remediation and wastewater treatment: a review. Journal of hazardous materials 267, 194-205.

Fu, F., and Wang, Q. 2011. Removal of heavy metal ions from wastewaters: a review. Journal of environmental management 92(3), 407-418.

Futalan, C. M., Kan, C.-C., Dalida, M. L., Pascua, C., and Wan, M.-W. 2011. Fixed-bed column studies on the removal of copper using chitosan immobilized on bentonite. Carbohydrate Polymers 83(2), 697-704.

Genç-Fuhrman, H., Mikkelsen, P. S., and Ledin, A. 2007. Simultaneous removal of As, Cd, Cr, Cu, Ni and Zn from stormwater: Experimental comparison of 11 different sorbents. water research 41(3), 591-602.

Goldberg, S., and Johnston, C. T. 2001. Mechanisms of arsenic adsorption on amorphous oxides evaluated using macroscopic measurements, vibrational spectroscopy, and surface complexation modeling. Journal of colloid and interface science 234(1), 204-216.

Gupta, K., and Ghosh, U. C. 2009. Arsenic removal using hydrous nanostructure iron (III)–titanium (IV) binary mixed oxide from aqueous solution. Journal of hazardous materials 161(2-3), 884-892.

Gupta, V., Saini, V., and Jain, N. 2005. Adsorption of As (III) from aqueous solutions by iron oxide-coated sand. Journal of colloid and interface science 288(1), 55-60.

He, Z. L., Yang, X. E., and Stoffella, P. J. 2005. Trace elements in agroecosystems and impacts on the environment. Journal of trace elements in medicine and biology 19(2-3), 125-140.

Herawati, N., Suzuki, S., Hayashi, K., Rivai, I., and Koyama, H. 2000. Cadmium, copper, and zinc levels in rice and soil of Japan, Indonesia, and China by soil type. Bulletin of environmental contamination and toxicology 64(1), 33-39.

Hiemstra, T., and Van Riemsdijk, W. 1999. Surface structural ion adsorption modeling of competitive binding of oxyanions by metal (hydr) oxides. Journal of colloid and interface science 210(1), 182-193.

Ho, Y.-S. 2006. Review of second-order models for adsorption systems. Journal of hazardous materials 136(3), 681-689.

Ho, Y.-S., and McKay, G. 2000. The kinetics of sorption of divalent metal ions onto sphagnum moss peat. water research 34(3), 735-742.

Hoins, U., Charlet, L., and Sticher, H. 1993. Ligand effect on the adsorption of heavy metals: The sulfate—Cadmium—Goethite case. Water, air, and soil pollution 68(1-2), 241-255.

Hu, X., Ding, Z., Zimmerman, A. R., Wang, S., and Gao, B. 2015. Batch and column sorption of arsenic onto iron-impregnated biochar synthesized through hydrolysis. water research 68, 206-216.

Huang, Y.-H., Hsueh, C.-L., Huang, C.-P., Su, L.-C., and Chen, C.-Y. 2007. Adsorption thermodynamic and kinetic studies of Pb (II) removal from water onto a versatile Al2O3-supported iron oxide. Separation and purification technology 55(1), 23-29.

Janga, Y.-C., Somannaa, Y., and Kimb, H. 2016. Source, Distribution, Toxicity and Remediation of Arsenic in the Environment–A review. International Journal of Applied Environmental Sciences 11(2), 559-581.

Janjaroen, D., Dilokdumkeng, P., and Jhandrta, P. 2018. Effect of Water Hardness and pH on Adsorption Kinetic of Arsenate on Iron Oxide. Engineering Journal 22(2), 13-23.

Jeong, Y., Fan, M., Van Leeuwen, J., and Belczyk, J. F. 2007. Effect of competing solutes on arsenic (V) adsorption using iron and aluminum oxides. JOURNAL OF ENVIRONMENTAL SCIENCES-BEIJING- 19(8), 910.

Jeong, Y., Maohong, F., Van Leeuwen, J., and Belczyk, J. F. 2007. E ect of competing solutes on arsenic (V) adsorption using ironand aluminum oxides. Journal of Environmental Sciences 19(8).

JohnD, H. 1963. Chemical equilibria affecting the behavior of manganese in natural water. Hydrological Sciences Journal 8(3), 30-37.

Kang, Y., et al. 2014. Removing arsenic from groundwater in Cambodia using high performance iron adsorbent. Environmental monitoring and assessment 186(9),

5605-5616.

Katsoyiannis, I. A., and Zouboulis, A. I. 2002. Removal of arsenic from contaminated water sources by sorption onto iron-oxide-coated polymeric materials. water research 36(20), 5141-5155.

Kitkaew, D., et al. 2018. Fast and Efficient Removal of Hexavalent Chromium from Water by Iron Oxide Particles.

Kong, Y., Kang, J., Shen, J., Chen, Z., and Fan, L. 2017. Influence of humic acid on the removal of arsenate and arsenic by ferric chloride: effects of pH, As/Fe ratio, initial As concentration, and co-existing solutes. Environmental Science and Pollution Research 24(3), 2381-2393.

Koretsky, C. 2000. The significance of surface complexation reactions in hydrologic systems: a geochemist's perspective. Journal of Hydrology 230(3-4), 127-171.

Lee, M., Paik, I. S., Kim, I., Kang, H., and Lee, S. 2007. Remediation of heavy metal contaminated groundwater originated from abandoned mine using lime and calcium carbonate. Journal of hazardous materials 144(1-2), 208-214.

Liu, J.-F., Zhao, Z.-s., and Jiang, G.-b. 2008. Coating Fe3O4 magnetic nanoparticles with humic acid for high efficient removal of heavy metals in water. Environmental science & technology 42(18), 6949-6954.

Luu, T. T. G., Sthiannopkao, S., and Kim, K.-W. 2009. Arsenic and other trace elements contamination in groundwater and a risk assessment study for the residents in the Kandal Province of Cambodia. Environment International 35(3), 455-460.

Meena, A. K., Mishra, G., Rai, P., Rajagopal, C., and Nagar, P. 2005. Removal of heavy metal ions from aqueous solutions using carbon aerogel as an adsorbent. Journal of hazardous materials 122(1-2), 161-170.

Meng, X., Bang, S., and Korfiatis, G. P. 2000. Effects of silicate, sulfate, and carbonate on arsenic removal by ferric chloride. water research 34(4), 1255-1261.

Meng, X., Korfiatis, G. P., Christodoulatos, C., and Bang, S. 2001. Treatment of arsenic in Bangladesh well water using a household co-precipitation and filtration system. water research 35(12), 2805-2810.

Ministry of Environment, M. (2012). *The Cambodian Government's Achievements and Future Direction in Sustainable Development, National Report for Rio+20 United Nations Conference on Sustainable Development*. Retrieved from https://sustainabledevelopment.un.org/content/documents/1022cambodia.pdf.

MoIMAE. (2004). DRINKING WATER QUALITY STANDARDS. MINISTRY OF INDUSTRY MINES AND ENERGY, Cambodia

Molis O'nilia, N. (2016). Cambodia: Arsenic Removal from Drinking Water through a

Variety of Options. Engineering without boder.

Mondal, P., Majumder, C., and Mohanty, B. 2008. Effects of adsorbent dose, its particle size and initial arsenic concentration on the removal of arsenic, iron and manganese from simulated ground water by Fe3+ impregnated activated carbon. Journal of hazardous materials 150(3), 695-702.

Mouton, M., van Deventer, J., and Vaarno, J. Oxidative precipitation of Fe and Mn by air/SO2. Paper presented at the The Fourth South African Conference on Base Metals. The Southern African Institute of Mining and Metallurgy. 2007.

Mustafa, S., Tasleem, S., and Naeem, A. 2004. Surface charge properties of Fe2O3 in aqueous and alcoholic mixed solvents. Journal of colloid and interface science 275(2), 523-529.

National Institute of Statistic. (2008). *General Population Census of Cambodia 2008*. Government of Cambodia.

Oladoja, N., Ololade, I., Alimi, O., Akinnifesi, T., and Olaremu, G. 2013. Iron incorporated rice husk silica as a sorbent for hexavalent chromium attenuation in aqueous system. Chemical Engineering Research and Design 91(12), 2691-2702.

Olcay YILMAZ, Erdal COKCA, and ¨UNL¨U, K. 2002. Comparison of Two Leaching Tests to Assess the E ectiveness of Cement-Based Hazardous Waste Solidi cation/Stabilization

Turkish J. Eng. Env. Sci. 27 201- 212.

Phuengprasop, T., Sittiwong, J., and Unob, F. 2011. Removal of heavy metal ions by iron oxide coated sewage sludge. Journal of hazardous materials 186(1), 502-507.

Pulsawat, W., Leksawasdi, N., Rogers, P., and Foster, L. 2003. Anions effects on biosorption of Mn (II) by extracellular polymeric substance (EPS) from Rhizobium etli. Biotechnology letters 25(15), 1267-1270.

Qdais, H. A., and Moussa, H. 2004. Removal of heavy metals from wastewater by membrane processes: a comparative study. Desalination 164(2), 105-110.

Roberts, L. C., et al. 2004. Arsenic removal with iron (II) and iron (III) in waters with high silicate and phosphate concentrations. Environmental science & technology 38(1), 307-315.

Sam Ol, O. (2011). Groundwater pollution and Risk Management in Cambodia, : Camboida National Petroleum Authority

Sang, Y., Li, F., Gu, Q., Liang, C., and Chen, J. 2008. Heavy metal-contaminated groundwater treatment by a novel nanofiber membrane. Desalination 223(1-3),

349-360.

Shallari, S., Schwartz, C., Hasko, A., and Morel, J. 1998. Heavy metals in soils and plants of serpentine and industrial sites of Albania. Science of the Total Environment 209(2-3), 133-142.

Silva, L. G., et al. 2018. Chemical and electrochemical advanced oxidation processes as a polishing step for textile wastewater treatment: A study regarding the discharge into the environment and the reuse in the textile industry. Journal of Cleaner Production 198, 430-442.

Smith, K. S. 1999. Metal sorption on mineral surfaces: an overview with examples relating to mineral deposits. The Environmental Geochemistry of Mineral Deposits. Part B: Case Studies and Research Topics 6, 161-182.

Snyder, K. V., Webster, T. M., Upadhyaya, G., Hayes, K. F., and Raskin, L. 2016. Vinegar-amended anaerobic biosand filter for the removal of arsenic and nitrate from groundwater. Journal of environmental management 171, 21-28.

Stohs, S. J., and Bagchi, D. 1995. Oxidative mechanisms in the toxicity of metal ions. Free radical biology and medicine 18(2), 321-336.

Su, C., and Puls, R. W. 2001. Arsenate and arsenite removal by zerovalent iron: effects of phosphate, silicate, carbonate, borate, sulfate, chromate, molybdate, and nitrate, relative to chloride. Environmental science & technology 35(22), 4562-4568.

Subramani, A., et al. 2012. Impact of intermediate concentrate softening on feed water recovery of reverse osmosis process during treatment of mining contaminated groundwater. Separation and purification technology 88, 138-145.

Thakur, L. S., and Mondal, P. 2017. Simultaneous arsenic and fluoride removal from synthetic and real groundwater by electrocoagulation process: parametric and cost evaluation. Journal of environmental management 190, 102-112.

Thirunavukkarasu, O., Viraraghavan, T., and Subramanian, K. 2003. Arsenic removal from drinking water using iron oxide-coated sand. Water, air, and soil pollution 142(1-4), 95-111.

Tiwari, M. K., Bajpai, S., Dewangan, U., and Tamrakar, R. K. 2015. Suitability of leaching test methods for fly ash and slag: A review. Journal of Radiation Research and Applied Sciences 8(4), 523-537.

Uy, D., et al. Kanchan arsenic filter: evaluation and applicability to Cambodia. Paper presented at the Water, sanitation and hygiene: sustainable development and multisectoral approaches. Proceedings of the 34th WEDC International Conference, United Nations Conference Centre, Addis Ababa, Ethiopia, 18-22 May 2009. 2009.

Vaaramaa, K., and Lehto, J. 2003. Removal of metals and anions from drinking water by ion exchange. Desalination 155(2), 157-170.

Viswanadham, B. V. S. (2015). Soil Mechanics. *Lecture - 7.*

Washington, U. S., and Off, G. P. Chemistry of Iron in Natural Water., 1962.

WHO. (2004). Guideline for Drinking water quality standard (Vol. 1).

Wilkie, J. A., and Hering, J. G. 1996. Adsorption of arsenic onto hydrous ferric oxide: effects of adsorbate/adsorbent ratios and co-occurring solutes. Colloids and Surfaces A: Physicochemical and Engineering Aspects 107, 97-110.

Yantasee, W., et al. 2007. Removal of heavy metals from aqueous systems with thiol functionalized superparamagnetic nanoparticles. Environmental science & technology 41(14), 5114-5119.

Yin, H., Kong, M., Gu, X., and Chen, H. 2017. Removal of arsenic from water by porous charred granulated attapulgite-supported hydrated iron oxide in bath and column modes. Journal of Cleaner Production 166, 88-97.

Yoon, S.-Y., et al. 2014. Kinetic, equilibrium and thermodynamic studies for phosphate adsorption to magnetic iron oxide nanoparticles. Chemical engineering journal 236, 341-347.

Yu, X., et al. 2013. One-step synthesis of magnetic composites of cellulose@ iron oxide nanoparticles for arsenic removal. Journal of Materials Chemistry A 1(3), 959-965.

Yuh-Shan, H. 2004. Citation review of Lagergren kinetic rate equation on adsorption reactions. Scientometrics 59(1), 171-177.

Zevi, Y., Dewita, S., Aghasa, A., and Dwinandha, D. 2018. Removal of Iron and Manganese from Natural Groundwater by Continuous Reactor Using Activated and Natural Mordenite Mineral Adsorption. IOP Conference Series: Earth and Environmental Science 111, 012016. doi: 10.1088/1755-1315/111/1/012016.

Zewail, T., and Yousef, N. 2015. Kinetic study of heavy metal ions removal by ion exchange in batch conical air spouted bed. Alexandria Engineering Journal 54(1), 83-90.

Zhang, G.-S., Qu, J.-H., Liu, H.-J., Liu, R.-P., and Li, G.-T. 2007. Removal mechanism of As (III) by a novel Fe− Mn binary oxide adsorbent: oxidation and sorption. Environmental science & technology 41(13), 4613-4619.

APPENDIX

Appendix 1. Photograph of raw materials for adsorbents synthesized Iron oxide particles, sand and Iron oxide coated sand

Appendix 2. Photograph of apparatus and experimental procedure
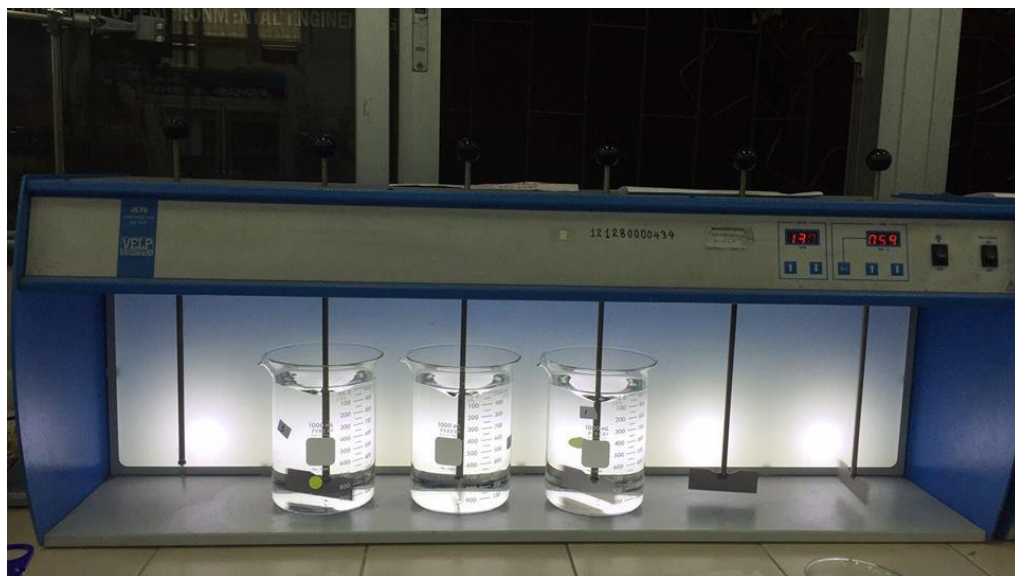
Figure 2.A. Adsorption of heavy metals by using IOP at 1 hr with 130 rpm by Jar test instrument

Figure 2. B. Leaching of heavy metals from adsorbents after process run at 18 hr with 30 rpm by TLCP test with using Multi RS-60 leaching machine.

Figure 2.C. Sieve analysis of both adsorbents

Figure 2.D. Water sampling preservation before ICP-OES analysis

Appendix 3. The analysis of pH water at differences dosages for adsorption operation
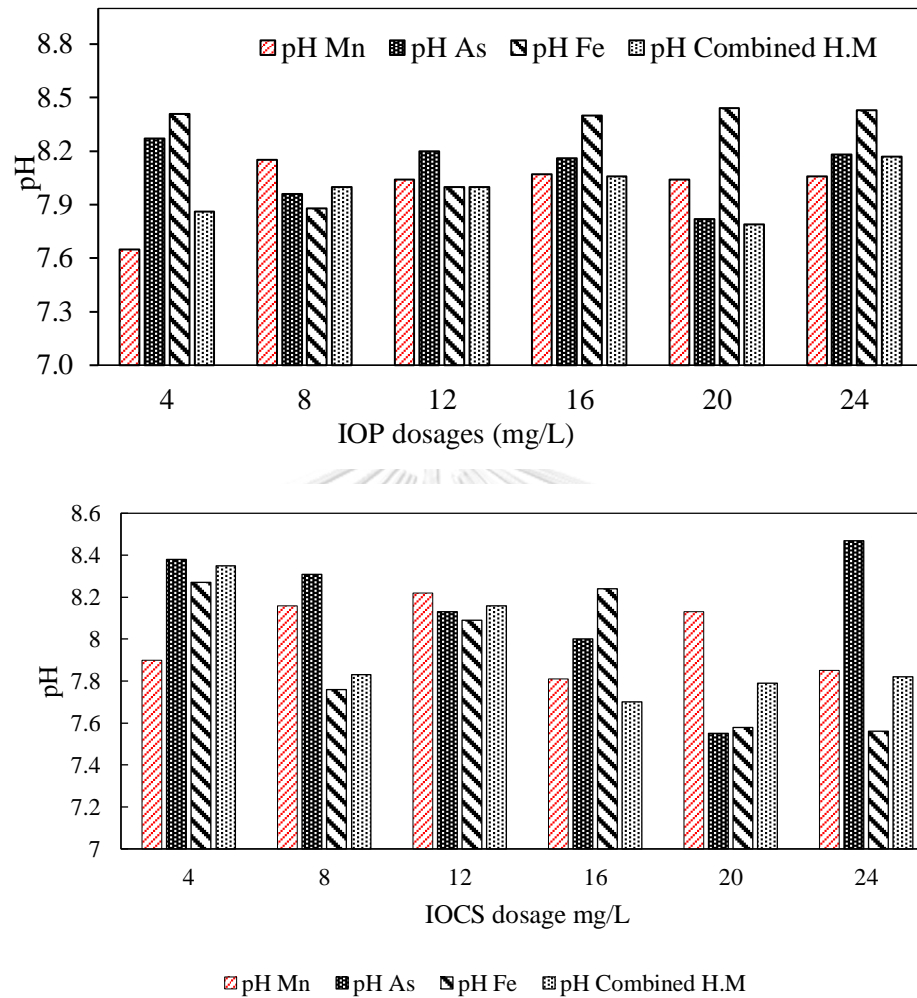
Figure 3 A. pH of water at difference adsorbents dosages a) IOP and b) IOCS

Appendix 4. The analysis of temperature of water at differences dosages for adsorption operation
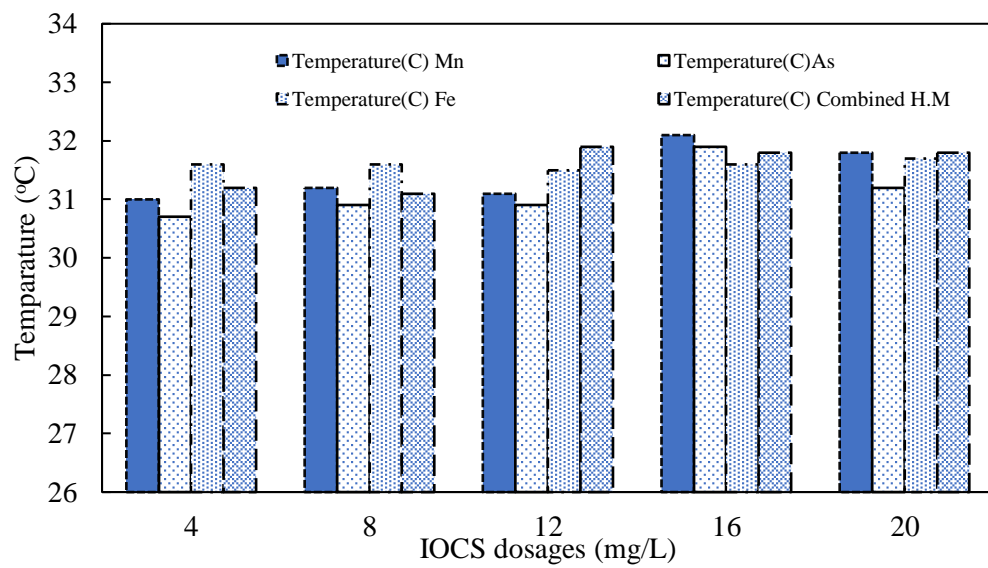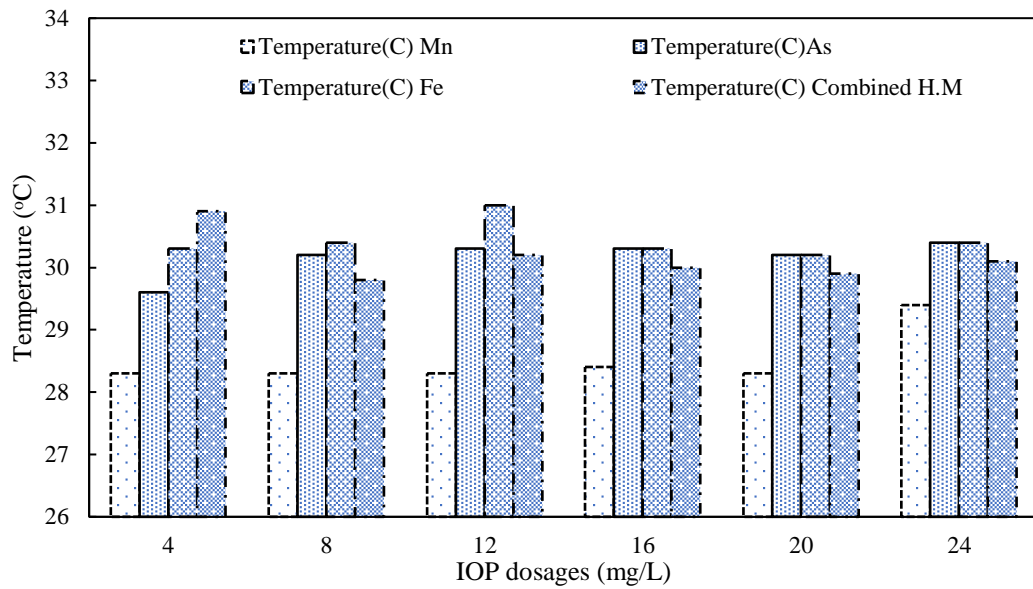
Figure 4.A. Temperature of water at difference adsorbents dosages a) IOP and b)IOCS

Appendix 4 Groundwater synthetic

This study was synthesized groundwater in four types including single manganese, arsenic and iron and a combined heavy metal. pH and temperature of water were analyzed and controlled by pH meter around 8 ± 0.5 and 30 ± 2 °C, respectively (Figure 3.and 4.A.). For concentration of heavy metals were examined by using ICP-OES with calibration curve plotted between concentration and intensity shown in
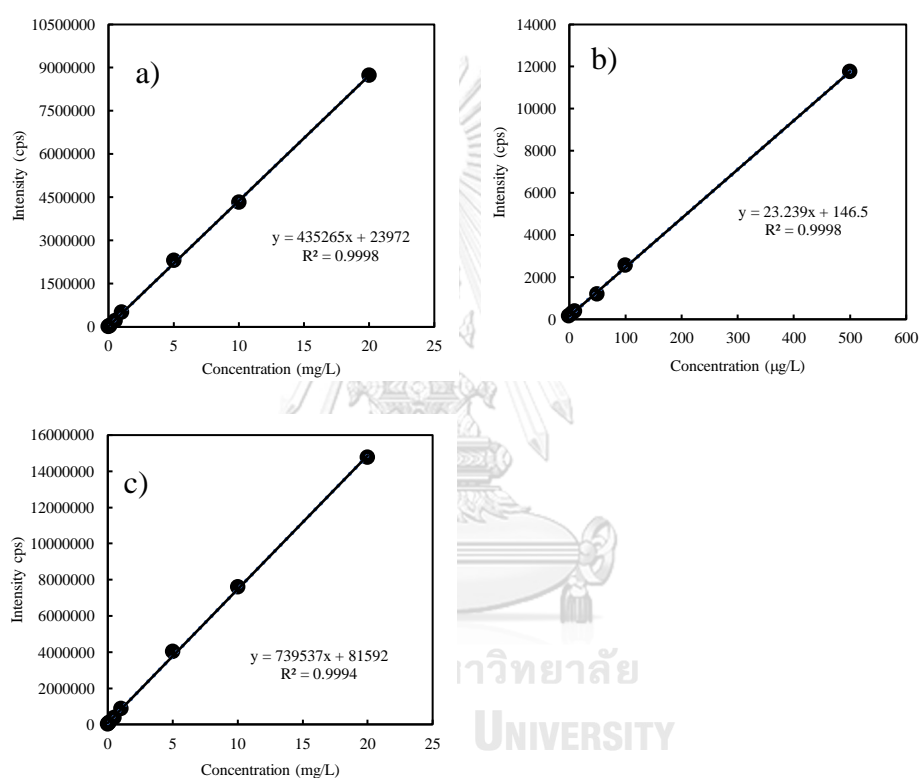
Figure 4.B Calibration curve between intensity and concentration including linear regression and R^2 for a)Mn, b)As and c)Fe for ICP-OES analysis

Appendix 5. Concentration of heavy metals along the times a) Mn, b)As and c)Fe in single heavy metals adsorption using IOP
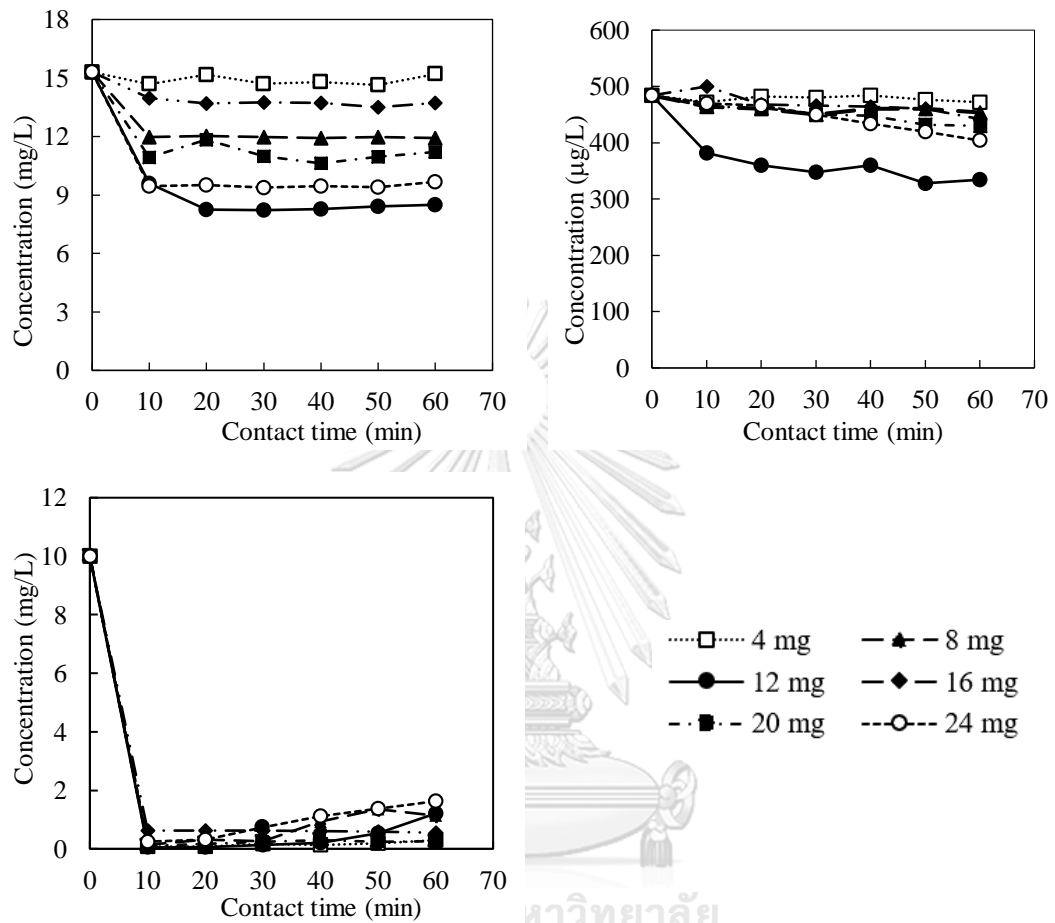
Appendix 6. Concentration of heavy metals along the times a) Mn, b)As and c)Fe in combined heavy metals adsorption using IOP
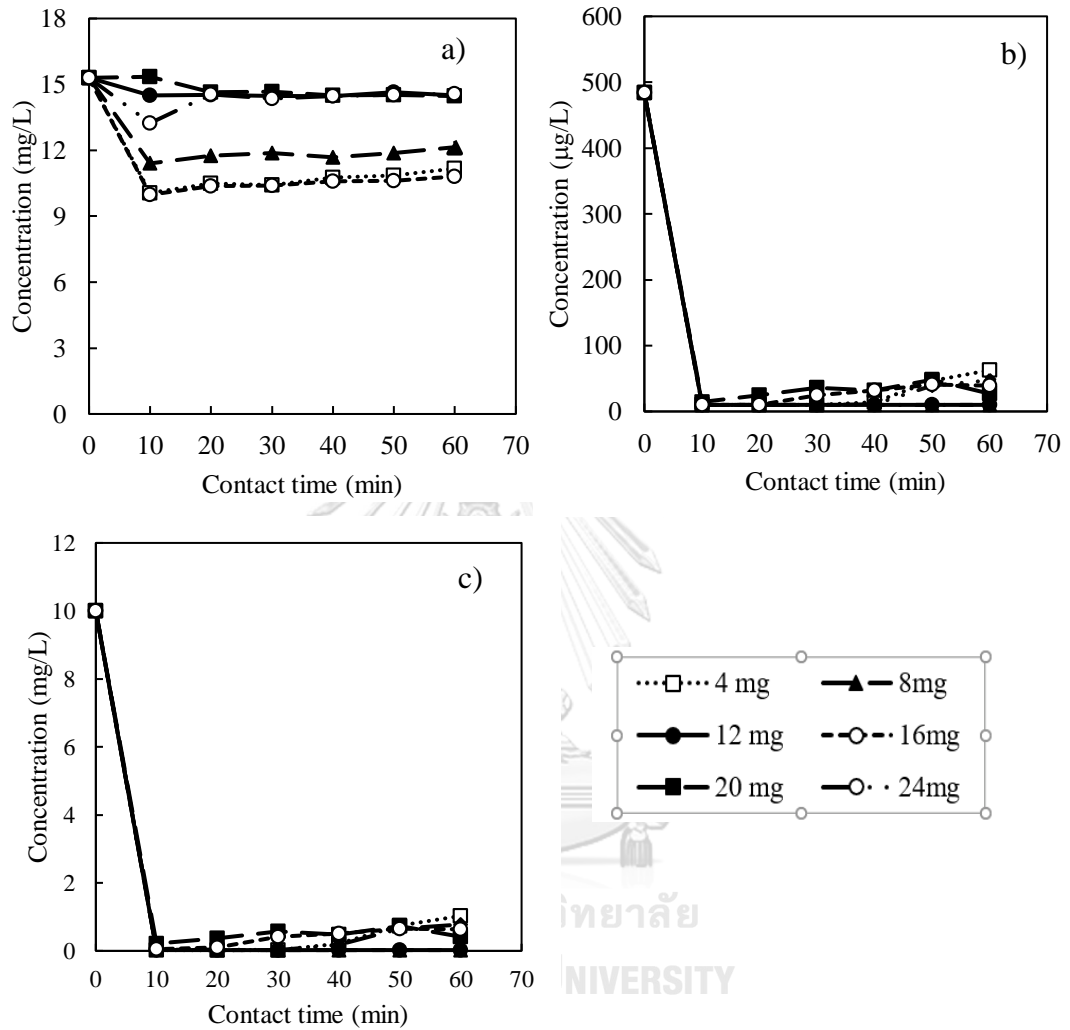
Appendix 7. Concentration of heavy metals along the times a) Mn, b)As and c)Fe in single heavy metals adsorption using IOCS
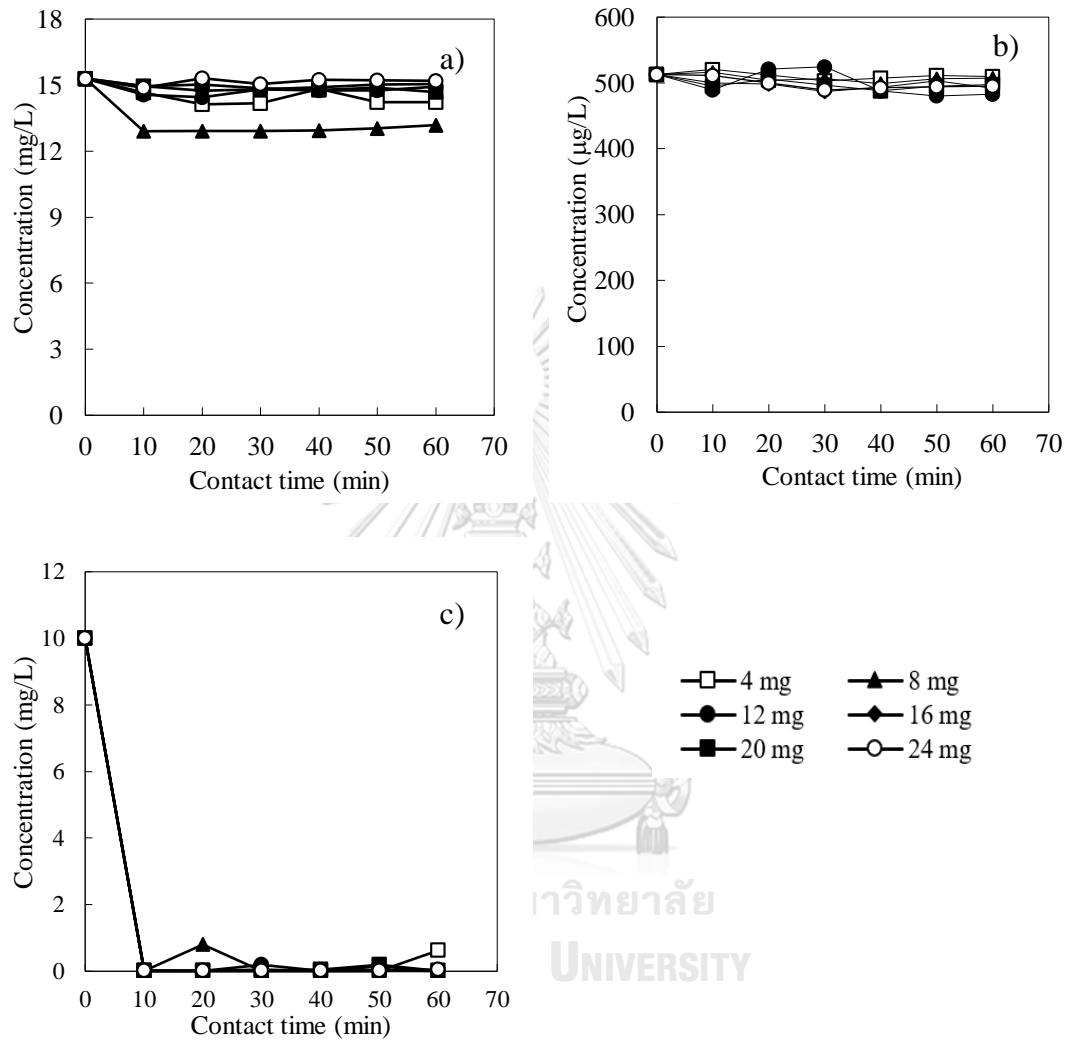
Appendix 8. Concentration of heavy metals along the times a) Mn, b)As and c)Fe in combined heavy metals adsorption using IOCS
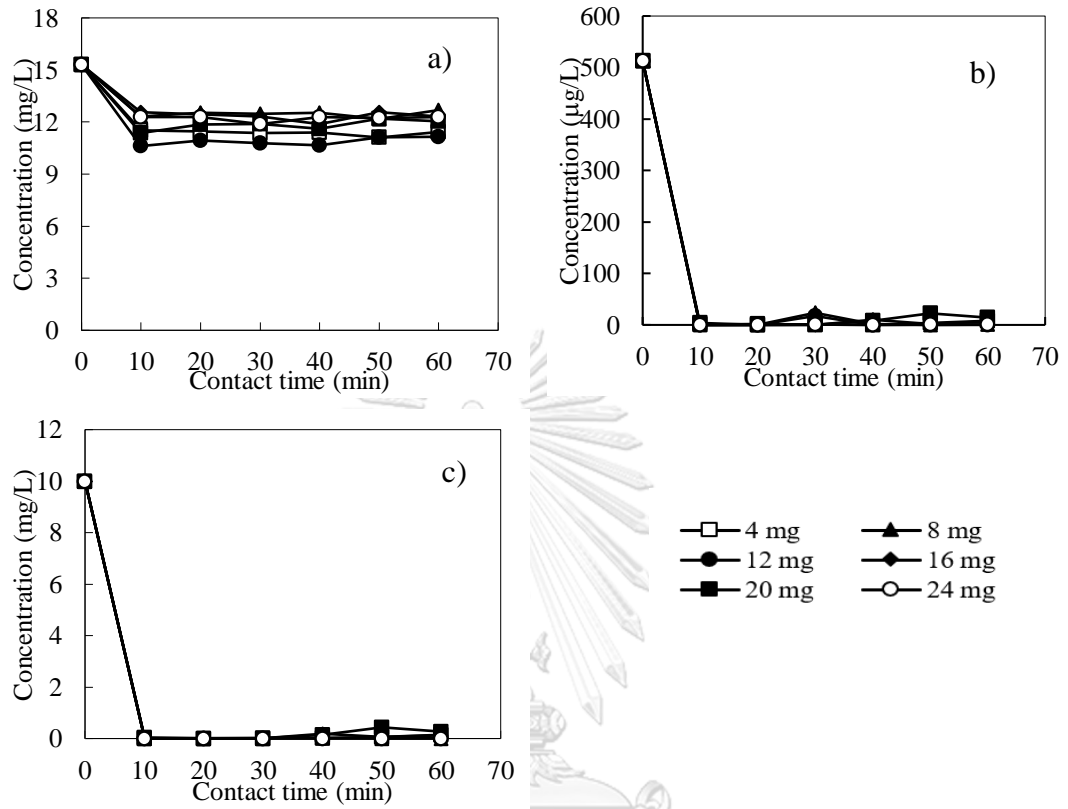
Appendix 9. Adsorption capacity of heavy metals in single adsorption using IOP

a)Mn

IOP weight (mg)	Volume (L)	Time (min)	Co (mg/L)	Ct (mg/L)	Co-Ct	q(t) (mg/mg Fe2O3)
0	1	0	15.3	15.30	0	0
4	1	10	15.3	14.68	0.62	0.155
4	1	20	15.3	15.16	0.14	0.035
4	1	30	15.3	14.70	0.60	0.15
4	1	40	15.3	14.80	0.50	0.125
4	1	50	15.3	14.64	0.66	0.165
4	1	60	15.3	15.2	0.10	0.025
8	1	10	15.3	11.98	3.32	0.415
8	1	20	15.3	12.02	3.28	0.41
8	1	30	15.3	11.96	3.34	0.417
8	1	40	15.3	11.92	3.38	0.422
8	1	50	15.3	11.96	3.34	0.417
8	1	60	15.3	11.92	3.38	0.422
12	1	10	15.3	9.58	5.72	0.476
12	1	20	15.3	8.26	7.04	0.586
12	1	30	15.3	8.22	7.08	0.59
12	1	40	15.3	8.28	7.02	0.585
12	1	50	15.3	8.40	6.90	0.575
12	1	60	15.3	8.50	6.80	0.566
16	1	10	15.3	13.96	1.34	0.08375
16	1	20	15.3	13.70	1.60	0.100
16	1	30	15.3	13.76	1.54	0.096
16	1	40	15.3	13.72	1.58	0.098
16	1	50	15.3	13.50	1.80	0.112
16	1	60	15.3	13.72	1.58	0.098
20	1	10	15.3	10.94	4.36	0.218
20	1	20	15.3	11.84	3.46	0.173
20	1	30	15.3	10.98	4.32	0.216
20	1	40	15.3	10.62	4.68	0.234
20	1	50	15.3	10.96	4.34	0.217
20	1	60	15.3	11.20	4.10	0.205
24	1	10	15.3	9.46	5.84	0.243
24	1	20	15.3	9.50	5.80	0.241
24	1	30	15.3	9.38	5.92	0.246
24	1	40	15.3	9.46	5.84	0.243
24	1	50	15.3	9.40	5.9	0.245
24	1	60	15.3	9.68	5.62	0.234

b) As

Weight (mg)	Volume (L)	Time (min)	Co (mg/L)	Ct(mg/L)	Ci-Ct	q(t)
4	1	10	0.484	0.472	0.012	0.003
4	1	20	0.484	0.482	0.002	0.001
4	1	30	0.484	0.480	0.004	0.001
4	1	40	0.484	0.484	0	0.000
4	1	50	0.484	0.476	0.008	0.002
4	1	60	0.484	0.472	0.012	0.003
8	1	10	0.484	0.464	0.02	0.003
8	1	20	0.484	0.460	0.024	0.003
8	1	30	0.484	0.450	0.034	0.004
8	1	40	0.484	0.460	0.024	0.003
8	1	50	0.484	0.460	0.024	0.003
8	1	60	0.484	0.454	0.03	0.004
12	1	10	0.484	0.382	0.102	0.009
12	1	20	0.484	0.360	0.124	0.010
12	1	30	0.484	0.348	0.136	0.011
12	1	40	0.484	0.360	0.124	0.010
12	1	50	0.484	0.328	0.156	0.013
12	1	60	0.484	0.334	0.15	0.013
16	1	10	0.484	0.500	-0.016	-0.001
16	1	20	0.484	0.468	0.016	0.001
16	1	30	0.484	0.466	0.018	0.001
16	1	40	0.484	0.464	0.02	0.001
16	1	50	0.484	0.460	0.024	0.002
16	1	60	0.484	0.442	0.042	0.003
20	1	10	0.484	0.464	0.02	0.001
20	1	20	0.484	0.462	0.022	0.001
20	1	30	0.484	0.450	0.034	0.002
20	1	40	0.484	0.448	0.036	0.002
20	1	50	0.484	0.432	0.052	0.003
20	1	60	0.484	0.430	0.054	0.003
24	1	10	0.484	0.470	0.014	0.001
24	1	20	0.484	0.466	0.018	0.001
24	1	30	0.484	0.450	0.034	0.001
24	1	40	0.484	0.434	0.05	0.002
24	1	50	0.484	0.420	0.064	0.003
24	1	60	0.484	0.404	0.08	0.003

C) Fe

Adsorbent weight (mg)	Volume (L)	Time (min)	Co (mg/L)	Ct (mg/L)	Co-Ct	q(t) (mg/mg Fe$_2$O$_3$)
0	1	0	10	10	0	#DIV/0!
4	1	10	10	0.082	9.918	2.4795
4	1	20	10	0.074	9.926	2.4815
4	1	30	10	0.160	9.840	2.4600
4	1	40	10	0.138	9.862	2.4655
4	1	50	10	0.188	9.812	2.4530
4	1	60	10	0.290	9.710	2.4275
8	1	10	10	0.138	9.862	1.2328
8	1	20	10	0.308	9.692	1.2115
8	1	30	10	0.250	9.750	1.2188
8	1	40	10	0.926	9.074	1.1343
8	1	50	10	1.356	8.644	1.0805
8	1	60	10	1.142	8.858	1.1073
12	1	10	10	0.076	9.924	0.8270
12	1	20	10	0.176	9.824	0.8187
12	1	30	10	0.334	9.666	0.8055
12	1	40	10	0.550	9.450	0.7875
12	1	50	10	0.622	9.378	0.7815
12	1	60	10	0.806	9.194	0.7662
16	1	10	10	0.050	9.950	0.6219
16	1	20	10	0.052	9.948	0.6218
16	1	30	10	0.132	9.868	0.6168
16	1	40	10	0.208	9.792	0.6120
16	1	50	10	0.532	9.468	0.5918
16	1	60	10	1.210	8.790	0.5494
20	1	10	10	0.102	9.898	0.4949
20	1	20	10	0.168	9.832	0.4916
20	1	30	10	0.240	9.760	0.4880
20	1	40	10	0.296	9.704	0.4852
20	1	50	10	0.238	9.762	0.4881
20	1	60	10	0.252	9.748	0.4874
24	1	10	10	0.246	9.754	0.4064
24	1	20	10	0.316	9.684	0.4035
24	1	30	10	0.734	9.266	0.3861
24	1	40	10	1.118	8.882	0.3701
24	1	50	10	1.362	8.638	0.3599
24	1	60	10	1.630	8.370	0.3488

Appendix 10. Adsorption capacity of heavy metals in combined adsorption using IOP
a)Mn,

Adsorbent weight (mg)	Time (min)	Co (mg/L)	Ct (mg/L)	Co-Ct	q(t) (mg/mg Fe_2O_3)
4	10	15.3	10.06	5.240	1.310
4	20	15.3	10.486	4.814	1.203
4	30	15.3	10.410	4.89	1.222
4	40	15.3	10.770	4.530	1.132
4	50	15.3	10.864	4.436	1.109
4	60	15.3	11.184	4.116	1.029
8	10	15.3	11.404	3.896	0.487
8	20	15.3	11.75	3.55	0.443
8	30	15.3	11.882	3.418	0.427
8	40	15.3	11.684	3.616	0.452
8	50	15.3	11.886	3.414	0.426
8	60	15.3	12.142	3.158	0.394
12	10	15.3	14.492	0.808	0.067
12	20	15.3	14.534	0.766	0.063
12	30	15.3	14.486	0.814	0.067
12	40	15.3	14.466	0.834	0.069
12	50	15.3	14.634	0.666	0.055
12	60	15.3	14.504	0.796	0.066
16	10	15.3	9.978	5.322	0.332
16	20	15.3	10.374	4.926	0.307
16	30	15.3	10.404	4.896	0.306
16	40	15.3	10.578	4.722	0.295
16	50	15.3	10.616	4.684	0.292
16	60	15.3	10.81	4.49	0.280
20	10	15.3	15.348	-0.048	-0.0024
20	20	15.3	14.652	0.648	0.0324
20	30	15.3	14.680	0.620	0.031
20	40	15.3	14.492	0.808	0.0404
20	50	15.3	14.522	0.778	0.0389
20	60	15.3	14.468	0.832	0.0416
24	10	15.3	13.238	2.062	0.085
24	20	15.3	14.548	0.752	0.031
24	30	15.3	14.346	0.954	0.039
24	40	15.3	14.486	0.814	0.033
24	50	15.3	14.526	0.774	0.032
24	60	15.3	14.566	0.734	0.0305

b)As

Adsorbent weight (mg)	Time (min)	Co (mg/L)	Ct(mg/L)	Co-Ct	q(t) (mg/mg Fe$_2$O$_3$)
4	0	0.484	0.484	0	0.000
4	10	0.484	0.010	0.474	0.119
4	20	0.484	0.010	0.474	0.119
4	30	0.484	0.010	0.474	0.119
4	40	0.484	0.014	0.470	0.117
4	50	0.484	0.046	0.438	0.109
4	60	0.484	0.063	0.421	0.105
8	10	0.484	0.010	0.474	0.059
8	20	0.484	0.010	0.474	0.059
8	30	0.484	0.010	0.474	0.059
8	40	0.484	0.010	0.474	0.059
8	50	0.484	0.010	0.474	0.059
8	60	0.484	0.010	0.474	0.059
12	10	0.484	0.010	0.474	0.040
12	20	0.484	0.010	0.474	0.040
12	30	0.484	0.010	0.474	0.040
12	40	0.484	0.010	0.474	0.040
12	50	0.484	0.010	0.474	0.040
12	60	0.484	0.010	0.474	0.040
16	10	0.484	0.010	0.474	0.030
16	20	0.484	0.010	0.474	0.030
16	30	0.484	0.010	0.474	0.030
16	40	0.484	0.011	0.473	0.030
16	50	0.484	0.039	0.445	0.028
16	60	0.484	0.047	0.437	0.027
20	10	0.484	0.014	0.470	0.023
20	20	0.484	0.025	0.459	0.023
20	30	0.484	0.036	0.448	0.022
20	40	0.484	0.032	0.452	0.023
20	50	0.484	0.048	0.436	0.022
20	60	0.484	0.027	0.457	0.023
24	10	0.484	0.010	0.474	0.020
24	20	0.484	0.010	0.474	0.020
24	30	0.484	0.025	0.459	0.019
24	40	0.484	0.032	0.452	0.019
24	50	0.484	0.041	0.443	0.018
24	60	0.484	0.039	0.445	0.019

C)Fe

Adsorbent weight (mg)	Time (min)	Co (mg/L)	Ct (mg/L)	Co-Ct	q(t) (mg/mg Fe2O3)
4	10	10	0.03	9.97	2.492
4	20	10	0.02	9.98	2.495
4	30	10	0.026	9.974	2.493
4	40	10	0.206	9.794	2.448
4	50	10	0.744	9.256	2.314
4	60	10	1.026	8.974	2.243
8	10	10	0.044	9.956	1.244
8	20	10	0.026	9.974	1.246
8	30	10	0.024	9.976	1.247
8	40	10	0.022	9.978	1.247
8	50	10	0.028	9.972	1.246
8	60	10	0.024	9.976	1.247
12	10	10	0.024	9.976	0.831
12	20	10	0.024	9.976	0.831
12	30	10	0.022	9.978	0.831
12	40	10	0.026	9.974	0.831
12	50	10	0.026	9.974	0.831
12	60	10	0.028	9.972	0.831
16	10	10	0.022	9.978	0.623
16	20	10	0.038	9.962	0.622
16	30	10	0.026	9.974	0.623
16	40	10	0.18	9.82	0.613
16	50	10	0.658	9.342	0.583
16	60	10	0.772	9.228	0.576
20	10	10	0.216	9.784	0.489
20	20	10	0.368	9.632	0.481
20	30	10	0.566	9.434	0.471
20	40	10	0.472	9.528	0.476
20	50	10	0.728	9.272	0.463
20	60	10	0.416	9.584	0.479
24	10	10	0.05	9.95	0.414
24	20	10	0.102	9.898	0.412
24	30	10	0.418	9.582	0.399
24	40	10	0.508	9.492	0.395
24	50	10	0.652	9.348	0.389
24	60	10	0.636	9.364	0.390

Appendix 11. Adsorption capacity of heavy metals in single adsorption using IOCS
a)Mn,

Volume (L)	IOCS (mg)	Time(min)	Ct. (mg/L)	Co (mg/L)	qt (mg/mgFe2O3)
1	0.4	10	14.666	15.3	1.585
1	0.4	20	14.126	15.3	2.935
1	0.4	30	14.168	15.3	2.83
1	0.4	40	14.834	15.3	1.165
1	0.4	50	14.228	15.3	2.68
1	0.4	60	14.222	15.3	2.695
1	0.8	10	12.906	15.3	2.9925
1	0.8	20	12.92	15.3	2.975
1	0.8	30	12.922	15.3	2.9725
1	0.8	40	12.944	15.3	2.945
1	0.8	50	13.034	15.3	2.8325
1	0.8	60	13.186	15.3	2.6425
1	1.2	10	14.554	15.3	0.622
1	1.2	20	14.448	15.3	0.710
1	1.2	30	14.806	15.3	0.412
1	1.2	40	14.75	15.3	0.458
1	1.2	50	14.768	15.3	0.443
1	1.2	60	14.936	15.3	0.303
1	1.6	10	14.964	15.3	0.21
1	1.6	20	14.746	15.3	0.34625
1	1.6	30	14.802	15.3	0.31125
1	1.6	40	14.892	15.3	0.255
1	1.6	50	15.03	15.3	0.16875
1	1.6	60	15.052	15.3	0.155
1	2	10	14.956	15.3	0.172
1	2	20	15.032	15.3	0.134
1	2	30	14.85	15.3	0.225
1	2	40	14.772	15.3	0.264
1	2	50	14.876	15.3	0.212
1	2	60	14.682	15.3	0.309
1	2.4	10	14.876	15.3	0.176666667
1	2.4	20	15.312	15.3	-0.005
1	2.4	30	15.038	15.3	0.109166667
1	2.4	40	15.242	15.3	0.024166667
1	2.4	50	15.21	15.3	0.0375
1	2.4	60	15.19	15.3	0.045833333

b)As

Volume (L)	IOCS (mg)	Time(min)	Ct(mg/L)	Co (mg/L)	qt (mg/mgFe2O3)
1	0.4	10	0.5206	0.513	-0.01900
1	0.4	20	0.512	0.513	0.00250
1	0.4	30	0.5032	0.513	0.02450
1	0.4	40	0.5076	0.513	0.01350
1	0.4	50	0.5112	0.513	0.00450
1	0.4	60	0.5098	0.513	0.00800
1	0.8	10	0.5162	0.513	-0.00400
1	0.8	20	0.5044	0.513	0.01075
1	0.8	30	0.5068	0.513	0.00775
1	0.8	40	0.499	0.513	0.01750
1	0.8	50	0.5068	0.513	0.00775
1	0.8	60	0.507	0.513	0.00750
1	1.2	10	0.4892	0.513	0.01983
1	1.2	20	0.5212	0.513	-0.00683
1	1.2	30	0.5246	0.513	-0.00967
1	1.2	40	0.4878	0.513	0.02100
1	1.2	50	0.4802	0.513	0.02733
1	1.2	60	0.4826	0.513	0.02533
1	1.6	10	0.4996	0.513	0.00837
1	1.6	20	0.4986	0.513	0.00900
1	1.6	30	0.487	0.513	0.01625
1	1.6	40	0.4934	0.513	0.01225
1	1.6	50	0.5032	0.513	0.00613
1	1.6	60	0.4922	0.513	0.01300
1	2	10	0.495	0.513	0.00900
1	2	20	0.5054	0.513	0.00380
1	2	30	0.4968	0.513	0.00810
1	2	40	0.4882	0.513	0.01240
1	2	50	0.4948	0.513	0.00910
1	2	60	0.4974	0.513	0.00780
1	2.4	10	0.511	0.513	0.00083
1	2.4	20	0.5	0.513	0.00542
1	2.4	30	0.4892	0.513	0.00992
1	2.4	40	0.4928	0.513	0.00842
1	2.4	50	0.4946	0.513	0.00767

C)Fe

Volume (L)	IOCS (mg)	Time (min)	Ct (mg/L)	Co (mg/L)	qt (mg/mgFe2O3)
1	0.4	0	10	10	0
1	0.4	10	0.02	10	24.950
1	0.4	20	0.01	10	24.975
1	0.4	30	0.01	10	24.975
1	0.4	40	0.01	10	24.975
1	0.4	50	0.01	10	24.975
1	0.4	60	0.624	10	23.440
1	0.8	10	0.01	10	12.488
1	0.8	20	0.802	10	11.498
1	0.8	30	0.01	10	12.488
1	0.8	40	0.01	10	12.488
1	0.8	50	0.14	10	12.325
1	0.8	60	0.01	10	12.488
1	1.2	10	0.01	10	8.325
1	1.2	20	0.01	10	8.325
1	1.2	30	0.188	10	8.177
1	1.2	40	0.01	10	8.325
1	1.2	50	0.026	10	8.312
1	1.2	60	0.01	10	8.325
1	1.6	10	0.01	10	6.244
1	1.6	20	0.01	10	6.244
1	1.6	30	0.052	10	6.218
1	1.6	40	0.01	10	6.244
1	1.6	50	0.01	10	6.244
1	1.6	60	0.01	10	6.244
1	2	10	0.01	10	4.995
1	2	20	0.01	10	4.995
1	2	30	0.01	10	4.995
1	2	40	0.052	10	4.974
1	2	50	0.192	10	4.904
1	2	60	0.01	10	4.995
1	2.4	10	0.01	10	4.163
1	2.4	20	0.01	10	4.163
1	2.4	30	0.01	10	4.163
1	2.4	40	0.01	10	4.163
1	2.4	50	0.01	10	4.163
1	2.4	60	0.046	10	4.148

Appendix 12. Adsorption capacity of heavy metals in combined adsorption using IOCS a)Mn

Volume (L)	IOCS (mg)	Time (min)	Ct (mg/L)	Co (mg/L)	qe (mg/mgFe2O3)
1	0.4	10	11.532	15.3	9.42
1	0.4	20	11.444	15.3	9.64
1	0.4	30	11.362	15.3	9.845
1	0.4	40	11.384	15.3	9.79
1	0.4	50	11.106	15.3	10.485
1	0.4	60	11.434	15.3	9.665
1	0.8	10	12.308	15.3	3.74
1	0.8	20	12.544	15.3	3.445
1	0.8	30	12.474	15.3	3.532
1	0.8	40	12.528	15.3	3.465
1	0.8	50	12.176	15.3	3.905
1	0.8	60	12.684	15.3	3.27
1	1.2	10	10.616	15.3	3.903
1	1.2	20	10.922	15.3	3.648
1	1.2	30	10.776	15.3	3.77
1	1.2	40	10.672	15.3	3.856
1	1.2	50	11.124	15.3	3.48
1	1.2	60	11.138	15.3	3.468
1	1.6	10	12.564	15.3	1.71
1	1.6	20	12.43	15.3	1.793
1	1.6	30	12.328	15.3	1.857
1	1.6	40	11.88	15.3	2.137
1	1.6	50	12.556	15.3	1.715
1	1.6	60	12.316	15.3	1.865
1	2	10	11.368	15.3	1.966
1	2	20	11.858	15.3	1.721
1	2	30	11.878	15.3	1.711
1	2	40	11.604	15.3	1.848
1	2	50	12.184	15.3	1.558
1	2	60	12.036	15.3	1.632
1	2.4	10	12.278	15.3	1.259
1	2.4	20	12.3	15.3	1.25
1	2.4	30	11.88	15.3	1.425
1	2.4	40	12.28	15.3	1.258
1	2.4	50	12.214	15.3	1.285
1	2.4	60	12.288	15.3	1.255

b)As

Volume (L)	IOCS (mg)	Time (min)	Ct (mg/L)	Co (mg/L)	qe (mg/mgFe2O3)
1	0.4	10	0.000946	0.513	1.280
1	0.4	20	0.001338	0.513	1.279
1	0.4	30	0.000152	0.513	1.282
1	0.4	40	0.00001	0.513	1.282
1	0.4	50	0.003826	0.513	1.273
1	0.4	60	0.0077	0.513	1.263
1	0.8	10	0.00001	0.513	0.641
1	0.8	20	0.00001	0.513	0.641
1	0.8	30	0.02348	0.513	0.612
1	0.8	40	0.00168	0.513	0.639
1	0.8	50	0.00001	0.513	0.641
1	0.8	60	0.000414	0.513	0.641
1	1.2	10	0.00001	0.513	0.427
1	1.2	20	0.00001	0.513	0.427
1	1.2	30	0.017278	0.513	0.413
1	1.2	40	0.00001	0.513	0.427
1	1.2	50	0.00001	0.513	0.427
1	1.2	60	0.00001	0.513	0.427
1	1.6	10	0.00001	0.513	0.321
1	1.6	20	0.00001	0.513	0.321
1	1.6	30	0.00001	0.513	0.321
1	1.6	40	0.009552	0.513	0.315
1	1.6	50	0.00185	0.513	0.319
1	1.6	60	0.00673	0.513	0.316
1	2	10	0.003326	0.513	0.255
1	2	20	0.00001	0.513	0.256
1	2	30	0.00001	0.513	0.256
1	2	40	0.007912	0.513	0.253
1	2	50	0.02206	0.513	0.245
1	2	60	0.014478	0.513	0.249
1	2.4	10	0.000018	0.513	0.214
1	2.4	20	0.00001	0.513	0.214
1	2.4	30	0.000892	0.513	0.213
1	2.4	40	0.00001	0.513	0.214
1	2.4	50	0.000172	0.513	0.214
1	2.4	60	0.000742	0.513	0.213

C) Fe

Volume (L)	IOCS (mg)	Time (min)	Ct (mg/L)	Co (mg/L)	qe (mg/mgFe$_2$O$_3$)
1	0.4	10	0.01	10	24.975
1	0.4	20	0.01	10	24.975
1	0.4	30	0.018	10	24.955
1	0.4	40	0.012	10	24.970
1	0.4	50	0.054	10	24.865
1	0.4	60	0.14	10	24.650
1	0.8	10	0.01	10	12.488
1	0.8	20	0.01	10	12.488
1	0.8	30	0.01	10	12.488
1	0.8	40	0.028	10	12.465
1	0.8	50	0.01	10	12.488
1	0.8	60	0.01	10	12.488
1	1.2	10	0.01	10	8.325
1	1.2	20	0.01	10	8.325
1	1.2	30	0.01	10	8.325
1	1.2	40	0.01	10	8.325
1	1.2	50	0.01	10	8.325
1	1.2	60	0.01	10	8.325
1	1.6	10	0.01	10	6.244
1	1.6	20	0.01	10	6.244
1	1.6	30	0.01	10	6.244
1	1.6	40	0.19	10	6.131
1	1.6	50	0.054	10	6.216
1	1.6	60	0.118	10	6.176
1	2	10	0.052	10	4.974
1	2	20	0.01	10	4.995
1	2	30	0.01	10	4.995
1	2	40	0.144	10	4.928
1	2	50	0.426	10	4.787
1	2	60	0.274	10	4.863
1	2.4	10	0.01	10	4.163
1	2.4	20	0.01	10	4.163
1	2.4	30	0.01	10	4.163
1	2.4	40	0.01	10	4.163
1	2.4	50	0.01	10	4.163
1	2.4	60	0.01	10	4.163

Appendix 13. Kinetic model results of single heavy metals adsorption by IOP in 1 hr, pH= 8± 0.5 and differences doses

Mn	Pseudo first-order reaction						Pseudo second-order reaction					
doses (mg)	Linear Equation	Log qe	$-K_1/2.303$	qe,cal	k_1	R^2	Linear Equation	1/qe	$1/k_2qe^2$	q_e	k_2	R^2
4	y=0.0172x-0.7438	-0.7438	0.0172	0.180	-0.040	0.375	y=26.52x-244.32	26.52	-244.32	0.038	-2.879	0.469
8	y=0.0095x-1.5728	-1.5728	0.0095	0.027	-0.022	0.035	y=2.3688x+0.5338	2.3688	0.5338	0.422	10.512	1.000
12	y=0.010x-0.4894	-0.4894	0.01	0.324	-0.023	0.313	y=1.7282x+0.6024	1.7282	0.6024	0.579	4.958	0.998
16	y=0.0238x-1.4899	-1.4899	0.0238	0.032	-0.055	0.230	y=9.564x+11.392	9.564	11.392	0.105	8.029	0.988
20	y=0.0127x-0.6933	-0.6933	0.0127	0.203	-0.029	0.223	y=4.6517x+2.5077	4.6517	2.5077	0.215	8.629	0.986
24	y=0.0068x-0.2928	-0.2928	0.0068	0.510	-0.016	0.375	y=4.1961x-1.6707	4.1961	-1.6707	0.238	-10.539	0.999

As

doses (mg)	Pseudo first-order reaction						Pseudo second-order reaction					
	Linear Equation	Log qe	$-K_1/2.303$	qe,cal	k_1	R^2	Linear Equation	1/qe	$1/k_2qe^2$	qe	k_2	R^2
4	y=0.0059x-2.0832	-2.0832	0.0059	0.008	-0.014	0.094	y=226.19x+10119	226.19	10119	0.004	5.056	0.093
8	y=0.0244x-2.8328	-2.8328	0.0244	0.001	-0.056	0.131	y=285.71x+532.21	285.71	532.21	0.004	153.380	0.946
12	y=0.0375x-2.9202	-2.9202	0.0375	0.001	-0.086	0.410	y=77.41x+288.57	77.41	288.57	0.013	20.766	0.973
16	y=0.0238x-3.0622	-3.0622	0.0238	0.001	-0.055	0.239	y=597.28x-81.633	597.28	-81.633	0.002	-437,0	0.609
20	y=0.0178x-3.1323	-3.1323	0.0178	0.001	-0.041	0.097	y=318.46x+6089.7	318.46	6089.7	0.003	16.654	0.735
24	y=0.021x-2.9766	-2.9766	0.021	0.001	-0.048	0.183	y=177.67x+11946	177.67	11946	0.006	2.642	0.217

Fe

doses (mg)	Pseudo first-order reaction						Pseudo second-order reaction					
	Linear Equation	Log qe	$K_1/2.303$	qe,cal	k_1	R^2	Linear Equation	1/qe	$1/k_2qe^2$	qe	k_2	R^2
4	y=-0.0041x+0.1788	0.1788	-0.0041	1.509	0.009	0.375	y=0.4108x-0.0928	0.4108	-0.0928	2.434	-1.818	1.000
8	y=-0.0117x+0.1329	0.1329	-0.0117	1.358	0.027	0.179	y=0.9292x-1.1816	0.9292	-1.1816	1.076	-0.731	0.997
12	y=0.0012x-0.0537	-0.0537	0.0012	0.884	-0.003	0.375	y=1.3038x-0.9936	1.3038	-0.9936	0.767	-1.711	0.999
16	y=0.0028x-0.1208	-0.1208	0.0028	0.757	-0.006	0.375	y=1.7774x-2.4701	1.7774	-2.4701	0.563	-1.279	0.994
20	y=-0.0061x-0.2398	-0.2398	-0.0061	0.576	0.014	0.018	y=2.0555x-0.1857	2.0555	-0.1857	0.486	-22.752	1.000
24	y=0.0049x-0.2124	-0.2124	0.0049	0.613	-0.011	0.375	y=2.8689x-4.5051	2.8689	-4.5051	0.349	-1.827	0.997

Appendix 14. Kinetic model results of combined heavy metals adsorption by IOP in 1 hr, pH= 8± 0.5 using differences doses

153

Mn	Pseudo first-order reaction						Pseudo second-order reaction					
doses (mg)	Linear Equation	Log qe	$-K_1/2.303$	qe,cal	k_1	R^2	Linear Equation	1/qe	$1/k_2qe^2$	qe	k_2	R^2
4	y=-0.0001x+0.0058	0.0058	-0.0001	1.0134	0.0002	0.375	y=0.959x-1.9848	0.959	-1.984	1.043	-0.463	0.993
8	y=0.0043x-0.1874	-0.1874	0.0043	0.6495	-0.0099	0.375	y=2.4738x-3.7182	2.473	-3.718	0.404	-1.646	0.993
12	y=0.0079x-1.0572	-1.0572	0.0079	0.0877	-0.0182	0.024	y=16.002x-10.767	16.002	-10.76	0.062	-23.782	0.975
16	y=0.0059x-0.2562	-0.2562	0.0059	0.5544	-0.0136	0.375	y=3.5481x-4.556	3.5481	-4.556	0.282	-2.763	0.998
20	y=0.0032x-1.8463	-1.8463	0.0032	0.0142	-0.0074	0.005	y=25.966x-21.435	25.966	-21.435	0.039	-31.455	0.938
24	y=0.0162x-0.7032	-0.7032	0.0162	0.1981	-0.0373	0.375	y=33.195x-109.99	33.195	-109.99	0.030	-10.018	0.982

As	Pseudo first-order reaction						Pseudo second-order reaction					
doses (mg)	Linear Equation	Log qe	$-K_1/2.303$	qe,cal	k_1	R^2	Linear Equation	1/qe	$1/k_2qe^2$	qe	k_2	R^2
4	y=0.0105x-0.454	-0.454	0.0105	0.352	-0.024	0.375	y=9.3842x-13.784	9.3842	-13.784	0.107	-6.38	0.995
8	y=0.0131x-0.5698	-0.5698	0.0131	0.269	-0.030	0.375	y=16.878x+2E-13	16.878	2E-13	0.059	1.424E+15	1.000
12	y=0.015x-0.6516	-0.6516	0.015	0.223	-0.035	0.375	y=25.316x+4E-13	25.316	4E-13	0.040	1.60E+15	1.000
16	y=0.0168x-0.7261	-0.7261	0.0168	0.188	-0.039	0.375	y=36.407x-38.744	36.407	-38.744	0.027	-34.21	0.997
20	y=-0.0167x-1.1609	-1.1609	-0.0167	0.069	0.038	0.046	y=44.695x-8.7132	44.695	-8.7132	0.022	-229.26	0.999
24	y=-0.0117x-0.5017	-0.5017	-0.0117	0.315	0.027	0.024	y=54.09x-33.043	54.09	-33.043	0.018	-88.54	0.999

Fe	Pseudo first-order reaction						Pseudo second-order reaction					
doses (mg)	Linear Equation	Log qe	$K_l/2.303$	qe,cal	k_1	R^2	Linear Equation	1/qe	$1/k_2qe^2$	q_e	k_2	R^2
4	y=-0.0038x+0.1629	0.1629	-0.0038	1.455	0.009	0.375	y=0.4419x-0.58	0.4419	-0.58	2.26	-0.34	0.996
8	y=0.0068x-1.5495	-1.5495	0.0068	0.028	-0.016	0.007	y=0.8019x+0.0052	0.8019	0.0052	1.25	123.66	1.000
12	y=-0.0009x-0.0373	-0.0373	-0.0009	0.918	0.002	0.375	y=1.2033x-0.0067	1.2033	-0.0067	0.83	-216.11	1.000
16	y=0.0026x-0.111	-0.111	0.0026	0.774	-0.006	0.375	y=1.7298x-1.7337	1.7298	-1.73	0.58	-1.73	0.998
20	y=-0.0186x-0.414	-0.414	-0.0186	0.385	0.043	0.124	y=2.1174x-0.2954	2.1174	-0.2954	0.47	-15.18	0.999
24	y=-0.0183x+0.0371	0.0371	-0.0183	1.089	0.042	0.112	y=2.5803x-1.5454	2.5803	-1.5454	0.39	-4.31	1.000

Appendix 15. Kinetic model results of single heavy metals adsorption by IOCS in 1 hr, pH= 8 ± 0.5 and differences dosages

Mn doses (mg)	Pseudo first-order reaction						Pseudo second-order reaction					
	Linear Equation	Log qe	-K₁/2.303	qe,cal	k₁	R²	Linear Equation	1/qe	1/k₂qe²	qe	k₂	R²
0.4	y=-0.0173x+0.353	0.353	-0.0173	2.254	0.040	0.0477	y=0.42502x+1.3892	0.42	1.38	2.353	0.130	0.615
0.8	y=-0.0045x+0.1959	0.1959	-0.0045	1.570	0.010	0.375	y=0.37x-5.145	0.36	0.51	2.703	0.266	0.994
1.2	y=0.0056x-0.2405	-0.2405	0.0056	0.575	-0.013	0.375	y=3.0211x-17.063	3.02	17.06	0.331	0.535	0.914
1.6	y=-0.1576x+2.3947	2.3947	-0.1576	248.142	0.363	0.375	y=6.2777x-39.47	6.27	39.47	0.159	0.998	0.904
2	y= 0.0023x-0.8638	-0.8638	0.0023	0.137	-0.005	0.131	y=3.3579x+31.016	3.35	31.01	0.298	0.364	0.826
2.4	y=-0.0018x-0.856	-0.856	-0.0018	0.139	0.004	0.0007	y=43.343x-1210.4	43.34	121,0	0.023	1.552	0.236

As

doses (mg)	Pseudo first-order reaction						Pseudo second-order reaction					
	Linear Equation	Log qe	-K$_1$/2.303	qe,cal	k$_1$	R^2	Linear Equation	1/qe	1/k$_2$qe^2	qe	k$_2$	R^2
0.4	y=0.0242x-1.9233	-1.9233	0.0242	0.012	-0.056	0.246	y=145.49x-40.159	145.49	-40.159	0.007	-527.088	0.481
0.8	y=0.0366x-1.6792	-1.6892	0.0366	0.020	-0.084	0.632	y=151.17x-1682.5	151.17	-1682.5	0.007	-13.582	0.814
1.2	y=0.0306x-2.2216	-2.2216	0.0306	0.006	-0.070	0.527	y=38.578+86.844	38.578	86.844	0.026	17.137	0.245
1.6	y=0.0188x-2.2662	-2.2662	0.0188	0.005	-0.043	0.142	y=102.96x-44.917	102.96	-44.917	0.010	-236.008	0.682
2	y=0.0311x-1.5782	-1.5782	0.0311	0.026	-0.072	0.381	y=106.45x+590.83	106.45	590.83	0.009	19.179	0.752
2.4	y=0.0479x-2.4341	-2.4341	0.0479	0.004	-0.110	0.702	y=50.37x+3916.3	50.37	3916.3	0.020	0.648	0.079

Fe

doses (mg)	Pseudo first-order reaction						Pseudo second-order reaction					
	Linear Equation	Log qe	-K$_1$/2.303	qe,cal	k$_1$	R^2	Linear Equation	1/qe	1/k$_2$qe^2	qe	k$_2$	R^2
0.4	y=-0.0147x+0.6361	0.6361	-0.0147	4.326	0.034	0.375	y=0.04172x-0.028	0.04172	-0.02795	23.969	-0.062	0.997
0.8	y=-0.0174x+0.5844	0.5844	-0.0174	3.841	0.040	0.0921	y=0.08x+0.03071	0.07996	0.03071	12.506	0.208	0.999
1.2	y=0.0233x+0.4429	0.4429	0.0233	2.773	-0.054	0.1299	y=0.1202x+0.00865	0.12019	0.00865	8.320	1.670	1.000
1.6	y=-0.0085x+0.1435	0.1435	-0.0085	1.392	0.020	0.0024	y=0.16016x+0.0029	0.16016	0.0029	6.244	8.845	1.000
2	y=-0.0209x+0.3388	0.3388	-0.0209	2.182	0.048	0.1564	y=0.20165x-0.0121	0.20165	-0.01206	4.959	-3.372	1.000
2.4	y=-0.0064x+0.2786	0.2786	-0.0064	1.899	0.015	0.375	y=0.2473x-0.1169	0.2408	-0.1169	4.153	-0.496	1.000

Appendix 16. Kinetic model results of combined heavy metals adsorption by IOCS in 1 hr, pH= 8± 0.5 and differences doses

Mn	Pseudo first-order reaction						Pseudo second-order reaction					
doses (mg)	Linear Equation	Log qe	$K_1/2.303$	qe,cal	k_1	R^2	Linear Equation	1/qe	$1/k_2qe^2$	q_e	k_2	R^2
0.4	y=-0.0005x-0.1613	-0.1613	-0.0005	0.6898	0.0012	0.181	y=0.1002x+0.0299	0.10018	0.02986	9.982	0.336	0.996
0.8	y=-0.0055x+0.2389	0.2389	-0.0055	1.7334	0.0127	0.375	y=0.2894x-0.1593	0.28945	-0.1593	3.455	-0.526	0.985
1.2	y=-0.0058x+0.2508	0.2508	-0.0058	1.7816	0.0134	0.375	y=0.2871x-0.3228	0.28714	-0.32278	3.483	-0.255	0.995
1.6	y=0.0011x-0.695	-0.695	0.0011	0.2018	-0.0025	0.080	y=0.5382x+0.0242	0.53418	0.02421	1.872	11.786	0.915
2	y=-0.0104x+0.1795	0.1795	-0.0104	1.5118	0.0240	0.033	y=0.6226x-0.8577	0.62261	-0.85772	1.606	-0.452	0.991
2.4	y=0.0072x-0.5295	-0.5295	0.0072	0.2955	-0.0166	0.140	y=0.7896x-0.3356	0.78965	-0.33565	1.266	-1.858	0.996

As

doses (mg)	Pseudo first-order reaction						Pseudo second-order reaction					
	Linear Equation	Log qe	$-K_1/2.303$	qe,cal	k_1	R^2	Linear Equation	$1/qe$	$1/k_2qe^2$	qe	k_2	R^2
0.4	y=-0.0011x+0.0471	0.0471	-0.0011	1.115	0.003	0.375	y=0.7892x-0.13189	0.78921	-0.13188	1.267	-4.723	1.000
0.8	y=-0.0079x-0.4098	-0.4098	-0.0079	0.389	0.018	0.000	y=1.561x+0.3145	1.561	0.31455	0.641	7.747	0.999
1.2	y=0.004x-0.4345	-0.4345	0.004	0.368	-0.009	0.081	y=2.3392x+0.3492	2.3392	0.34922	0.427	15.669	1.000
1.6	y=-0.0045x-0.3304	-0.3304	-0.0045	0.467	0.010	0.002	y=3.158x-0.3992	3.158	-0.39922	0.317	-24.981	1.000
2	y=-0.0108x-0.1072	-0.1072	-0.0108	0.781	0.025	0.014	y=4.0409x-1.6599	4.0409	-1.6599	0.247	-9.837	1.000
2.4	y=0.0072x-0.912	-0.912	0.0072	0.122	-0.017	0.039	y=4.6833x-0.0421	4.6833	-0.04211	0.214	-520.857	1.000

Fe

doses (mg)	Pseudo first-order reaction						Pseudo second-order reaction					
	Linear Equation	Log qe	$-K_1/2.303$	qe,cal	k_1	R^2	Linear Equation	$1/qe$	$1/k_2qe^2$	qe	k_2	R^2
0.4	y=-0.0149x+0.6462	0.6462	-0.0149	4.4279	0.0343	0.375	y=0.0404x-0.0061	0.04044	-0.00614	24.728	-0.266	1.000
0.8	y=-0.0176x+0.4502	0.4502	-0.0176	2.8197	0.0405	0.051	y=0.0801x+0.0002	0.0801	0.00021	12.484	30.552	1.000
1.2	y=-0.0099x+0.4273	0.4273	-0.0099	2.6749	0.0228	0.375	y=0.12012x-1E-15	0.12012	-1.00E-15	8.325	-1.4E+13	1.000
1.6	y=-0.0133x+0.319	0.319	-0.0133	2.0845	0.0306	0.023	y=0.162x-0.0171	0.16196	0.01709	6.174	1.535	1.000
2	y=-0.0154x+0.3989	0.3989	-0.0154	2.5055	0.0355	0.375	y=0.2071x-0.0824	0.20713	0.08238	4.828	0.521	1.000
2.4	y=-0.0066x+0.2876	0.2876	-0.0066	1.9391	0.0152	0.373	y=0.2402x-3E-15	0.24024	3.00E-15	4.163	1.92E+13	1.000

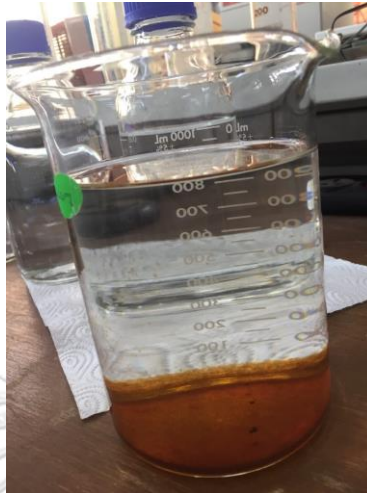**Appendix 17.** Photograph of co-precipitated As and Fe in water after adsorption process using IOP and IOCS

Figure 17.A. photograph of co-precipitation As and Fe in combined heavy metals using IOP 12 mg/L, pH = 8 ± 0.5 at 1 hr

Figure 17.B. Photographs of co-precipitation As and Fe in combined heavy metals using IOCS, pH= 8 ± 0.5 at 1 hr

Appendix 18. Research plan

The work schedule conducts of this study showed in Table 5.1.

Table 5.1. Research schedule and planning

Works Description/Date	2018							2019						
	Jun	Jul	Aug	Sep	Oct	Nov	Dec	Jan	Feb	Mar	Apr	May	Jun	Jul
Literatures review	■	■	■											
Thesis proposal				■										
Adsorbents Preparation					■	■								
Batch test														
Study adsorbent dose and contact time						■	■							
Study effect of anion sulfate in groundwater								■	■					
Leaching test									■					
Results analyst					■	■	■	■	■					
Conference paper									■	■	■	■		
Thesis writing					■	■	■	■	■	■	■	■		
Thesis defense													■	
Thesis revision and submission														■

Appendix 19. Cost of adsorbents estimation

Approximately cost estimation of adsorbents generation was summarized in this table.

IOP		IOCS	
Name	**Price (Baths)**	**Name**	**Price (Baths)**
Cast iron rod	1,000	Sand	90
Transportation	600	$Fe(NO_3)_3.9H_2O$	1,092
Milling process	0	NaOH	461
Total	1,600	*Total*	1,643

Appendix 20. Leaching test analysis

Loading concentration (mg/mg IOP or IOCS) = (leachate con. × Volume of leaching) / 1L× Mass of IOP or IOCS

1. Leaching of IOP after single heavy metals adsorption

Me tals	Leachate con mg/L	Volume leaching (μL)	Volume leaching (mL)	Mass IOP (mg)	loading con (μg/mg IOP)	loading con (mg/mg IOP)
Mn	145.4	210	0.21	10	3.0534	0.00305
As	0.0582	140.7	0.1407	6.7	0.00122	1.22E-06
Fe	1541	483	0.483	23	32.361	0.0323

2. Leaching of IOP after combined heavy metals adsorption

Me tals	Leachate con mg/L	Volume leaching (μL)	Volume leaching (mL)	Mass IOP (mg)	loading con (μg/mg IOP)	loading con (mg/mg IOP)
Mn	190.6	325.5	0.3255	15.5	4.0026	0.004
As	0.001	325.5	0.3255	15.5	0.000021	21E-09
Fe	2166	325.5	0.3255	15.5	45.486	0.045486

3. Leaching of IOCS after single heavy metals adsorption

Meta ls	Leacha te con mg/L	Volume leaching (μL)	Volume leaching (mL)	Mass IOCS (mg)	loading con (μg/mg IOCS)	loading con (mg/mg IOCS)
Mn	0.3777	909.3	0.9093	43.3	0.00793	7.933E-06
As	0.0102	1352.4	1.3524	64.4	0.00021	2.142E-07
Fe	0.85	894.6	0.8946	42.6	0.0179	0.00001785

4. Leaching of IOCS after combined heavy metals adsorption

Meta ls	Leachate con mg/L	Volume leaching (μL)	Volume leaching (mL)	Mass IOCS (mg)	loading con (μg/mg IOCS)	loading con (mg/mg IOCS)
Mn	0.16	1352.4	1.3524	64.4	0.00336	33.6E-07
As	0.00334	1352.4	1.3524	64.4	0.00007	7.014E-08
Fe	1.48	1352.4	1.3524	64.4	0.0311	0.000031

VITA

NAME	Ramy Lun
DATE OF BIRTH	08 June 1995
PLACE OF BIRTH	Kompong Cham Province, Cambodia
INSTITUTIONS ATTENDED	Institute of Technology of Cambodia
HOME ADDRESS	Phnom Penh, Cambodia
AWARD RECEIVED	Mr. Ramy Lun awarded ADB scholarship for conducting his bachelor's degree majoring water resources and rural infrastructure engineering and AUN/SEED-Net for pursuing his master's degree majoring environmental engineering.

จุฬาลงกรณ์มหาวิทยาลัย
CHULALONGKORN UNIVERSITY